

SETTLEMENT BEHAVIOUR OF CONCRETE FACED ROCKFILL DAMS:
A CASE STUDY

A THESIS SUBMITTED TO
THE GRADUATE SCHOOL OF NATURAL AND APPLIED SCIENCES
OF
MIDDLE EAST TECHNICAL UNIVERSITY

BY

RIZA SAVAŞ ÖZKUZUKIRAN

IN PARTIAL FULFILLMENT OF THE REQUIREMENTS
FOR
THE DEGREE OF MASTER OF SCIENCE
IN
CIVIL ENGINEERING

JANUARY 2005

Approval of the Graduate School of Natural and Applied Sciences

Prof. Dr. Canan ÖZGEN
Director

I certify that this thesis satisfies all the requirements as a thesis for the degree of Master of Science.

Prof . Dr. Erdal ÇOKÇA
Head of Department

This is to certify that we have read this thesis and that in our option it is fully adequate, in scope and quality, as a thesis for the degree of Master of Science.

Gülru S. YILDIZ
Co-Supervisor

Prof . Dr. M. Yener ÖZKAN
Supervisor

Examining Committee Members

Prof. Dr. Ufuk ERGUN (METU, CE) _____

Prof . Dr. M. Yener ÖZKAN (METU, CE) _____

Assoc. Prof. Dr. K. Önder ÇETİN (METU, CE) _____

Dr. Oğuz ÇALIŞAN (Geotechnical Consultant) _____

Gülru S. YILDIZ (State Hydraulic Works) _____

I hereby declare that all information in this document has been obtained and presented in accordance with academic rules and ethical conduct. I also declare that, as required by these rules and conduct, I have fully cited and referenced all material and results that are not original to this work.

Name, Last name : Rıza Savaş ÖZKUZUKIRAN

Signature :

ABSTRACT

SETTLEMENT BEHAVIOUR OF CONCRETE FACED ROCKFILL DAMS: A CASE STUDY

ÖZKUZUKIRAN, Rıza Savaş

M.S., Department of Civil Engineering

Supervisor : Prof. Dr. M. Yener ÖZKAN

Co-Supervisor: Gülru S. YILDIZ

January 2005, 150 Pages

In this study settlement behaviour of Kürtün dam, which is the first concrete faced rockfill dam in Turkey, is investigated. Two dimensional plane strain finite element analyses are carried out in order to determine the total stresses and displacements during construction and reservoir filling conditions. Hardening soil model is used in order to represent the non-linear, inelastic and stress dependent behaviour of rockfill material. Material model parameters are selected mainly referring to the previous studies on the dams consisting of similar materials. Calculated stresses and settlements are compared with the observed values and in general, they were found to be in good agreement for the construction stages. It is seen that, due to the relatively narrow valley and steep abutment slopes, arching is a significant parameter as far as the stresses and settlements are concerned. For the

reservoir impounding condition, calculated settlements were found to be slightly larger than the observed values, which may indicate that during the reservoir impounding, the rockfill embankment behaves in a stiffer manner as compared to that of during construction stages.

Keywords: Concrete faced rockfill dams, stress, settlement, finite element analysis, hardening soil model

ÖZ

ÖN YÜZÜ BETON KAPLI KAYA DOLGU BARAJLARIN OTURMA DAVRANIŞI: BİR ÖRNEK ÇALIŞMA

ÖZKUZUKIRAN, Rıza Savaş

Yüksek Lisans, İnşaat Mühendisliği Bölümü

Tez Yöneticisi : Prof. Dr. M. Yener ÖZKAN

Ortak Tez Yöneticisi : İnş. Yük. Müh. Gülru S. YILDIZ

Ocak 2005, 150 sayfa

Bu çalışmada Türkiye'deki ilk ön yüzü beton kaplı kaya dolgu baraj olan Kürtün barajının oturma davranışı incelenmiştir. İnşaat durumu ile su tutma durumuna ait toplam gerilmelerin ve yer değiştirmelerin belirlenmesi amacıyla iki boyutlu düzlem şekil değiştirme prensibi kullanılarak, sonlu elemanlar metodu analizleri gerçekleştirilmiştir. Kaya dolgu malzemesinin doğrusal ve elastik olmayan, gerilme bağımlı davranışını temsil etmek için sertleşen zemin modeli kullanılmıştır. Malzeme model parametreleri, temelde, benzer malzemeler içeren önceki çalışmalar kaynak gösterilerek seçilmiştir. Hesaplanan gerilme ve oturmalar, ölçülen değerler ile karşılaştırılmış ve inşaat evreleri için uyumun genelde iyi olduğu görülmüştür. Gerilmeler ve oturmalar açısından bakıldığında, dar vadi ve dik mesnet eğimleri nedeniyle, kemerlenme etkisinin önemli bir parametre olduğu görülmüştür. Su tutma

durumunda, baraj kaya dolgu seddesinin inşaat durumuna göre daha katı davranışının belirtisi olarak hesaplanan oturmalar gözlenen değerlerden bir parça yüksek bulunmuştur.

Anahtar Kelimeler: Ön yüzü beton kaplı kaya dolgu barajlar, gerilme, oturma, sonlu elemanlar analizi, sertleşen zemin modeli

To My Family

ACKNOWLEDGMENTS

The author wishes to express his sincere appreciation to his supervisor Prof. Dr. M. Yener ÖZKAN and co-supervisor Gülru S. YILDIZ (M.S) for their guidance, advice, criticism, encouragements and insight throughout the research.

Mr. Mehmet ÖZYAZICIOĞLU and Mr. A. Anıl YUNATCI are also sincerely acknowledged for their valuable support.

Finally the author is grateful for all continuous support, understanding and encouragement he has received from his family and friends.

TABLE OF CONTENTS

PLAGIARISM	iii
ABSTRACT	iv
ÖZ	vi
DEDICATION	viii
ACKNOWLEDGEMENTS	ix
TABLE OF CONTENTS	x
CHAPTER	
1. INTRODUCTION	1
2. CONCRETE FACED ROCKFILL DAMS, SHEAR STRENGTH AND MODELING OF ROCKFILL MATERIAL	3
2.1 General	3
2.2 Evolution, Characteristics and Current Design Trends of CFRDs	4
2.2.1 Evolution of Modern CFRDs	4
2.2.2 General Considerations	5
2.2.2.1 Design of Dam Section	5
2.2.2.2 Toe Slab	6
2.2.2.3 Concrete Face	6
2.2.2.4 Zoning in CFRDs	8
2.2.3 Materials for Rockfill Dams and Rockfill Grading	9

2.2.4 Sluicing	11
2.3 Shear Strength Characteristics of Rockfill Material	11
2.3.1 Previous Studies	12
2.3.2 Summary of the Studies	36
2.4 Constitutive Laws	37
2.4.1 Linear Elasticity	37
2.4.2 Non-Linear Material Models	38
2.4.2.1 Duncan and Chang's Hyperbolic Model	38
2.4.2.2 Hardening Soil Model	44
3. SETTLEMENT OF CONCRETE FACED ROCKFILL DAMS	47
3.1 General	47
3.2 A Review of Previous Studies	48
3.2.1 Observed Settlement Behaviour of CFRDs	48
3.2.2 Settlement Analyses of Earth and Rockfill Dams	58
3.2.2.1 Assessment of Behaviour of Fill Dams by Finite Element Method	58
3.2.2.2 Empirical Approaches on Determining Deformation Moduli of CFRDs	70
3.2.3 Assessment of Settlement Behaviour of CFRDs by Finite Element Method.....	76
4. SETTLEMENT ANALYSES OF KÜRTÜN DAM BY FINITE ELEMENT METHOD	92
4.1 Kürtün Dam	92
4.2 Instrumentation	95
4.2.1 Hydraulic Settlement Devices	101

4.2.2 Hydraulic Pressure Cells	101
4.2.3 Strainmeters	102
4.2.4 Surface-Mount Jointmeters	103
4.3 Observed Settlement Behaviour of Kürtün Dam	103
4.3.1 Construction Period	104
4.3.2 Impoundment Period	105
4.3.3 Operation Period	105
4.4 Preliminary Finite Element Analyses of Kürtün Dam	110
4.4.1 Material Model and Material Parameters	110
4.4.2 Elements and Finite Element Mesh Used in the Analyses	112
4.4.3 Analysis Technique	114
4.4.4 Determination of Layer Thicknesses	115
4.5 Analyses and Results	116
4.5.1 Determination of Material Model Parameters and EoC Analyses	116
4.5.2 Effects of Zone 3C	121
4.5.3 Reservoir Full Condition (RFC)	124
4.5.4 Assessment of Total Stresses	131
4.5.5 Behaviour of Concrete Membrane due to Reservoir Impounding	134
4.5.6 Displacement and Total Stress Contours	137
5. SUMMARY and CONCLUSIONS	144
REFERENCES	147

CHAPTER 1

INTRODUCTION

With the developments in dam engineering and the technology used, concrete faced rockfill dams (CFRDs) became popular in recent years, especially in the regions with a shortage of impervious soils.

In fact, these type of dams have been built all over the world for almost 150 years. Heights of CFRDs has passed 200 m where Shuibuya dam which is under construction in China, is 230 m high and will be the highest CFRD in the world.

Today, the design of concrete face rockfill dams are mostly depend on experience and engineering judgment (Cooke, 1984). For these kind of huge structures, it is essential to predict the behaviour both for the construction and the reservoir impounding conditions.

Clough et al. were the first researchers who utilized finite element method in predicting the behaviour of an earth dam in 1967. Since then finite element method became a powerful tool for predicting the behaviour of both earth and rockfill dams.

In their study, Clough et al. used linear elastic model to analyze stresses and deformations in the dam. However with the development of powerful computers, more complex models are developed to represent the stress-strain behaviour of materials and used in the finite element analysis such as the non-linear hyperbolic model developed by Duncan and Chang, in 1970.

In this study, two dimensional plane strain analyses of 133 m high Kürtün dam which is the first CFRD in Turkey are carried out to compute the stresses and deformation behaviour both for construction and reservoir impounding conditions. The analyses are carried out by using the Plaxis v7.2 finite element program.

Hardening soil model which is a non-linear elasto-plastic model is utilized to represent the rockfill material behaviour. The model material parameters are estimated from appropriate studies in the literature. Later, the results are compared with the observed values.

In Chapter 2, current trends in CFRD design are outlined with the literature overview relating shear strength characteristics of rockfill material. Constitutive laws used in representing the stress-strain behaviour of rockfill material are also outlined in Chapter 2. Chapter 3 reviews the settlement behaviour of CFRDs. In Chapter 4, the results of the analyses are represented together with the observed settlement behaviour of Kürtün dam. Chapter 5 includes the summary and conclusions of the study.

CHAPTER 2

CONCRETE FACED ROCKFILL DAMS, SHEAR STRENGTH AND MODELING OF ROCKFILL MATERIAL

2.1 General

The currently accepted definition of a rockfill dam is given by the ASCE Symposium on Rockfill Dams in 1960 as "a dam that relies on rock, either dumped in lifts or compacted in layers, as a major structural element."

Rockfill dams can be examined in two categories; (1) rockfill dams with impervious membranes, (2) rockfill dams with earth cores. The large majority of impervious membranes are of cement concrete which is dealt in this study, followed by asphalt-concrete, which has been used on many dams up to medium heights. There are a few examples of steel and timber membranes. The membrane is mostly placed on the upstream slope but has been provided inside the rockfill embankment in a few cases (Singh et al., 1995).

This chapter is divided in three main parts. First current trends in CFRD design are outlined. Second the studies of determination of shear strength characteristics of rockfill material are overviewed. In the final part constitutive models used in modeling rockfill material behaviour are briefly outlined.

2.2 Evolution, Characteristics and Current Design Trends of CFRDs

2.2.1 Evolution of Modern CFRDs

According to Cooke, the evolution of rockfill dams can be considered under three main categories. These are; early period (1850-1940), transition period (1940-1965) and modern period (1965-). The early period of rockfill dams date back to the California gold rush. The gold miners in California sierras developed the construction of dumped rockfill dams. These dams were timber faced, having heights up to 25 m. Very steep slopes [0.5:1 to 0.75:1 (H:V)] are used in the embankments. The first rockfill dam known to use concrete facing was Chatworth Park dam which was constructed in California, in 1895. The 84 m high Dix River dam in Kentucky and 101 m high Salts Springs dam in California are early high concrete face dams. Despite the occurrence of some leakage problems, Salt Springs dam has been operating since 1931. The rockfill dams were constructed with impervious membrane faces until earth core designs began to be developed about 1940 (Cooke, 1984).

In the transition period, there were certain limitations and problems with CFRDs higher than 300 ft (91 m). Availability of suitable rockfill material was one of the problems since dumped rockfill was widely considered to be a rock type of having high unconfined compressive strength. Another problem was the compressibility of the rockfill since dumped rockfill was placed in thick lifts as 18-60m. Serious leakage problems occurred frequently with these type of dumped rockfill dams due to high settlement of rockfill embankment in the reservoir impounding period. In this period, the important CFRDs could be summarized as 75 m high Lower Bear River No.1 dam, 46 m high Lower Bear River No.2 dam and 110 m high Paradela dam. 150 m high New Exchequer dam located in California which was constructed in 1958 is the last example in transition period. The dam was built with a partially compacted rockfill of 1.2-3.0 m lifts and dumped rockfill of 18 m lifts (Cooke, 1984).

In the 1955-1965 period, the transition from dumped rockfill to compacted rockfill is forced by need for higher dams, the unavailability of high quality rock at many dam sites and the development of heavy, smooth drum, vibratory rollers. In this period 18-60 m lifts changed to 3 m in some dams. At Ambuklao dam in 1955, most of the dumped rockfill was changed to 0.6 m layer rockfill due to the low strength and small sizes of some available rock (Cooke, 1984).

The transition from dumped rockfill to compacted rockfill was very rapid. With the development of vibratory rollers, the usage of relatively weak rock particles become possible with compaction in thin layers. 110m high Cethana dam located in Australia, 140 m high Alto Anchicaya dam located in Colombia and 160 m high Foz do Areia dam located in Brazil are the CFRDs that contributed to the state-of-the-art of rockfill dam design.

CFRDs are now being considered as an alternative at most sites to the earth core rockfill dams when compared in cost and schedule. Lots of CFRDs are presently under construction throughout the world and their popularity is increasing everyday.

2.2.2 General Considerations

As mentioned earlier, the design of CFRDs is mainly empirical and based on experience and judgment. In the following paragraphs, a brief outline about the current CFRD design practice is given.

2.2.2.1 Design of Dam Section

In CFRDs all the rockfill is located downstream from the reservoir water loading. According to Cooke (1984), in these type of dams relatively high safety ratios against horizontal sliding and slope stability is maintained. The majority of the water load goes into the foundation through the dam axis. Cooke (1984) indicated

that it is hardly possible to recommend a verified realistic method of stability analysis from wedge or circle analysis since no rockfill dam has ever failed because of inadequate stability. Therefore, traditionally 1.3H:1V to 1.5H:1V design slopes are selected in CFRDs generally.

2.2.2.2 Toe Slab

Hard, non-erodible and groutable rock is the most desirable rock for a toe slab. However, foundations which do not suit with the above statement can also be used in CFRDs with proper engineering. Generally the toe slab is placed in 6-8 m lengths and dowelled to well cleaned rock prior to grouting. There is no such current design practice about the width of the toe slab. Widths are determined by engineering judgment and varies with the quality of rock and the dam height. One layer of reinforcing is used near the top of the toe slab (Cooke et al., 1987).

2.2.2.3 Concrete Face

In CFRDs, durability and impermeability are more important than strength for the concrete face where C20 concrete is considered as adequate. Current design practice provides a permanent and watertight face (Cooke et al., 1987).

The thickness of early dumped rockfill dams was taken traditionally as $0.3 \text{ m} + 0.0067H$ where H represents the dam height. Nowadays the increment value is reduced to $0.003H$. In some CFRDs to $0.002H$ or less increments are used. These slabs have given satisfactory performance and there is a current general trend towards thinner slabs (Cooke et al., 1987). Also, there are some CFRDs which have a constant slab thickness such as Murchison dam where a constant slab thickness of 0.30 m is used.

The concrete face is reinforced in order to resist the tension forces without cracking. In early designs 0.5% reinforcing is used traditionally in each direction. Nowadays this ratio is being reduced to 0.4%. But in the literature, there are dams where lower reinforcing ratios are used. Reinforcing is placed as a single layer at the center of the slab or a little above the slab centerline. Here, the purpose is to make the slab as flexible as possible, allowing it to follow small differential settlements without developing high bending stresses and to provide equal bending resistance in both directions (Cooke et al., 1987).

On almost all the recent CFRDs, a double row of small bars (anti-spalling reinforcement) has been used at the perimeter joint. Usually ordinary reinforcing steel is used but there are some dams where high-yield steel has been used without changing the amount of steel such as in Areia dam (Cooke et al., 1987).

The concrete slabs are placed in vertical strips with the form of continuous slips from bottom to the top with simple horizontal construction joints. No waterstops are used in these horizontal construction joints. The slab is usually placed in 12-18 m-wide strips where 15 m is very common in practice.

The concrete face mostly placed after the rockfill embankment has been completed to full height. However, there are some CFRDs, in which the concrete face is placed where the construction of the embankment are in progress such as Areia, Salvajina and Khao Laem dams. At the 160 m high Areia dam, the concrete slab was placed on the lower 80 m of the dam height before the rest of the embankment was completed (Cooke et al., 1987).

Parapet walls are used in order to reduce the amount of rockfill at the crest level and contributes to the economy of the dam. A parapet wall of 3-5 m in height can be taken as the current design practice. The freeboard of the CFRDs is calculated from top of the parapet wall if the wall is extended into the abutments.

2.2.2.4 Zoning in CFRDs

A typical zoning of a CFRD is given in Figure 2.1. Here, Zone 1 can be considered as a blanket which consists of impervious soils. The purpose of using this zone is to cover the perimeter joints and the slab in the lower elevations with an impervious soil, preferably silt, which would seal any cracks or joint openings. It is mostly preferred in high dams but it is not a must in CFRD design. There are dams in operation without Zone 1, indicating that this it is not necessarily useful. Actually it is useful only when a problem occurs. Zone 1 can be placed from bottom to several meters above from the original riverbed (Cooke et al., 1987).

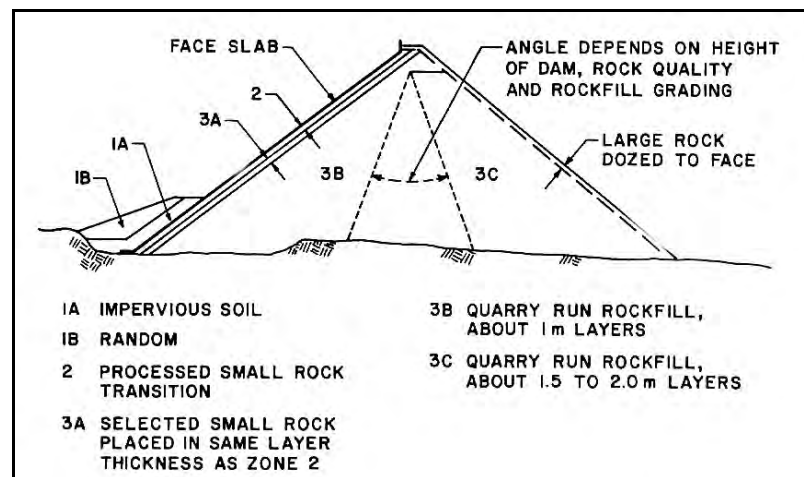


Figure 2.1 Typical zoning of CFRDs (Cooke et al., 1987)

Zone 2 consists of finer rock. The purpose of using this zone, directly under the slab, is to provide a firm and uniform support for the slab. Here, rockfill materials having particle sizes between 7.5 and 15 cm are used with 40% sand sizes and fines. Compaction is carried out in 0.4-0.5 m layers using smooth-drum vibratory rollers. Generally four coverage of a 10 t. smooth drum vibratory roller is taken as sufficient.

Zone 2 provides a semi-impervious barrier, preventing any large leakage which can be developed through a crack in the concrete slab. According to Cooke et al. (1987), current design practice is to use more sand sized particles in Zone 2 to achieve more workability and less permeability. However, at rainy sites, care must be taken since Zone 2 material can be lost by erosion.

The main zone in a CFRD is Zone 3. This zone consists of three internal zones; Zone 3A, Zone 3B and Zone 3C.

Zone 3A is a transition zone between Zone 2 and the main rockfill and compacted in 0.4-0.5 m layers similar to Zone 2. The main purpose of compaction is to limit the size of the voids in Zone 3A and ensure that Zone 2 material could not be washed into large voids into the main rockfill zones (Cooke et al., 1987).

Mostly, Zone 3B is compacted in 1 m layers with 4-6 passes of a 10 t. smooth drum vibratory roller. In order to control the slab displacements, compressibility of Zone 3B must be as low as practical and in most cases the compaction effort mentioned above gives a satisfactory performance (Cooke et al., 1987).

Zone 3C has a little influence on the slab settlement and takes negligible water load. This zone is compacted in 1-2 m layers with a four passes of a 10 t. smooth drum vibratory rollers. At the downstream face of the dam, large rock particles are placed such as in Areia dam.

2.2.3 Materials for Rockfill Dams and Rockfill Grading

Specifications for the rockfill dams are not as rigid as for concrete aggregates. The rock which will be used in the dam, should be sound and should not be liable to disintegration by weathering. The most suitable rock types are the massive igneous or metamorphic rocks where rocks which will split into flat pieces on blasting are undesirable. In the literature granites, diorites, gneisses, basalts, dense sandstones and limestones and dolomitic quartzites are satisfactorily used for the rockfill dams. There are also rockfill dams where relatively soft rocks are used such as siltstones, schists and argillites (Singh et al., 1995).

The range of unconfined compressive strength of the rockfill used in CFRDs lies between 100-200 kg/cm² (very low) to more than 2500 kg/cm² (highest) with the majority of 500-1500 kg/cm². Generally, hard rocks with unconfined compressive strengths of as low as 300 kg/cm² is thought to be adequate for CFRDs. Rockfill of higher strength have no technical advantage since the rockfill of 300-400 kg/cm² strength are not more compressible in the completed dam than those of much harder rocks. On the contrary, the use of rockfill from rock of low to moderate compressive strength have several cost advantages since it is less costly to blast and gives considerably less damage to rubber-tired equipment (Cooke et al., 1987).

According to Cooke (1984), one of the key points in selecting the rock type is its behaviour upon wetting. If after wetting, a blasted rockfill is strong enough to support construction trucks and a 10 t vibratory roller, it may be considered as suitable for compacted rockfill dams. If the rock breaks down and does not remain free-draining after compaction, it is necessary to provide zones of hard, pervious rockfill for internal drainage.

The most important properties of the CFRD embankments are their low compressibility and high shear strength. Usually rockfill is highly pervious. As a general rule any quarried hard rock with an average particle size distribution having 20% or less finer than the No.4 sieve and 10% or less finer than the No.200 sieve will have the needed rockfill of high shear strength and low compressibility (Cooke et al., 1987).

According to Cooke et al.(1987), a stable construction surface under the traffic loads caused by heavy trucks, demonstrates that the wheel loads are being carried by a rockfill skeleton where an unstable construction surface shows that loads are carried by the fines. If an unstable surface exists, the resulting embankment may not have the properties desired for a pervious rockfill zone.

2.2.4 Sluicing

Sluicing is the addition of water to rockfill in the construction. The main object of adding water is to wet the material. Upon wetting, the fines are softened and the compressive strength of the rockfill reduces and thus embankment shows relatively low post-construction settlements. However, if the water absorption of the rock used is very low, the improvement in compressibility is very small and can be taken as negligible especially for dams of moderate height and for Zone 3C.

High pressure sluicing apparatus is not needed since it is not necessary to wash the fines into the larger rockfill voids. The quantity of water used in sluicing ranges between 10-20% of the rockfill embankment volume.

Cooke et al. (1987) suggest the following general statements about the sluicing of rockfill:

1. For most hard rocks and CFRDs of low to moderate height, the addition of water has negligible effect on the dam behaviour.
2. For high dams and for rock having significantly lower unconfined compressive strength when tested in saturated condition, water should probably be added routinely for the upstream shell (Zone 3B).
3. For rocks with questionably high contents of earth and sand-sized particles, water should nearly always be used. For dirty rock, the water softens the fines so that larger rocks can be forced into contact with each other by the vibrating roller.

2.3 Shear Strength Characteristics of Rockfill Material

Shear strength is an important topic in soil mechanics. However determination of the shear strength characteristics of rockfill was always a difficult subject for geotechnical engineers. Since in many conditions rockfill materials contain particles up to 1200 mm particle sizes, they can not be tested with the

conventional triaxial testing apparatus. In order to carry out this kind of triaxial tests, very large apparatus are needed which are very expensive thus not available in many cases. To overcome this difficulty, some special methods are developed to reduce size of the rockfill particles for triaxial testing. Commonly used methods can be summarized as; (1) the scalping technique (Zeller et al., 1957), (2) parallel gradation technique (Lowe, 1964), (3) generation of quadratic grain size distribution curves (Fumagalli, 1969) and (4) the replacement technique (Frost, 1973). Parallel gradation technique of Lowe is the commonly used one among all.

Despite its difficulty, there are many valuable studies about shear strength of rockfill materials which can be summarized as Marsal 1967, Fumagalli 1969, Marachi et al. 1972 and Varadarajan et al. 2003. Some correlations are also, carried out such as Leps 1970, Barton et al. 1981. In the following sections these studies are briefly outlined.

2.3.1 Previous Studies

In 1967, Marsal carried out several triaxial and one dimensional compression tests on rockfill specimens in order to use the results in the design of 148 m high El Infiernillo dam which is located in Mexico. In triaxial tests, 113 cm in diameter, 250 cm high specimens were used with a max. particle size of 20 cm thus special testing devices are developed.

In Figure 2.2, the gradations of three of the materials used in Marsal's study are shown. Here, Material 1 consists of basalt fragments produced in a crushing plant. The fragments are sound and unconfined compressive strength (q_u) is estimated to be more than 1000 kg/cm^2 . Material 2, formed by granitic gneiss particles and obtained by quarry blasting; particles contain thin layers of schist and their q_u value is in average of 740 kg/cm^2 . Material 3 is of the same origin as Material 2 but has a much more uniform gradation (Marsal, 1967).

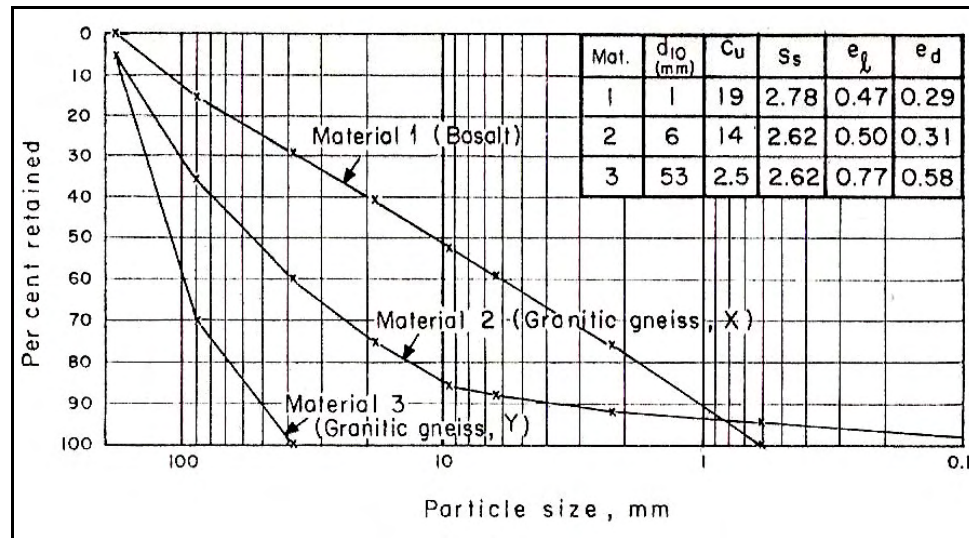


Figure 2.2 Grading curves of three rockfill materials (Marsal, 1967)

Marsal conducted the tests on drained conditions. The specimens were fully saturated before testing. The tests were conducted in three different confining stress values of 5, 10 and 25 kg/cm². In Figure 2.3, the relationships between principal stress ratio at failure and confining pressure are shown together with other rockfill materials used in Marsal's study. It is seen from this figure that, saturation has a significant effect on the shear strength of rockfill materials. Another important point is that, as the confining pressure increases, shear strength of rockfill decreases considerably where relatively high principal stress ratios are achieved when the specimens are tested under low confining pressures.

In Figure 2.4, the final gradations of the materials tested at the confining pressure of 25 kg/cm² is shown. He observed that, Material 1 shows fragmentation in the order of 12% while this value is about 10% to 24% in Material 2 and 23% to 53% in Material 3.

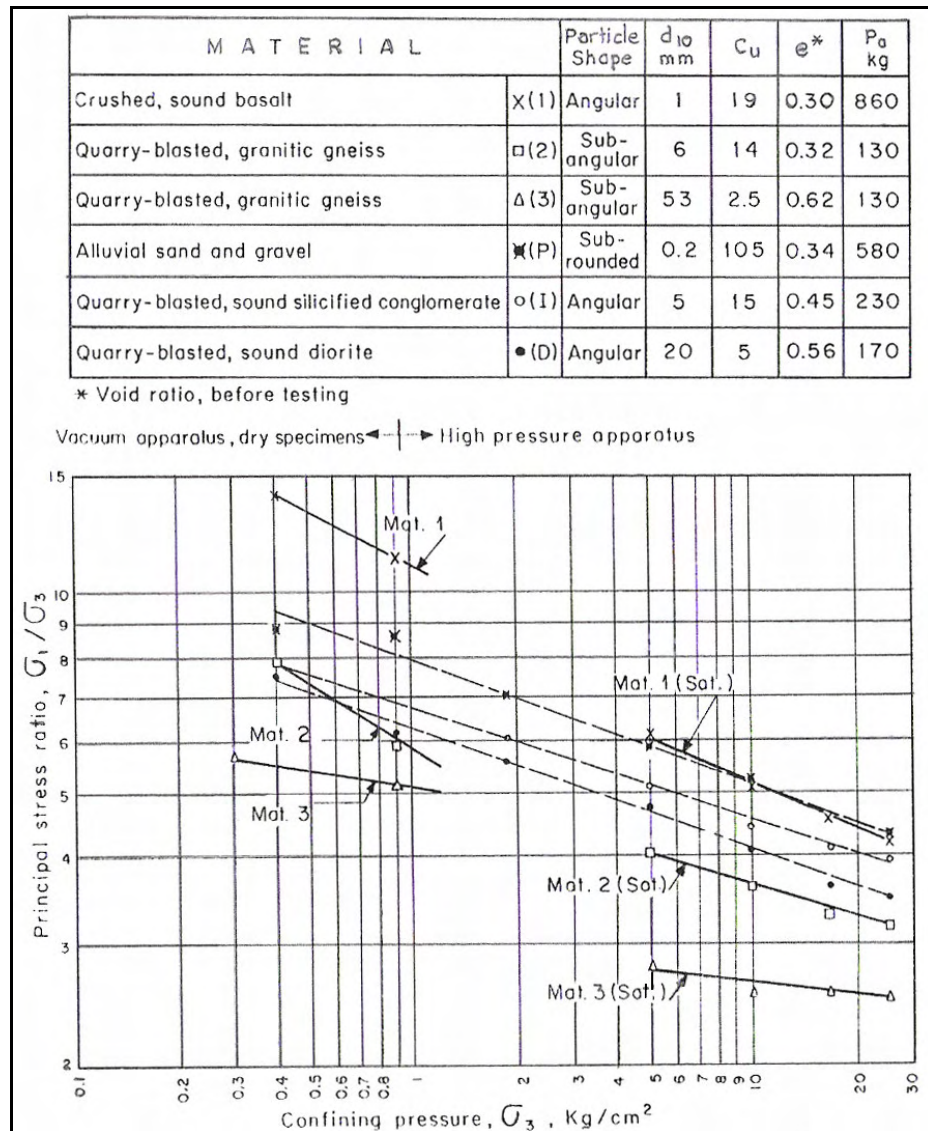


Figure 2.3 Principal stress ratio vs. confining stress relationship (Marsal, 1967)

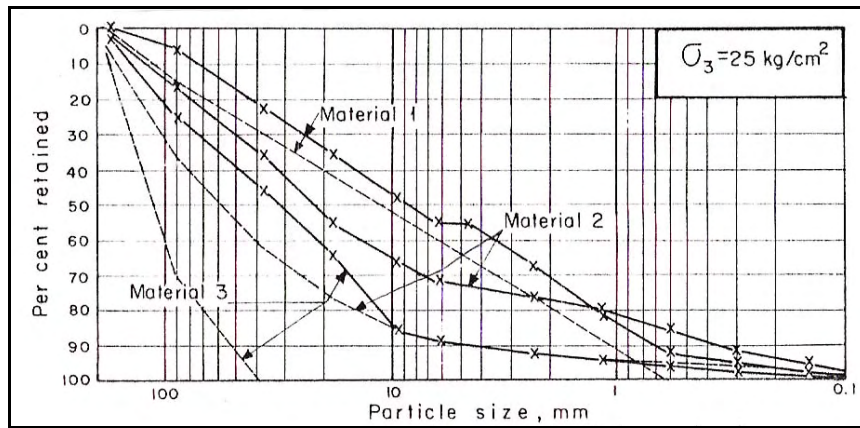


Figure 2.4 Grading of rockfill specimens after testing (Marsal, 1967)

After the tests, Marsal concluded that one of the most important factors that affect both the shear strength and the compressibility of the rockfill is the breakage of the particles or the fragmentation. In Figure 2.5, the relationship between the principal stress ratio at failure and particle breakage is shown. In this figure, B represents the breakage factor (in %) and according to Marsal, it can be determined by the following simple definition:

Before testing, the sample is sieved using a set of standard sieves and the percentage of particles retained in each sieve is calculated. After testing, the sample is again sieved and the percentage of particles retained in each sieve is calculated. Due to the breakage of particles, the percentage of particles retained in larger sieves will decrease and the percentage of particles retained in small size sieves will increase. The sum of decreases in percentage retained will be equal to the sum of increases in the percentage retained. The sum of decreases or increases is the value of the breakage factor B (Marsal, 1967).

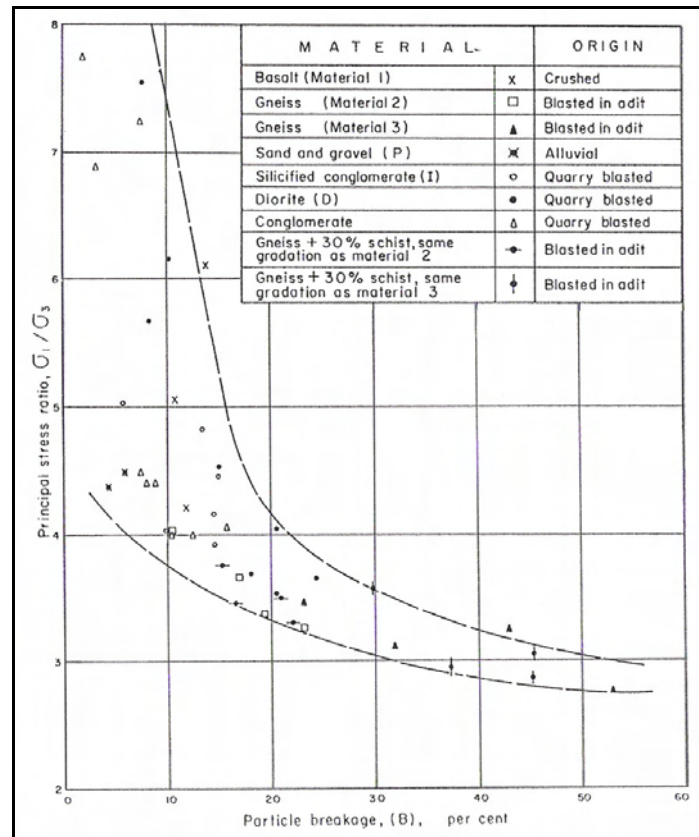


Figure 2.5 Breakage factor vs principal stress ratio relationship (Marsal, 1967)

From the compressibility point of view, Marsal concluded that compressibility is a complex phenomenon which is a result of displacements between particles combined with particle breakage and the deformation of the contact surfaces where the latter has a minor importance. From the shear strength point of view, he reached the following considerations:

The shear strength is larger in well graded materials with a low void ratio, and is independent from the origin of the rock. Materials with similar gradations present an appreciable variation in shear strength, probably due to intrinsic characteristics of the particles. The strength of materials decreases as particle breakage increases (Marsal, 1967).

In 1970, Leps collected the published data for individual large scale tests on gravels and rockfill up to that time and showed them in a single chart as shown in

Figure 2.6. The data consists of 15 different materials where Leps grouped them in three categories according to their gradation and compressive strength. Weak rock particles has strength of 500 psi to 2500 psi, average rock particles has strength of 2500 psi to 10000 psi and strong rock particles have strength of 10000 psi to 30000 psi. (1Mpa = 145 psi.)

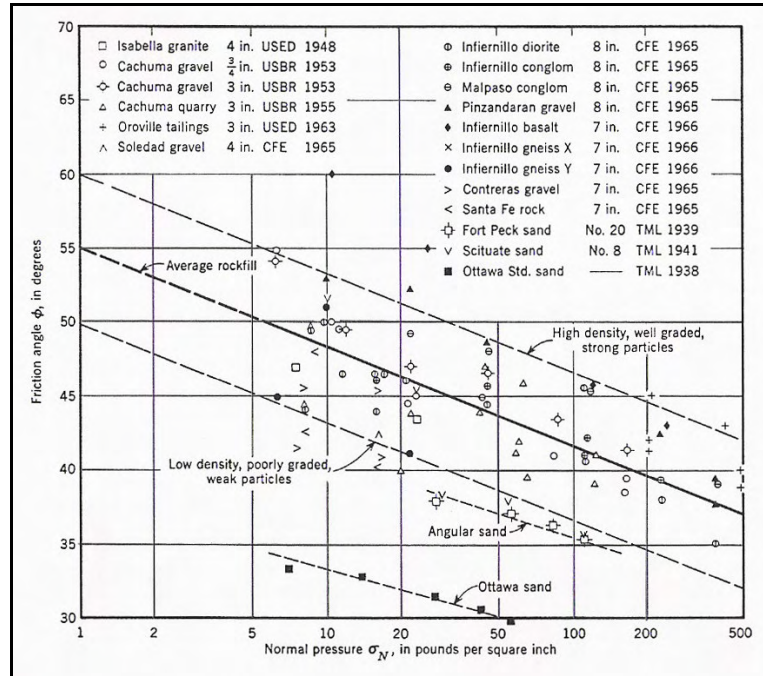


Figure 2.6 Effect of confining pressure on the peak friction angle of rockfill specimens (Leps, 1970)

According to Leps, Figure 2.6 gives a good overall perspective in understanding of the relation of friction angle to normal pressure in rockfill however it has some shortcomings, such as: (1) It only roughly indicates the effects of relative density. (2) It only roughly indicates the effects of gradation of the rockfill. (3) The effects of crushing strength of the dominant sized rock particles is only vaguely suggested. (4) It gives no clue as to the influence of particle shape of the dominant rock particles. (5) It gives no evaluation of the influence of degree of saturation of

the rock particles (Leps, 1970). Leps achieved the following conclusions at the end of his study:

- At a given normal pressure, friction angle increases with the increased relative density. This increase is more appreciable in the low pressure levels than in the higher pressure levels. Also at any given normal pressure, the improvement of the gradation of the rockfill increases the friction angle if it is not done with the help of fines.
- When all other factors kept constant, more angular particles give higher friction angles than the rounded particles. This increase may be as much as 10° - 15° at low normal pressure conditions. When the rockfill particles are saturated, their strength reduces a considerable degree. This decrease is much higher in relatively weaker particles.
- The friction angle decreases significantly if the confining pressure increases. In the average line which consists of about 100 test data, the friction angle decreases from 55° at 1 psi to 48° at 10 psi but decreases less than 2° for a further 9 psi increase. From this statement, it is clearly seen that the low pressure range of Figure 2.10 (1 psi to 10 psi) should be curved not straight (Leps,1970).

One of the valuable studies about shear strength of rockfill materials is presented in 1972 by Marachi et al. They conducted three series of isotropically consolidated, drained triaxial compression tests on typical rockfill materials. The tests were performed on 36 in., 12 in. and 2.8 in. diameter specimens with four different confining pressures of 30, 140, 420 and 650 psi. Three different materials are used in their study; (1) Pyramid dam material, (2) crushed basalt rock and (3) Oroville dam shell material.

First of the materials, Pyramid dam material, was produced by quarry blasting. The individual particles were very angular, comparatively weak and anisotropic in their strength properties. The source rock was a fine grained sedimentary rock. The second material, crushed basalt rock, had been quarry blasted and then crushed into smaller sizes in a crushing plant. The source rock was a fine grained olivine basalt having very random jointing and can be considered quite isotropic. Individual rock particles were angular and quite sound.

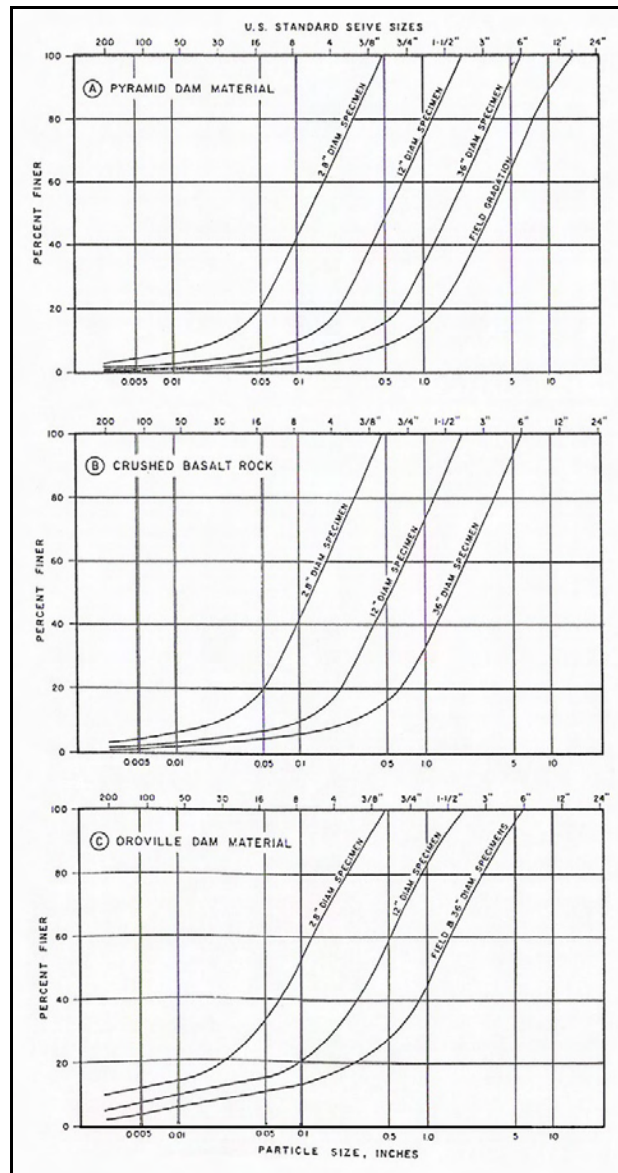


Figure 2.7 Grading curves of three rockfill materials (Marachi et al., 1972)

The last material, Oroville dam material was taken from the shell material of Oroville dam. The gravel sized particles of this material were well rounded to rounded however the particle shape was not the same throughout the range of grain sizes. It was almost impossible to break the medium gravel sized particles with a hammer. Jointing in the rock was very random and the rock was isotropic. In

Figure 2.7, the grain size distribution of the materials and the test specimens are shown. Marachi et al. set the max. particle diameter in each of the specimens to 1/6 of the diameter of the specimen.

In Figure 2.8, the isotropic consolidation behaviour of the materials is shown. Marachi et al, found the results as inconclusive, since they do not indicate that rockfill materials is affected materially by modeling the grain size distribution.

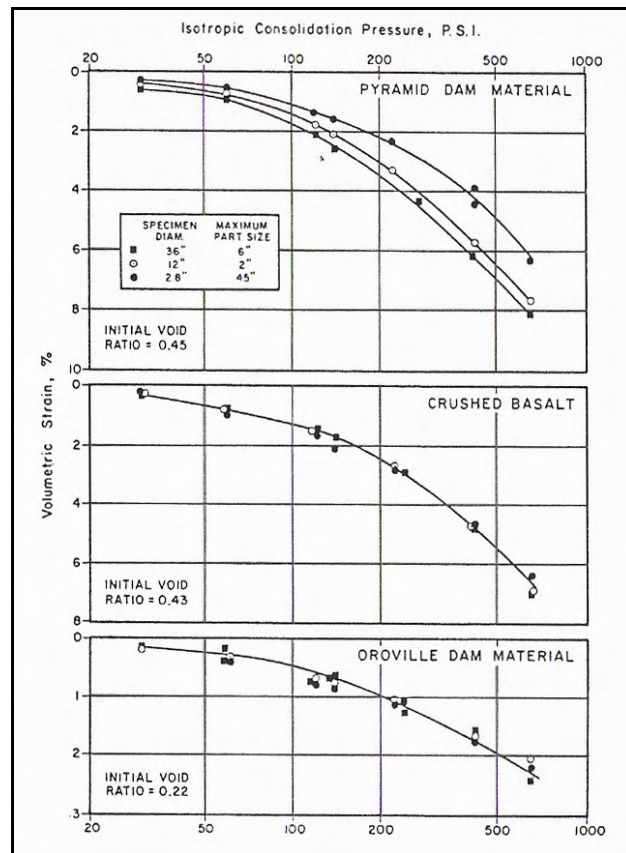
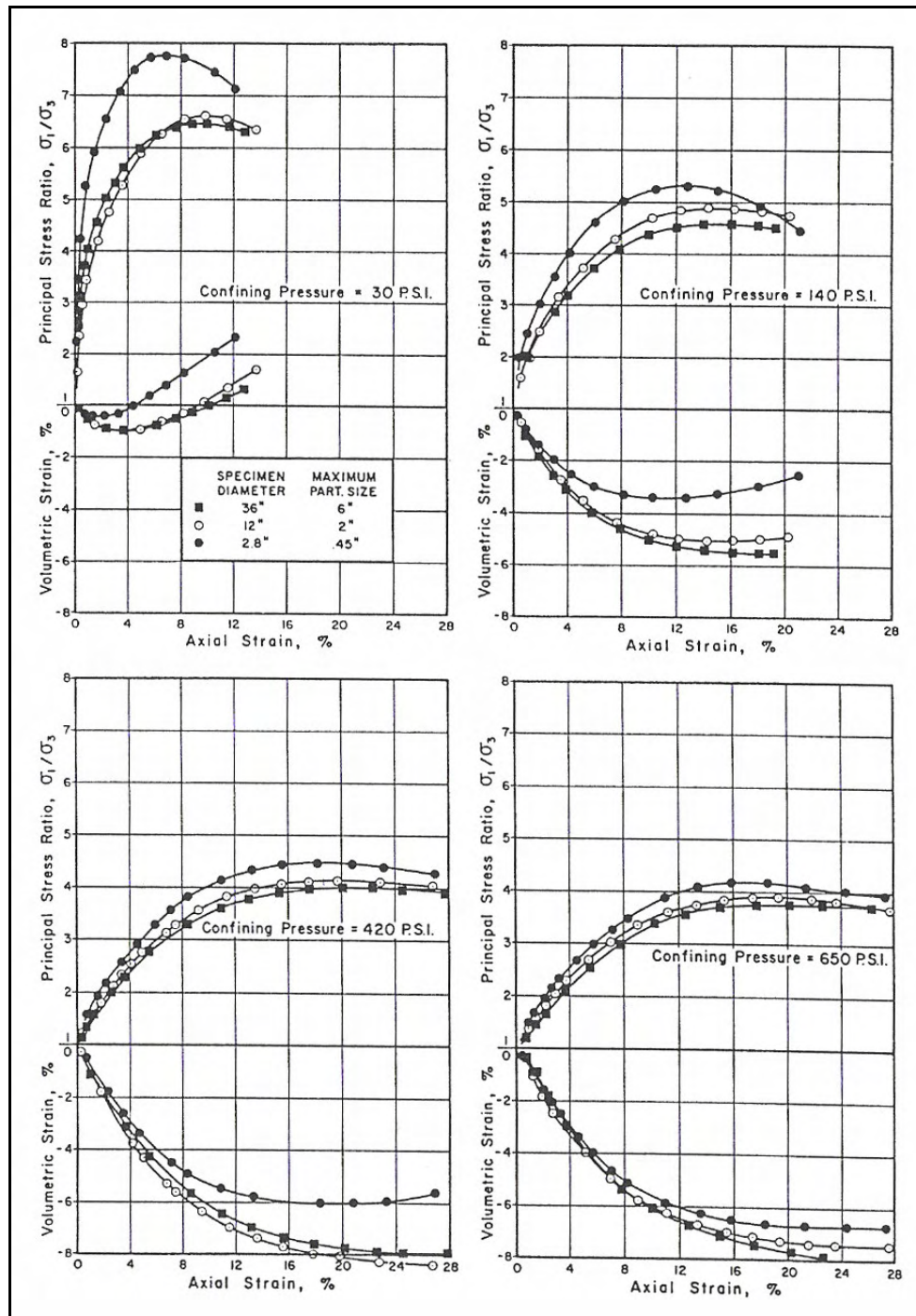


Figure 2.8 Isotropic compression of rockfill materials (Marachi et al., 1972)

In Figures 2.9, 2.10 and 2.11 the tests results of 40 saturated and isotropically consolidated, drained triaxial compression tests obtained from the modeled rockfill materials are shown. These curves indicate that, the principal stress ratio are greatest for small specimens and least for the large specimens.



**Figure 2.9 Drained triaxial test results of modeled Pyramid dam material
(Marachi et al., 1972)**

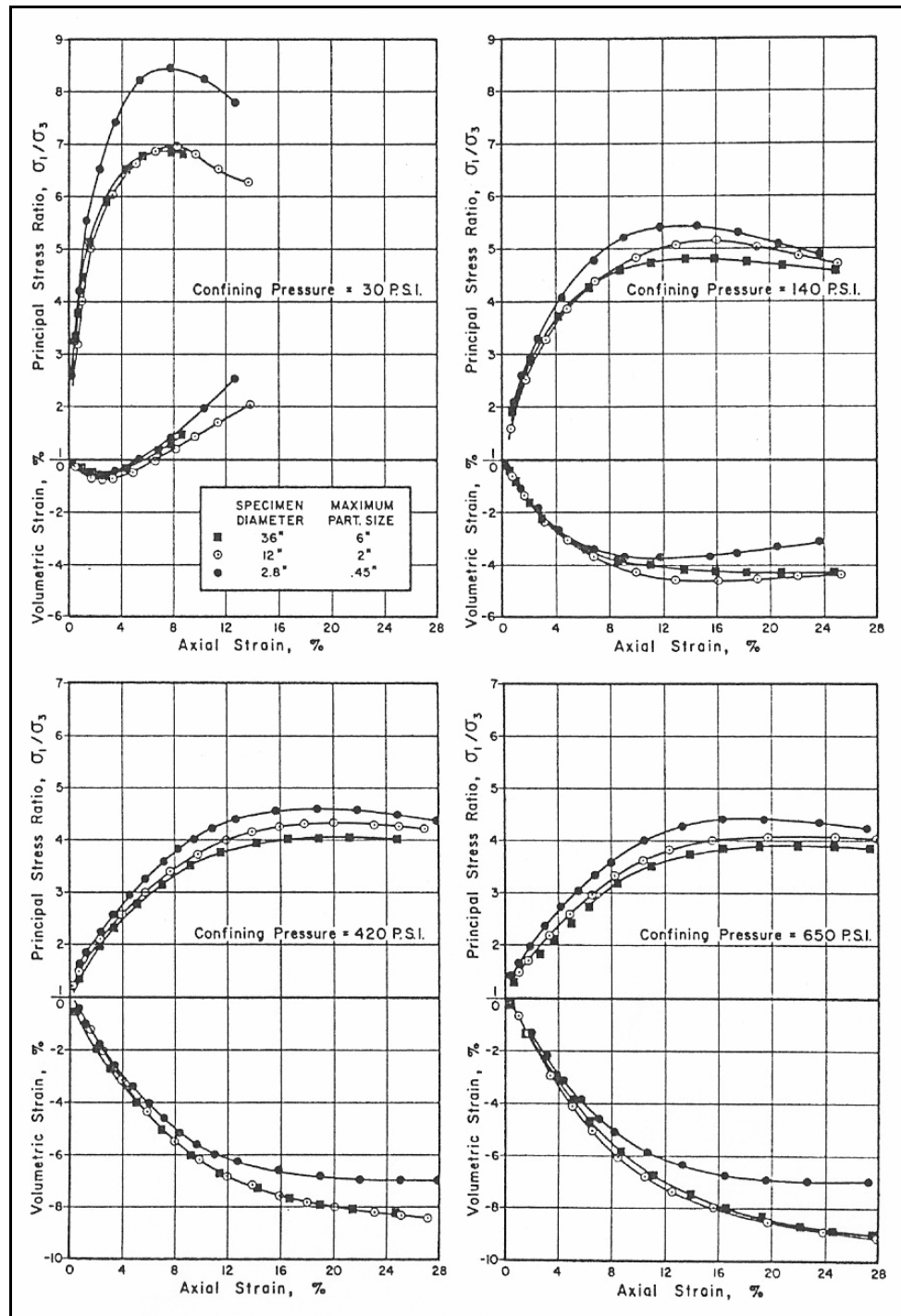


Figure 2.10 Drained triaxial test results of modeled crushed basalt material (Marachi et al., 1972)

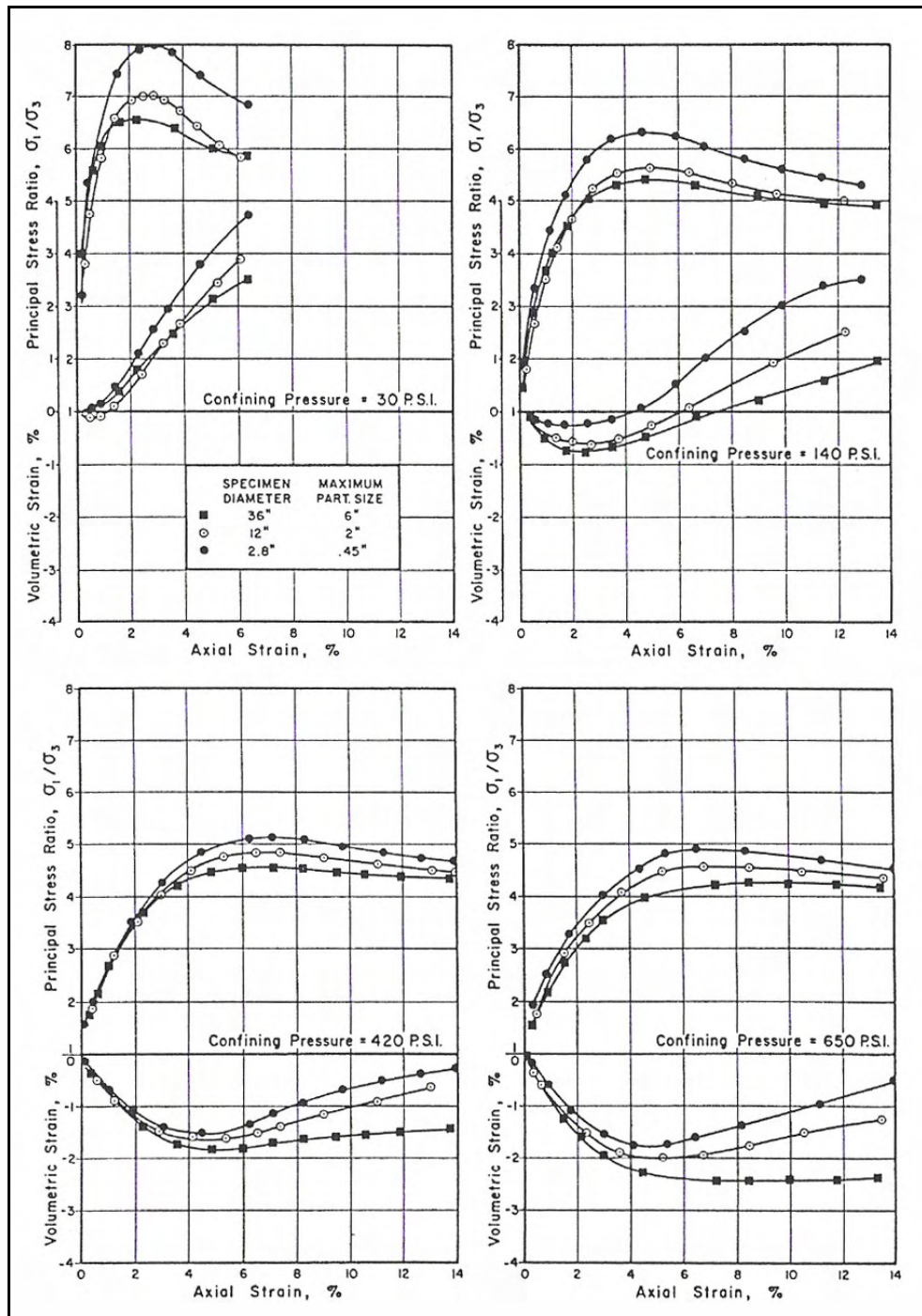


Figure 2.11 Drained triaxial test results of modeled Oroville dam shell material
(Marachi et al., 1972)

The compressibility behaviour of three materials are shown in Figures 2.12 and 2.13. The volumetric strains and the axial strains are increasing with confining pressure. The increase is more distinguishable in the low confining pressure range than the higher pressures which diminishes about 420 psi.

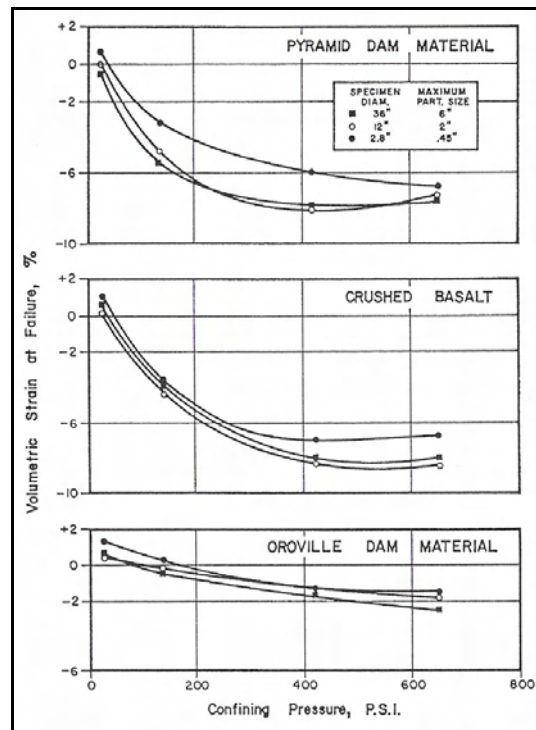


Figure 2.12 Failure volumetric strain – confining pressure relationship of modeled three rockfill materials (Marachi et al., 1972)

Marachi et al. depicted the relationship between internal friction angles, the confining pressures and max particle sizes as shown in Figures 2.14 and 2.15. It is clear in Figure 2.14 that the friction angle decreases with a decreasing rate as the confining pressure increases but not beyond pressures of 650 psi. It can also be seen that, the friction angle is least for large specimens and greatest for small specimens. Figure 2.15 indicates that the friction angle decreases as the max. particle size increases. For the materials having a max. particle size of 6 in., the internal friction

angles were in general 3° to 4° less than those of the materials having a max. particle size of 0.5 in. For the max particle sizes which do not exist in Figure 2.15, the curves can be extrapolated to the max. particle size in the field where the materials are too large for testing (Marachi et al., 1972).

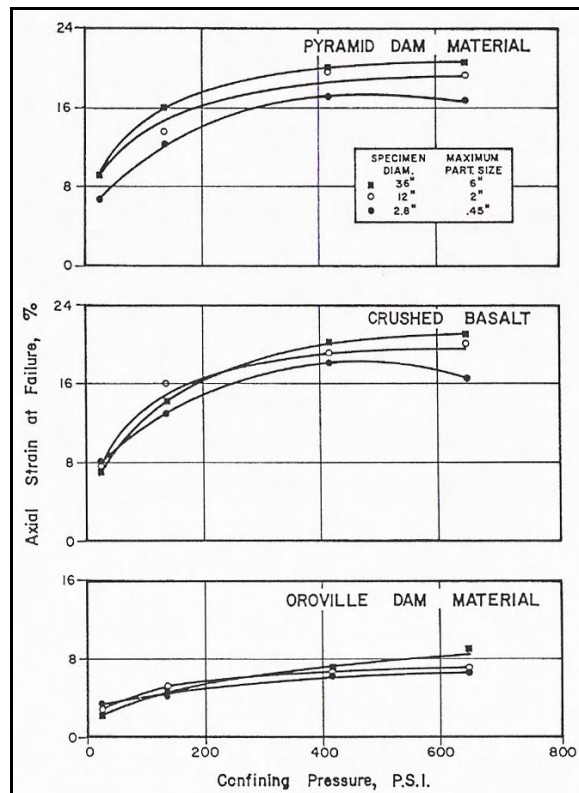


Figure 2.13 Failure axial strain – confining pressure relationship of modeled three rockfill materials (Marachi et al., 1972)

Marachi et al., summarized the results of their study with the one of Marsal's in Figure 2.16 for comparison. It may be seen that the angles of internal friction (except for granitic gneiss and El Granero shale) are within a relatively narrow range of a few degrees (Marachi et. al, 1972). The friction angles are given in the table of Figure 2.16, together with the axial strains (ϵ_1) at failure, volumetric strains (ϵ_v) at failure and the estimated critical confining pressures (σ_3^f).

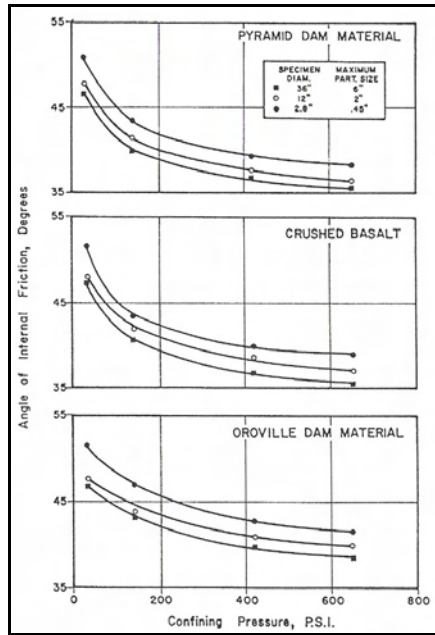


Figure 2.14 Peak friction angle – confining pressure relationship of modeled three rockfill materials (Marachi et al., 1972)

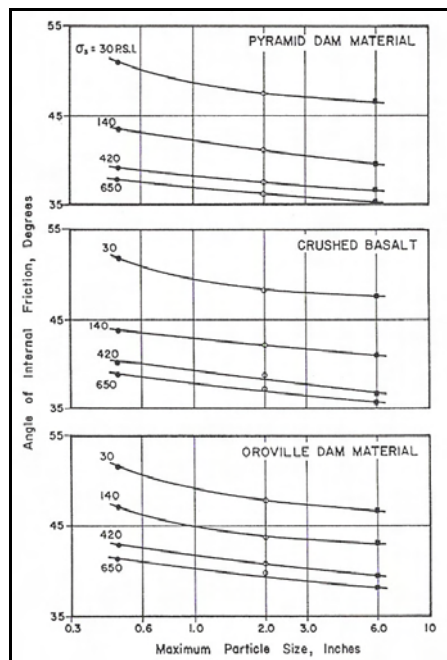
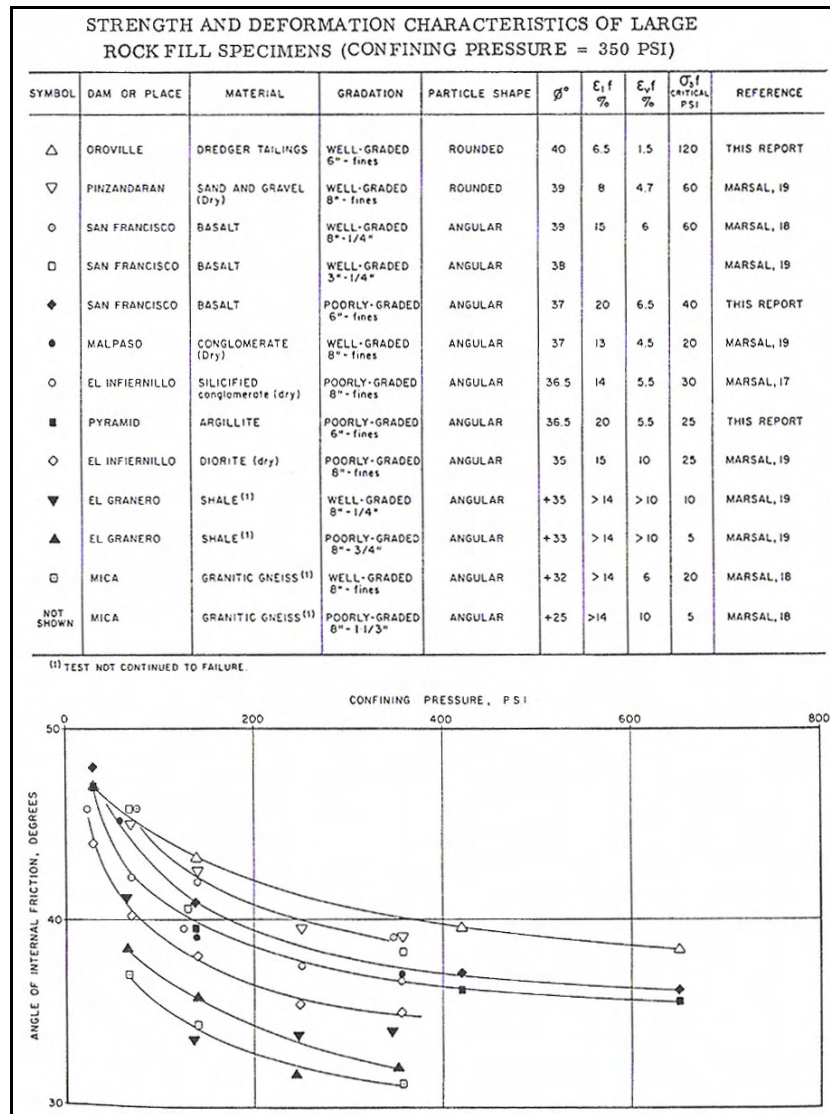


Figure 2.15 Peak friction angle – max. particle size relationship of modeled three rockfill materials (Marachi et al., 1972)



**Figure 2.16 Effect of confining pressure on friction angle of rockfill materials
(Marachi et al., 1972)**

In 1981, Barton et al. developed a relationship for determination of the peak drained friction angle of rockfill materials. They suggested the following equation.

$$\phi' = R \cdot \log \left(\frac{S}{\sigma_n} \right) + \phi_b \quad (2.1)$$

Here, R represents equivalent roughness, S represents equivalent strength of particles, σ_n' represents the effective total stress with ϕ' and ϕ_b representing the peak drained friction angle and basic friction angle of the rockfill, respectively. According to Barton et al., ϕ_b can be taken conventionally between 25° - 35° and equivalent strength (S) and equivalent roughness (R) of rockfill materials can be determined from Figures 2.17 and 2.18, respectively using d_{50} particle size, uniaxial compression strength (σ_c) and the porosity (n) of rockfill materials.

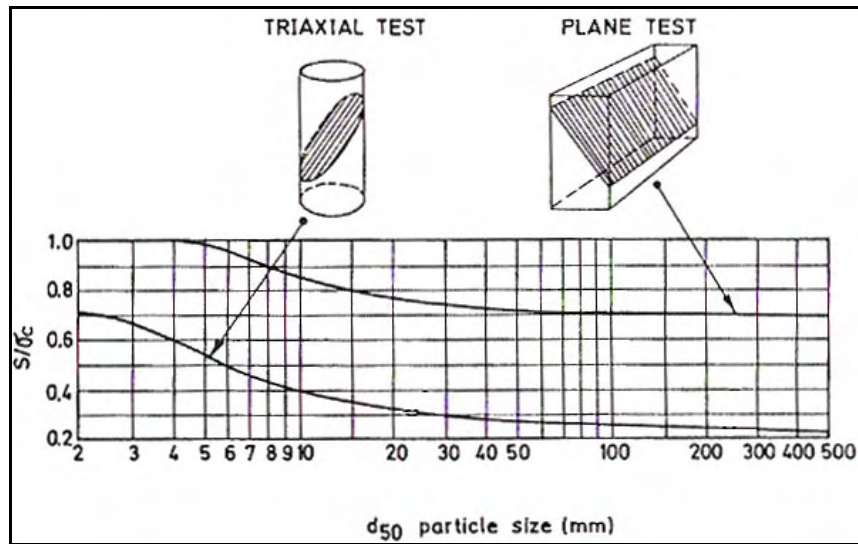


Figure 2.17 Equivalent strength of rockfill particles (Barton et al., 1981)

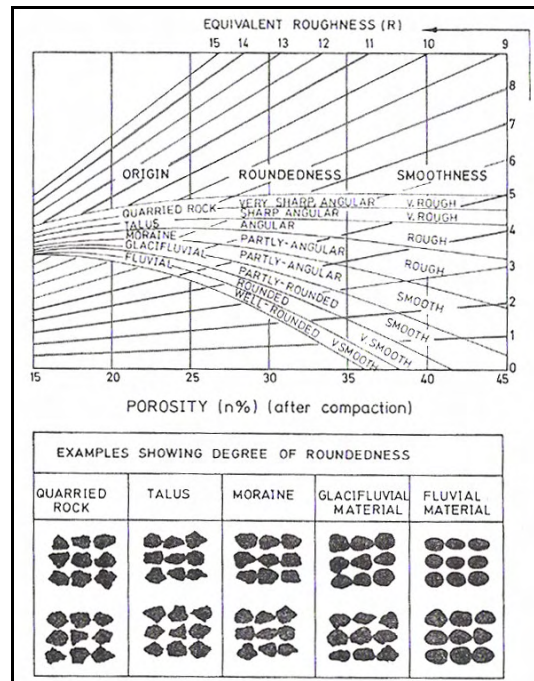


Figure 2.18 Equivalent roughness of rockfill particles (Barton et al., 1981)

Barton et al., compared the results obtained by using Eq. 2.1 with the measured values of Marachi et al.'s study as shown in Figure 2.19. Here, for Pyramid dam material, σ_c was taken as 15805 psi whereas it was taken as 28565 psi for Oroville dam material. The agreement was quite satisfactory. The effects of equivalent roughness (R) and equivalent strength (S) on rockfill friction angles are depicted in Figure 2.20 where ϕ_b was taken as 27.5° . Barton et al. concluded that, Leps (1970) was correct in drawing straight line envelopes (ϕ' inversely proportional to $\log \sigma'_n$), but he may have been incorrect in drawing parallel upper and lower boundaries (Barton et al., 1981).

In order to show the stress dependency of the friction angle, Barton et al. arranged the data in Figure 2.21 where it is clearly seen from the figure that, very high friction angles are obtained in the rockfill dam close to the toe. Barton et al. indicated that the stress dependency is a very positive factor in the critical toe region of a rockfill dam and according to them, high ϕ' values in this region help to explain the high resistance to raveling during extreme leakage.

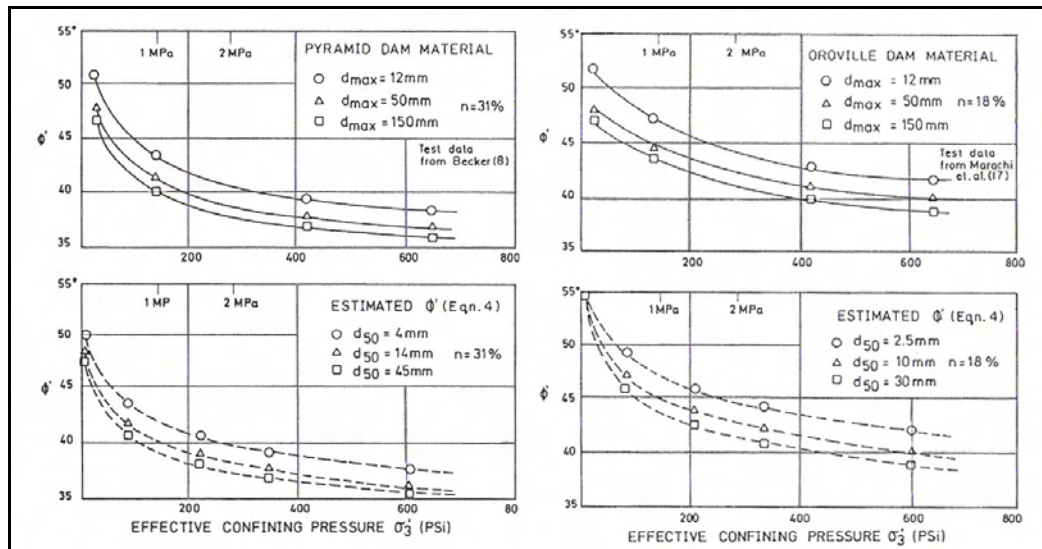


Figure 2.19 Comparison of estimated and measured friction angle relationships using Eq. 2.1 (Barton et al., 1981)

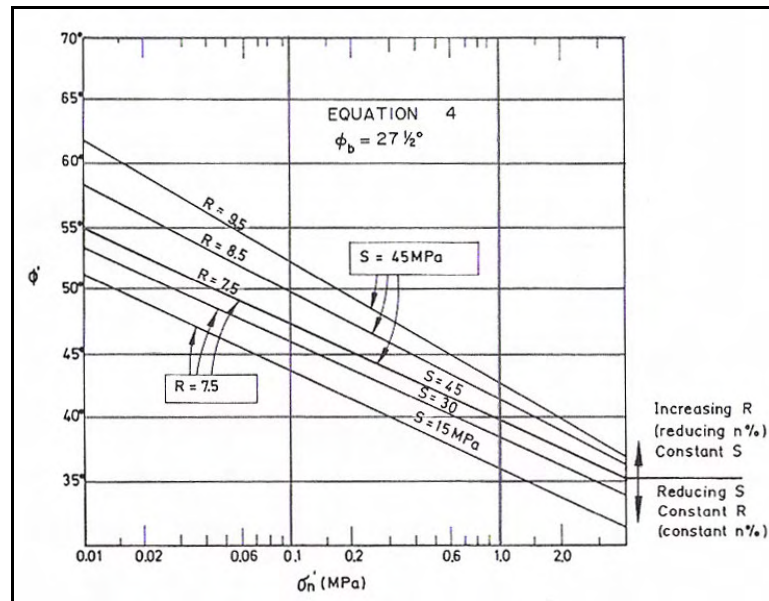
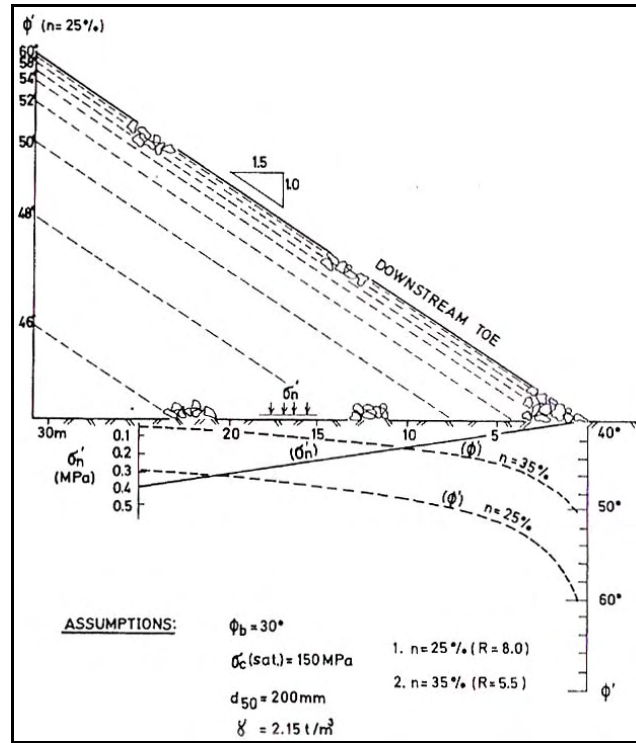


Figure 2.20 Effect of equivalent roughness and equivalent strength on rockfill friction angle (Barton et al., 1981)



**Figure 2.21 Effect of confining pressure on rockfill friction angle
(Barton et al., 1981)**

The last study outlined in this section is the one published by Varadarajan et al. in 2003. They arranged triaxial tests results on two rockfill materials, which were carried out by Gupta for his PhD dissertation where the rockfill materials are selected from different dam sites in India.

First rockfill material is taken from Ranjit Sagar dam site which is located at the north of India and the second rockfill material is taken from Purulia dam site which is located at the eastern part of India. It was indicated that, first rockfill material contains rounded to sub-rounded particles up to 320 mm max particle size and have a sedimentary origin however second rockfill material contains angular to sub-angular particles up to 1200 mm max particle size which are obtained by blasting from a metamorphic rock. When the materials were tested in impact, crushing and LA abrasion tests it is seen that, the Ranjit Sagar rockfill particles were stronger than the other rockfill material.

In Figure 2.22, gradation curves of the prototype and modeled rockfill materials are shown which were obtained by using Lowe's parallel gradation technique (Varadarajan et al., 2003).

In triaxial tests, 381 mm diameter 813 mm long and 500 mm diameter 600 mm long specimens are used. Tests are carried out in drained conditions with the specimens having 25, 50 and 80 mm max particle sizes. 350, 700, 1100 and 1400 kPa confining stresses are used for the Ranjit Sagar rockfill material while 300, 600, 900, 1200 kPa confining stresses are used for the Purulia rockfill material. The results of the triaxial tests are shown in Figure 2.23.

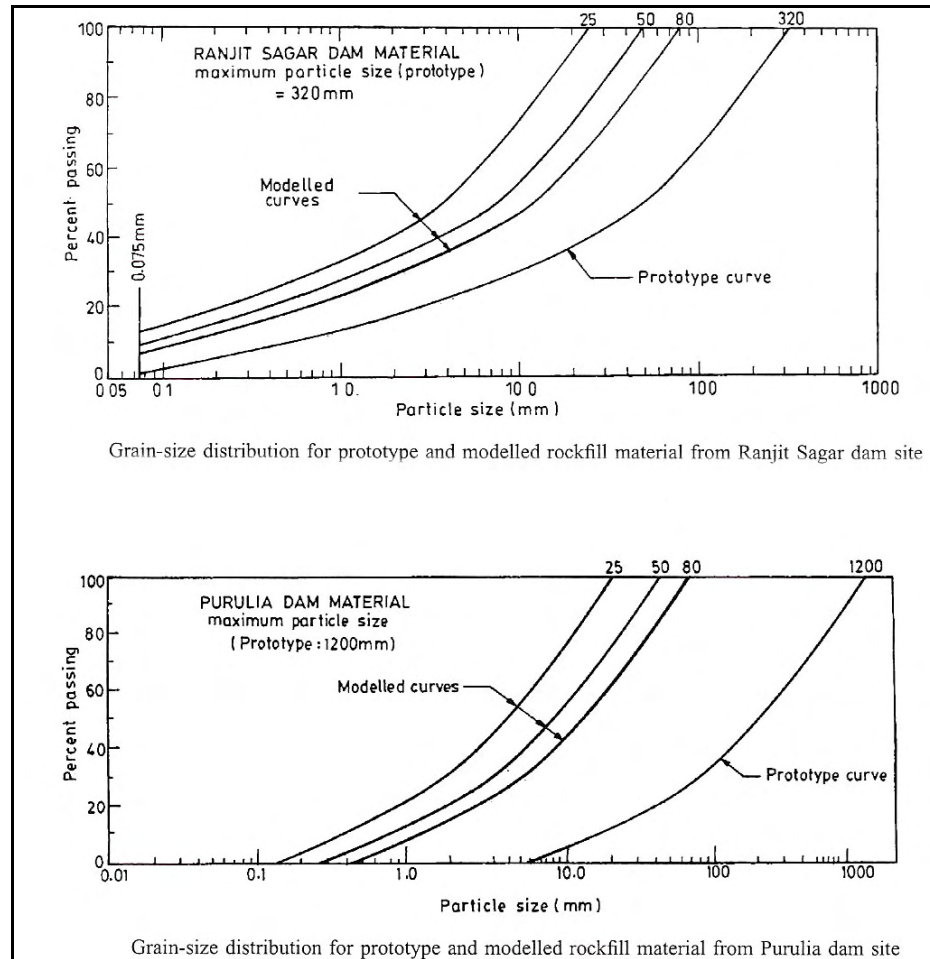


Figure 2.22 Grading curves of two rockfill materials (Varadarajan et al., 2003)

When Figure 2.23 is examined, it is seen that, the axial strains in the Ranjit Sagar rockfill material are higher than the Purulia rockfill material and when the volumetric strains are considered, the behaviour of two materials differ from each other clearly. Varadarajan et al. concluded that, Ranjit Sagar rockfill material undergoes volume compression due to compression of particles and rearrangement of particles due to the sliding of the rounded particles. The breakage of the particles is also a factor and this material shows a continuous volume compression throughout the test. On the other hand, Purulia rockfill material volume compression is due to the compression of particles and particle breakage. The angular particles show a high degree of interlocking and this causes dilatation.

In Figure 2.24, the variation of breakage factor of the rockfill materials with confining pressures is shown. As it is seen, breakage factor increases with size of the particles and confining pressure. Here, Purulia rockfill material shows relatively high particle breakage when compared with Ranjit Sagar dam material. This difference is due to the relatively low strength of particles. The results are given in Figure 2.25 together with other studies in the literature.

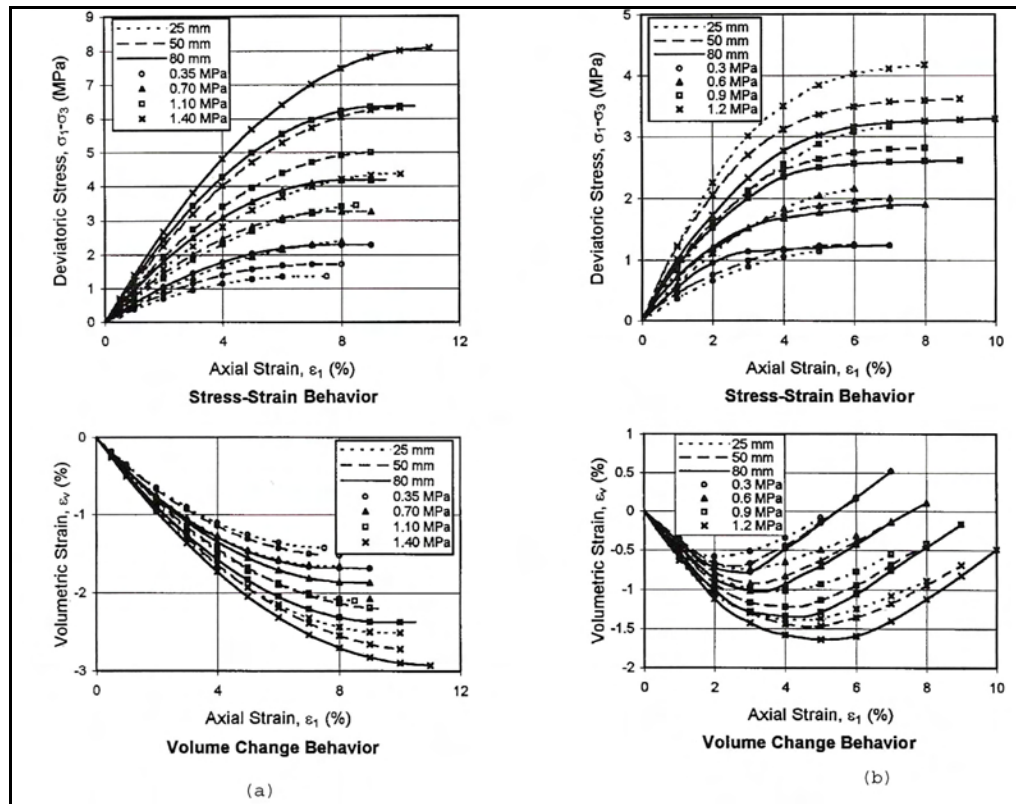


Figure 2.23 Triaxial test results of two rockfill materials ; a) Ranjit Sagar dam material, b) Purulia dam material (Varadarajan et al., 2003)

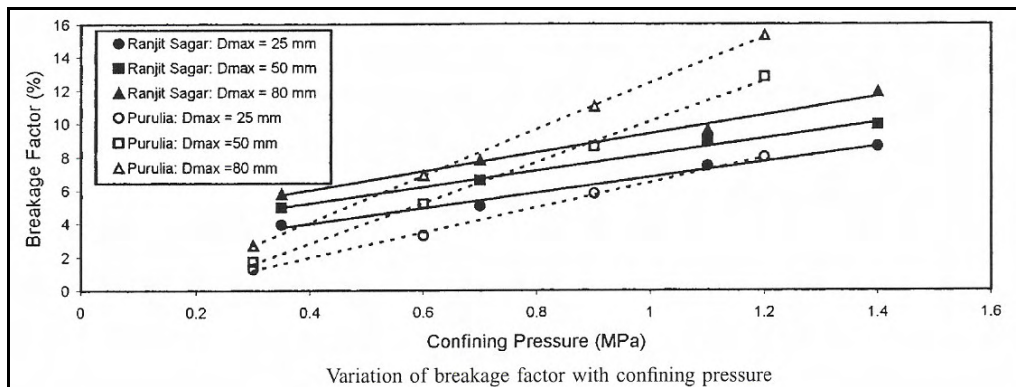


Figure 2.24 Confining pressure-breakage factor relationship of two rockfill materials (Varadarajan et al., 2003)

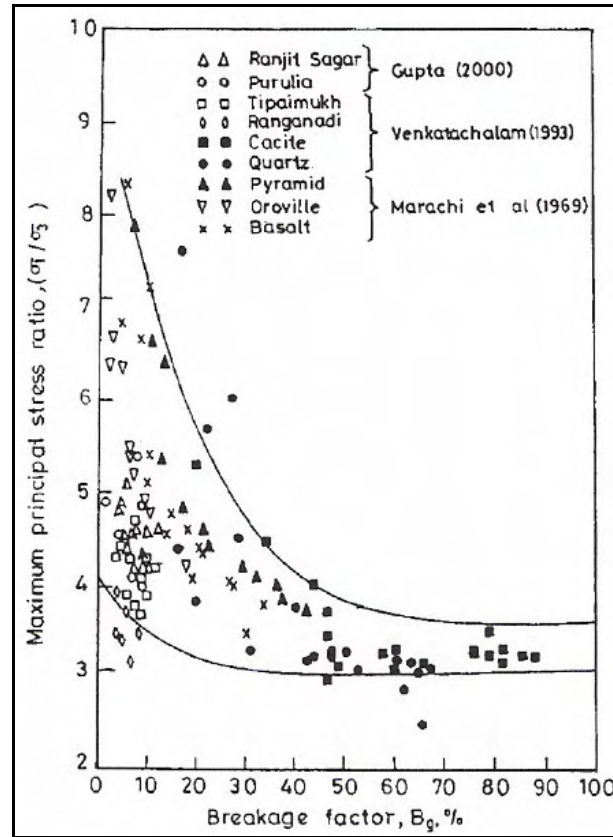


Figure 2.25 Breakage factors of rockfill particles (Varadarajan et al., 2003)

In Table 2.1, the friction angles of the materials are listed where the behaviour is completely different. As max particle size increases, the internal friction angle increases for the Ranjit Sagar dam material however an opposite trend is seen for the Purulia Dam material. Varadarajan et al. concluded that, as the particle size increases, greater interlocking is achieved for the same stress level and friction angle increases. On the other hand, as the particle size increases, the breakage effect increase and the friction angle decreases. As a result, the net effect is positive for Ranjit Sagar material and the friction angle increases with increased particle size however it is negative for Purulia material and friction angle decreases with increased particle size.

Table 2.1 Internal friction angles from triaxial tests (Varadarajan et al., 2003)

	Ranjit Sagar Dam Material				Purulia Dam Material			
D_{\max} (mm)	25	50	80	320	25	50	80	1200
ϕ (deg.)	31.5	33.2	35.4	40.31	32.5	31.4	30.6	26.62

2.3.2 Summary of the Studies

The following statements can be concluded about the shear strength of rockfill material:

Particle size: According to Singh et al. (1995), this concept has not achieved a solution; but if the max particle size is reduced by removing all the material above a certain size, while the remaining fraction remains unchanged, friction angle increases. However if materials obtained from the parallel gradation technique are used in the tests, the friction angle increases with the increasing max particle size (Singh et al., 1995).

Confining pressure: As the confining pressure increases, the friction angle of the rockfill material decreases with a decreasing rate. This result is obtained from all of the studies related with the rockfill behaviour.

Particle breakage: Particle breakage is one of the important factors that affect the shear strength of rockfill material. As the confining pressure increases, particle breakage increases but about a confining pressure of 70 kg/cm² the breakage effect comes to a static value and beyond this value it does not increase. The breakage effect also increases with the max. particle size. (Singh et al., 1995)

Gradation: The well graded materials show higher strength than uniformly graded materials.

2.4 Constitutive Laws

A constitutive law or a material model is a set of mathematical equations that describes the relationships between stress and strain. The constitutive laws used to model the behaviour of the rockfill materials are mostly based on linear elastic and non-linear elastic analysis. As shown in the previous sections; the behaviour of rockfill is inelastic, non-linear and highly stress dependent, thus application of a non-linear model is more realistic in the analysis of rockfill dams.

In the following sections, non-linear material models is briefly outlined with the constitutive laws used in the finite element analysis of dams such as Duncan and Chang's hyperbolic model and hardening soil model which is the selected model to represent the rockfill behaviour in this study. Linear elasticity theory is also summarized.

2.4.1 Linear Elasticity

Linear elasticity is the basic and thus the simplest model used in the soil engineering. In this model, generalized Hooke's laws are used in the constitutive equations. The behaviour is modeled using only two parameters; (1) elastic modulus (E), (2) Poisson's ratio, (ν) where stress-strain equations, in x-direction are:

$$\varepsilon_x = \sigma_x / E \quad (2.2a)$$

$$\varepsilon_y = -\nu \cdot \sigma_x / E \quad (2.2b)$$

$$\varepsilon_z = -\nu \cdot \sigma_x / E \quad (2.2c)$$

$$\gamma_{yz} = G \cdot \tau_{yz} \quad (2.3)$$

In the above equations, σ_x represents the normal stress in x direction, ε_x , ε_y and ε_z represents the strains in x, y and z directions respectively, γ_{yz} and τ_{xy} represents the

shear strain and stress in y-z plane respectively and G represents the shear modulus which can be evaluated as:

$$G = \frac{E}{2(1 + \nu)} \quad (2.4)$$

Similar equations can be written in y and z directions. In the above equations, it is seen that the stress strain relationship is taken as linear which means the elastic modulus is constant at all stress levels. However, as mentioned before, the rockfill behaviour (as well as the soil behaviour) is highly non-linear; so linear elasticity is not a realistic approach in prediction of a rockfill dam behaviour.

2.4.2 Non-Linear Material Models

2.4.2.1 Duncan and Chang's Hyperbolic Model

In 1963, Kondner have shown that the nonlinear stress strain curves of both clay and sand may be approximated by a hyperbola with a high degree of accuracy. The equation of hyperbola is given below.

$$(\sigma_1 - \sigma_3) = \frac{\varepsilon}{a + b \cdot \varepsilon} \quad (2.5)$$

Here σ_1 and σ_3 are the major and minor principal stresses, ε is the axial strain, a and b are the coefficients which can be determined using traditional triaxial tests as shown in Figure 2.26a. However it is much simple to use the transformed axes as in Figure 2.26b.

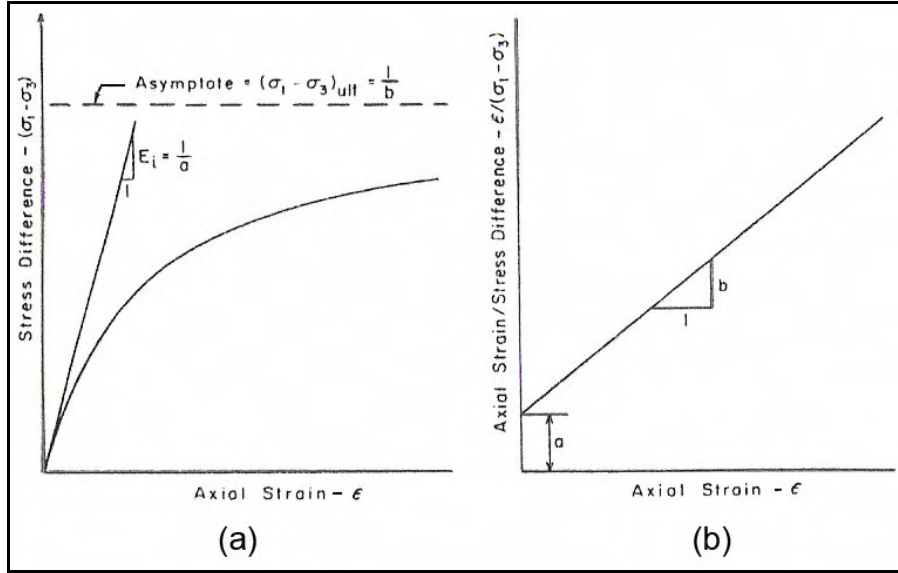


Figure 2.26 Hyperbolic stress-strain curve (Duncan and Chang, 1970)

As seen in Figure 2.26a, the asymptotic value of the deviator stress remains just above the hyperbola which can be determined using the compressive strength of the soil, such as:

$$(\sigma_1 - \sigma_3)_f = R_f (\sigma_1 - \sigma_3)_{ult} \quad (2.6)$$

where $(\sigma_1 - \sigma_3)_f$ is the compressive strength, $(\sigma_1 - \sigma_3)_{ult}$ is the asymptotic value of deviatoric stress and R_f is the failure ratio. Kondner found that R_f is independent of the confining pressure and it has a range between 0.75 and 1.00 for a number of soils (Duncan and Chang, 1970). By using initial tangent modulus and the compressive strength, the general equation can be written in the following form:

$$(\sigma_1 - \sigma_3) = \frac{\epsilon}{\frac{1}{E_i} + \frac{\epsilon \cdot R_f}{(\sigma_1 - \sigma_3)_f}} \quad (2.7)$$

The relationship developed by Kondner is an effective way of representing the non-linear behaviour of soils and it forms the fundamentals of Duncan and Chang's hyperbolic model.

In 1963, Janbu indicated that there is such a relationship between initial tangent modulus and the confining pressure as shown in Eq. 2.8.

$$E_i = K \cdot p_a \left(\frac{\sigma_3}{p_a} \right)^n \quad (2.8)$$

where E_i is the initial tangent modulus, σ_3 is the minor principle stress, p_a is the atmospheric pressure (expressed in the same units as E_i and σ_3), K is the modulus number and n is the exponent which determines the rate of the variation of E_i with σ_3 . K and n are dimensionless numbers and can be determined using the axis shown in Figure 2.27 (Duncan and Chang, 1970).

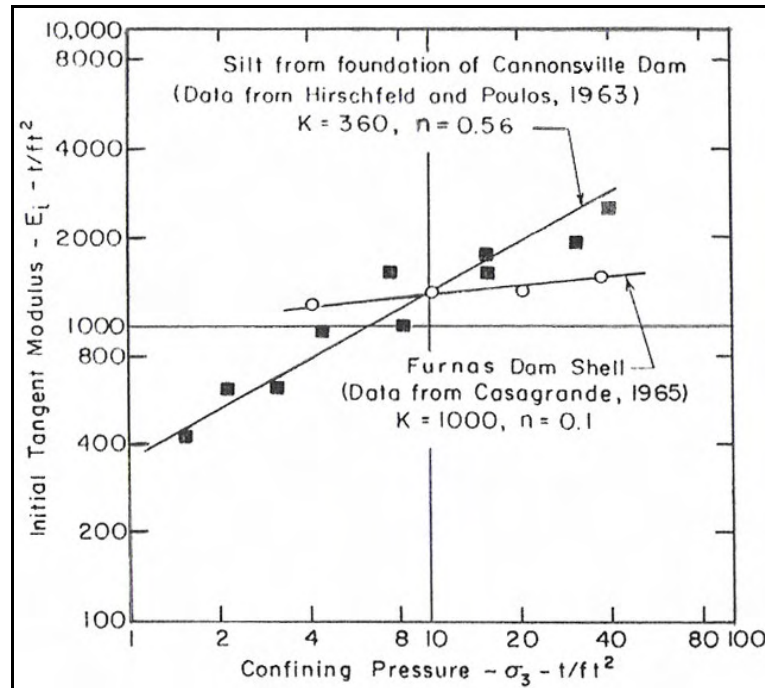


Figure 2.27 Determination of hyperbolic parameters (Duncan and Chang, 1970)

Duncan and Chang indicated that, if the minor principal stress kept constant, the tangent modulus can be determined using Eq. 2.9.

$$E_t = \frac{\partial(\sigma_1 - \sigma_3)}{\partial \varepsilon} \quad (2.9)$$

Here E_t represents the tangent elastic modulus. With combining Eq. 2.7 with Eq. 2.9, the following equation is achieved.

$$E_t = \frac{\frac{1}{E_i}}{\left(\frac{1}{E_i} + \frac{R_f \cdot \varepsilon}{(\sigma_1 - \sigma_3)_f} \right)^2} \quad (2.10)$$

Note that, Eq. 2.10 includes both the stress difference and the strain, which can have different reference states. In order to overcome this error, Duncan and Chang eliminated the strain in Eq. 2.10 by rewriting Eq. 2.7 in the following form.

$$\varepsilon = \frac{\sigma_1 - \sigma_3}{E_i \left(1 - \frac{R_f (\sigma_1 - \sigma_3)}{(\sigma_1 - \sigma_3)_f} \right)} \quad (2.11)$$

Duncan and Chang included the well known Mohr-Coulomb failure criterion in their hyperbolic model as:

$$(\sigma_1 - \sigma_3)_f = \frac{2c \cdot \cos \phi + 2\sigma_3 \sin \phi}{1 - \sin \phi} \quad (2.12)$$

where c is the cohesion and ϕ is the internal friction angle of the soil. Finally, combining Eq. 2.12 with 2.10 and 2.11, Eq. 2.13 is achieved.

$$E_t = \left[1 - \frac{R_f (1 - \sin \phi) (\sigma_1 - \sigma_3)}{2c \cdot \cos \phi + 2\sigma_3 \sin \phi} \right]^2 K \cdot p_a \left(\frac{\sigma_3}{p_a} \right)^n \quad (2.13)$$

Note that, the above equation can be used both in the effective stress analysis and in the total stress analysis. For the unloading-reloading condition, Duncan and Chang suggested that the following relationship can be used.

$$E_{ur} = K_{ur} \cdot p_a \left(\frac{\sigma_3}{p_a} \right)^n \quad (2.14)$$

where K_{ur} is the unloading-reloading modulus number. Note that, the modulus exponent n is the same both for the primary loading and for the unloading-reloading conditions.

In Duncan and Chang's hyperbolic model, there is no correlations made with the Poisson's ratio. This situation is updated in 1972 by Kulhawy et al. who developed a relationship to determine the tangent Poisson's ratio in a similar manner with the hyperbolic model. According to them, tangent Poisson's ratio can be evaluated using the following equation.

$$v_t = \frac{G - F \log \left(\frac{\sigma_3}{p_a} \right)}{\left(1 - \frac{d(\sigma_1 - \sigma_3)}{K \cdot p_a \left(\frac{\sigma_3}{p_a} \right)^n \left(1 - \frac{R_f (1 - \sin \phi) (\sigma_1 - \sigma_3)}{2c \cdot \cos \phi + 2\sigma_3 \sin \phi} \right)} \right)^2} \quad (2.15)$$

where, v_t is the tangent Poisson's ratio and G , F , d are the parameters whose values can be determined from the results of triaxial tests with volume change measurements (Kulhawy et al., 1972).

In 1980, Duncan et al. updated this subject again and suggested a bulk modulus parameter varying with the confining pressure and corresponds stress changes with volumetric strains such as:

$$B = K_b \cdot p_a \left(\frac{\sigma_3}{p_a} \right)^m \quad (2.16)$$

where B is the bulk modulus, K_b is the bulk modulus number and m is the bulk modulus exponent. They also indicated that, in the case of cohesionless soils, such as sands, gravels and rockfills it is difficult to select a single value of ϕ where it is usually found that the ϕ values decrease in proportion with the logarithm of the confining pressure. They suggested that, this variation may be represented by Eq. 2.17.

$$\phi = \phi_0 - \Delta\phi \cdot \log_{10} \left(\frac{\sigma_3}{p_a} \right) \quad (2.17)$$

In this equation ϕ_0 is the value of ϕ for σ_3 equal to p_a and $\Delta\phi$ is the reduction in ϕ for a ten-fold increase in σ_3 . Finally, Duncan et al. (1980) suggested the following statements about the hyperbolic model:

- a) Tangent values of Young's modulus (E_t) vary with confining pressure and the percentage of strength mobilized.
- b) Values of bulk modulus (B), vary with confining pressure and are independent of the percentage of strength mobilized.

2.4.2.2 Hardening Soil Model

As mentioned earlier, Hardening Soil Model is the selected model to represent the stress-strain behaviour of rockfill which is a modified version of Duncan-Chang model however it is an elasto-plastic model and uses theory of plasticity rather than theory of elasticity (Schanz et al., 1999).

This is such a complex model and the theory of this model will be outlined using the general conditions of a drained triaxial test. In the case of primary deviatoric loading, soil shows a decreasing stiffness and plastic strains develop. As described in the previous section, in a drained triaxial test, the stress-strain behaviour of the soil can be well approximated by a hyperbola which was first developed by Kondner et al. in 1963. In the hardening soil model, the following equation is used to represent the hyperbolic behaviour which is depicted in Figure 2.28.

$$\varepsilon_1 = \frac{1}{2E_{50}} \frac{q}{1 - q/q_a} , q < q_f \quad (2.18)$$

In Eq. 2.18, q is the deviatoric stress, q_a is the asymptotic value of the shear strength q_f is the ultimate deviatoric stress and E_{50} is the confining stress dependent stiffness modulus for primary loading corresponding to 50% of q_f which can be determined from Eq. 2.19 (see Figure 2.28).

$$E_{50} = E_{50}^{ref} \left(\frac{c \cdot \cot \phi - \sigma'_3}{c \cdot \cot \phi + p^{ref}} \right)^m \quad (2.19)$$

where E_{50}^{ref} is a reference stiffness modulus corresponding to the reference confining pressure p^{ref} . In the hardening soil model, the actual stiffness depends on the minor principal stress, σ'_3 which is the confining pressure in a triaxial test. Note that, σ'_3 is negative for compression. The power m controls the stress dependency as

the exponent n in the Duncan-Chang model. As in the Duncan-Chang model, Mohr-Coulomb failure criterion is used for evaluation of q_f in hardening soil model.

$$q_f = (c \cdot \cot \phi - \sigma'_3) \frac{2 \sin \phi}{1 - \sin \phi} \quad (2.20)$$

$$q_a = q_f / R_f \quad (2.21)$$

The failure ratio term is used as in the Duncan-Chang model to represent the similar relation between q_a and q_f . For the unloading-reloading condition another stress-dependent stiffness modulus is used:

$$E_{ur} = E_{ur}^{ref} \left(\frac{c \cdot \cot \phi - \sigma'_3}{c \cdot \cot \phi + p^{ref}} \right)^m \quad (2.22)$$

where E_{ur}^{ref} is a reference stiffness modulus for unloading-reloading condition, corresponding to the reference confining pressure p^{ref} . In many practical cases, E_{ur}^{ref} can be taken as equal to $3E_{50}^{ref}$ which is the default setting in the hardening soil model. For one-dimensional compression E_{oed} is used which can be evaluated using Eq. 2.23.

$$E_{oed} = E_{oed}^{ref} \left(\frac{c \cdot \cot \phi - \sigma'_3}{c \cdot \cot \phi + p^{ref}} \right)^m \quad (2.23)$$

where E_{oed} is a tangent stiffness modulus as indicated in Figure 2.29. Note that only σ_1 is considered to depict the one dimensional compression behaviour. If such a test result is not available as shown in Figure 2.29, $E_{oed}^{ref} \approx E_{50}^{ref}$ relation can be used.

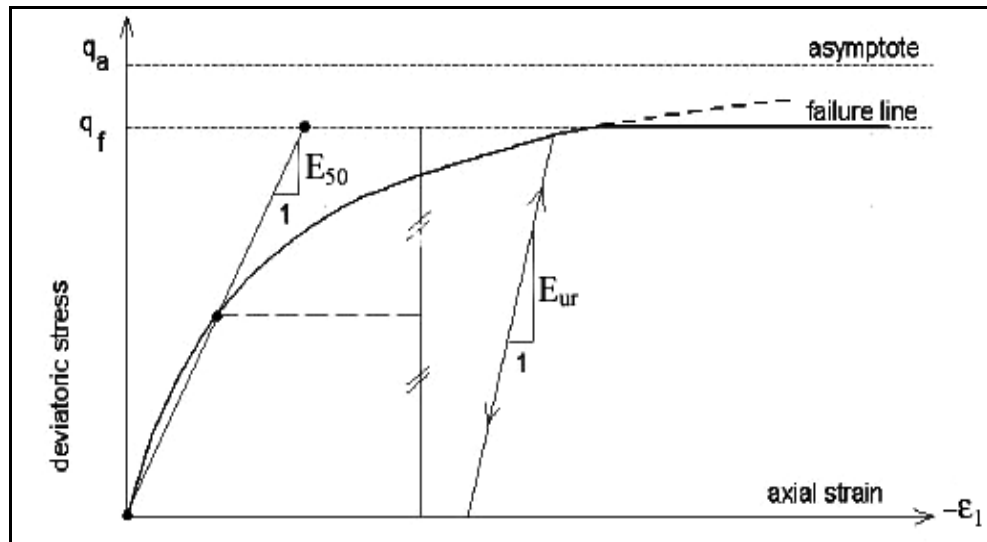


Figure 2.28 Hyperbolic stress-strain curve used in Hardening soil model
(negative values indicate compression, Schanz et al., 1999)

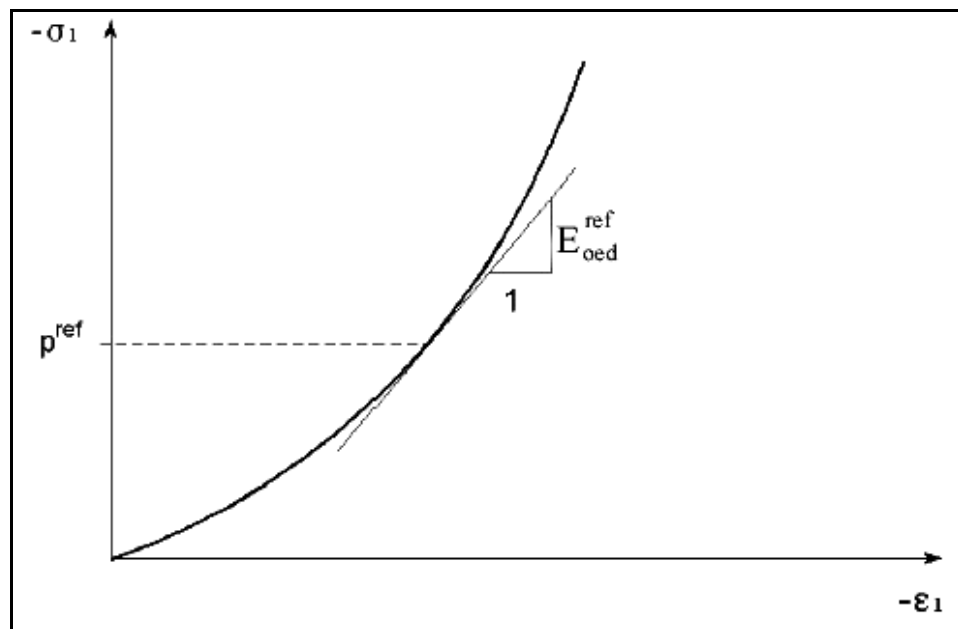


Figure 2.29 Definition of E_{oedr}^{ref} in oedometer test results (Schanz et al., 1999)
(negative values indicate compression)

CHAPTER 3

SETTLEMENT OF CONCRETE FACED ROCKFILL DAMS

3.1 General

Rockfill dams consists of rock fragments and voids of various sizes where rock-to-rock contact may be on edges, points and surfaces where crushing is a significant parameter contributing to displacements in contacts on edges and points. During construction of a dam, internal deformations take place due to changes in total stresses and pore pressures and due to creep. After the construction is completed, significant movements of the crest may take place during the first filling of the reservoir. Thereafter the rate of movement generally diminishes with time though time dependent creep may continue at a slow rate for several years. The displacements observed in a dam can be divided into three main components (Singh et al., 1995):

- Vertical displacements (settlements)
- Horizontal displacements, in upstream-downstream direction and normal to dam axis
- Horizontal displacements in the cross-valley direction and parallel to dam axis

In concrete face rockfill dams, the displacements must be limited to avoid cracking of the concrete membrane (Saboya et al., 1993).

In this chapter, settlement behaviour of CFRDs is overviewed where important studies in the literature about observed settlement behaviour and settlement analyses are briefly outlined.

3.2 A Review of Previous Studies

3.2.1 Observed Settlement Behaviour of CFRDs

In general every dam has its own deformation characteristics. The behaviour largely depends on construction techniques, construction time, the valley conditions and the material used for the embankment.

In order to demonstrate the settlement behaviour of CFRDs both for construction and for reservoir full condition, two case studies are selected where observed settlement behaviour of Foz de Areia and Salvajina CFRDs are presented.

Areia dam is 160 m high and located in Brazil when its construction was completed, it was the highest CFRD in the world. The crest length is 828 m. The zoning of the dam is shown for the max. section in Figure 3.1 with classification and methods of compaction of the materials. In Figure 3.2, contours of recorded settlements at the end of construction is shown. Here, the max. settlement is 358 cm and found at about mid-height of the dam (Pinto et al., 1985).

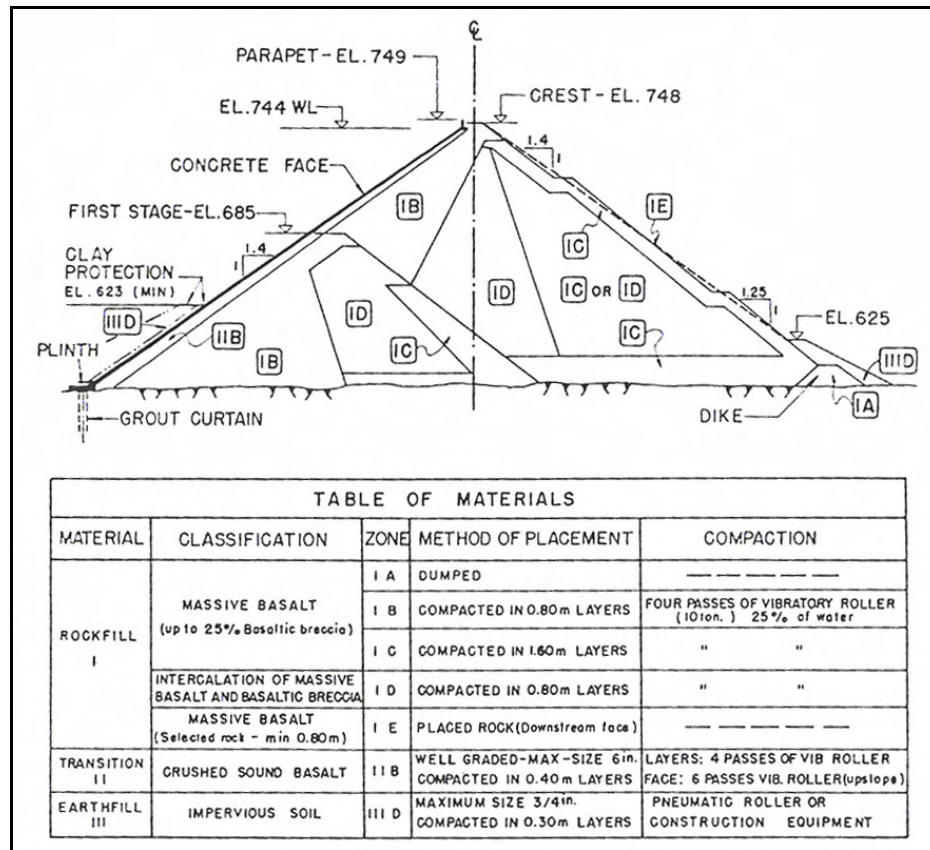


Figure 3.1 Areia dam, zoning and material properties (Pinto et al., 1985)

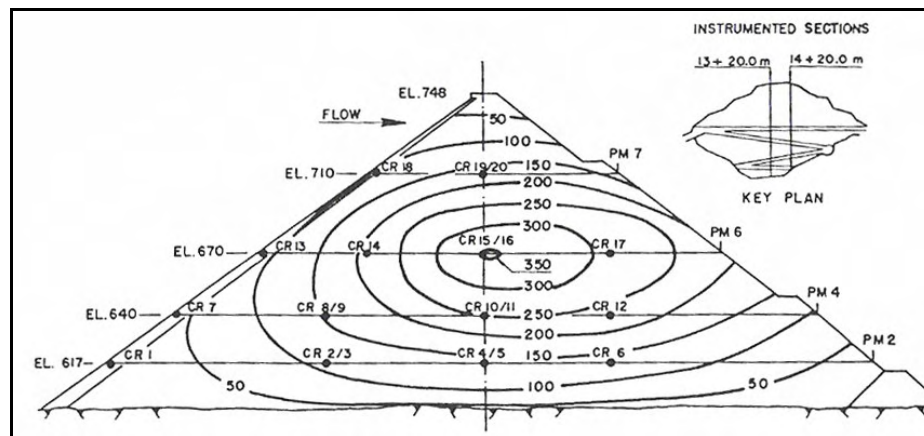


Figure 3.2 Areia dam, equal settlement curves after construction
(settlements are in cm, Pinto et al., 1985)

The deformation of rockfill embankment and concrete membrane of Areia dam after reservoir filling are shown in Figures 3.3 and 3.4, respectively. The max settlement normal to concrete face was recorded as 77.5 cm which is considerably higher than those of observed settlements for other dams in narrower valleys since in Areia dam the concrete face was constructed while the construction of main rockfill embankment was in progress. However general performance of the concrete face was excellent. In Figure 3.5, behaviour of downstream slope is shown after reservoir filling. It is seen that, in impounding condition displacements occur at the downstream face, as the upstream face (Pinto et al., 1985).

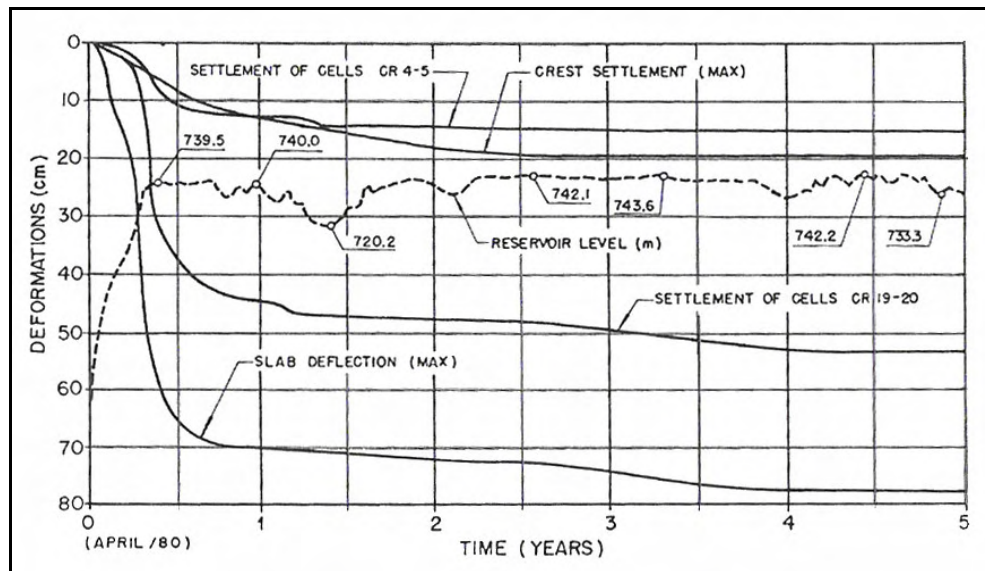


Figure 3.3 Areia dam, displacements after reservoir filling (Pinto et al., 1985)

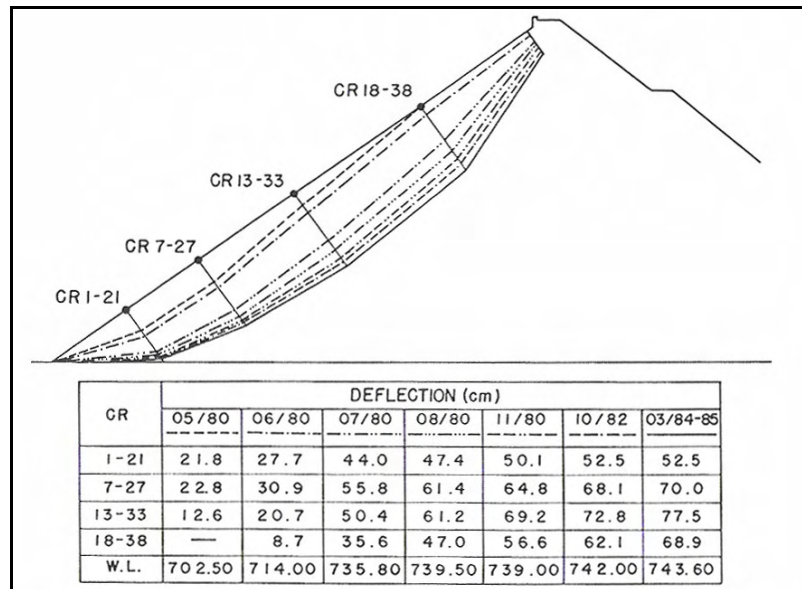


Figure 3.4 Areia dam, concrete slab displacements after reservoir filling
(displacements are not to scale, Pinto et al., 1985)

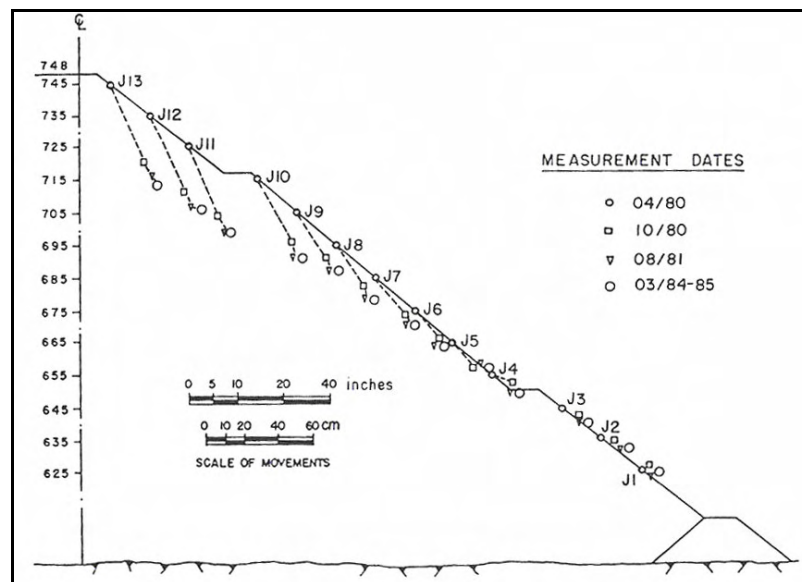


Figure 3.5 Areia dam, settlement and deflection of downstream slope after
reservoir filling (Pinto et al., 1985)

The 148 m high Salvajina dam which is located in Colombia is the second CFRD which is selected to demonstrate the settlement behaviour. When the construction of the dam was completed, it was the second highest CFRD in the world. In Figure 3.6, zoning and construction stages of the embankment are shown.

Zone 1 consists of gravel fill material up to 10-15 cm max particle sizes which was compacted in 0.45 m layers. Zone 2 consists of natural gravels up to 30 cm max particle size. This zone covers the upstream half and one fourth of downstream half of the embankment. The rockfill material in Zone 4 was obtained from spillway excavation and consists of weak sandstones and siltstones. Zone 4 was compacted in 0.9 m layers. A chimney drain (Zone 2A), consists of rather uniform material was included in the embankment, in order to anticipate lower than desirable permeabilities of Zones 2 and 4. The alluvial material found to be a dense deposit consisting of boulders and gravels in a sandy-silty matrix and not removed from the foundation.

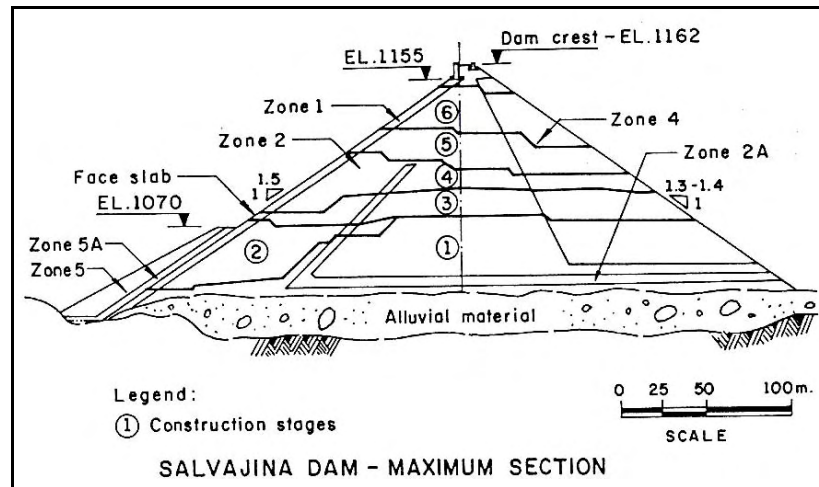


Figure 3.6 Salvajina dam, zoning and construction stages (Hacelas et al., 1985)

Salvajina dam was extensively instrumented in order to watch the dams performance during construction, first reservoir filling and operation stages. Location and description of instruments are illustrated at the max section in Figure 3.7.

The following paragraphs describe the dam behaviour during construction and first reservoir filling up to El 1144, which is equivalent to 92% of the total hydrostatic head (Hacelas et al., 1985). The equal settlement contours during construction and impounding are shown in Figures 3.8 and 3.9, respectively. For construction phase, rockfill material (Zone 4) settles almost twice of gravel material (Zone 2). For the reservoir filling phase, max settlement corresponding 92% of the total head reached 5 cm at the lower 1/3 of the dam, close to the upstream face and gradually decreasing in the downstream direction. Only half of the upstream part showed significant movement due to water load. Neither the alluvial material of the foundation nor the rockfill in the downstream shell suffered any significant movement during reservoir filling (Hacelas et al., 1985).

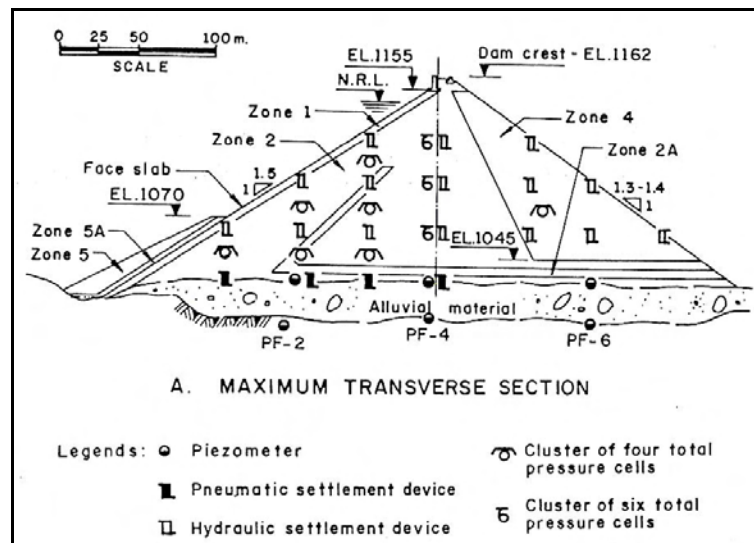


Figure 3.7 Salvajina dam instrumentation details (Hacelas et al., 1985)

Figure 3.10 shows the variation of vertical stresses during construction along the dam height at the five measuring sections. Figure 3.11 shows the increment of the normal stress within the fill on planes parallel to the concrete face due to hydrostatic load when the reservoir reached El 1144. Hacelas et al. also computed the direction of principal planes as shown in Figure 3.12. The ratio between these stresses within

the gravel fill was on the order of 10, while for the rockfill at the downstream part it was 2, which shows the striking difference in response of gravels and rockfill under similar gravity loading conditions. It was determined from the strain measurements that, gravel fill material deformation modulus was 7 times greater than that of rockfill which shows that gravel is remarkably incompressible and that it is the ideal material for higher concrete face dams (Hacelas et al., 1985).

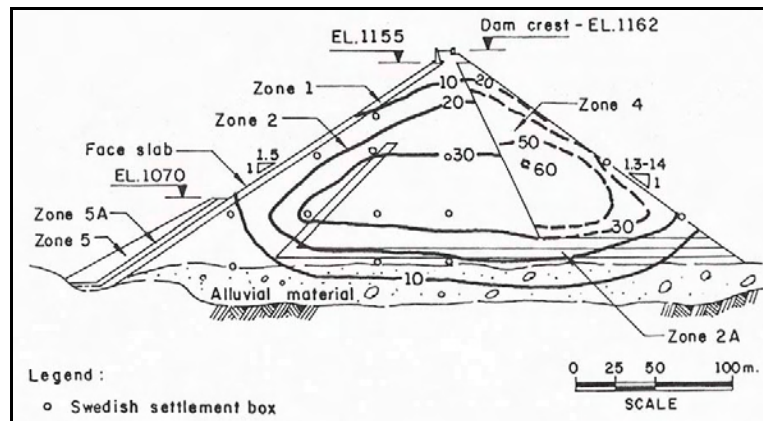


Figure 3.8 Salvajina dam, equal settlement contours during construction (in cm) (Hacelas et al., 1985)

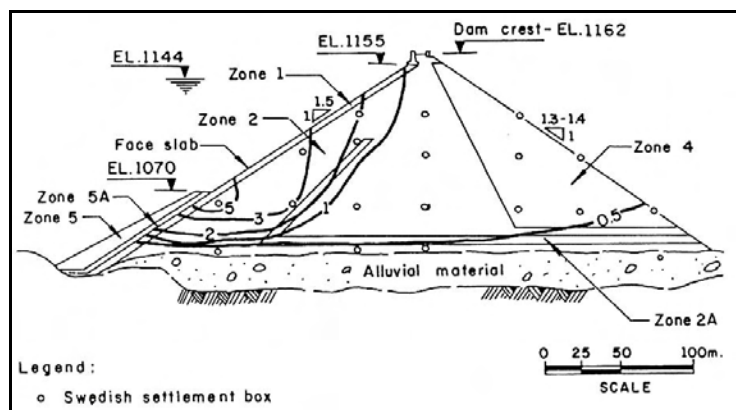


Figure 3.9 Salvajina dam, equal settlement contours during reservoir filling (in cm) (Hacelas et al., 1985)

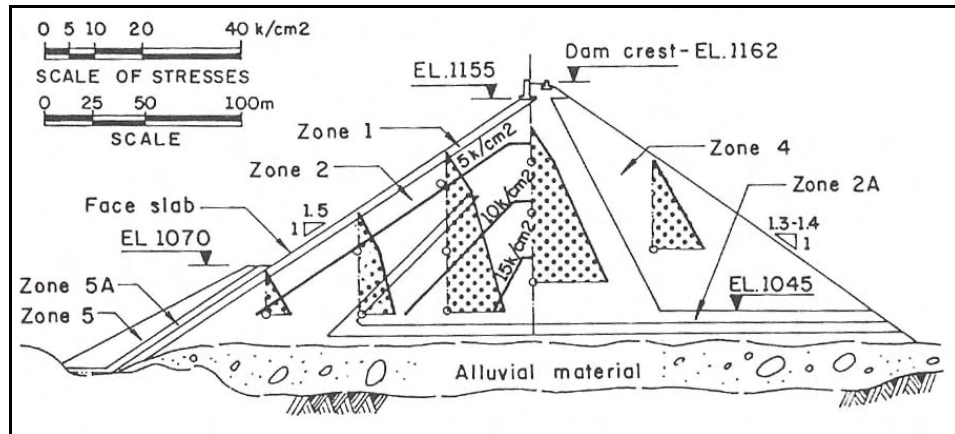


Figure 3.10 Salvajina dam, vertical normal stress at the end of construction
(Hacelas et al, 1985)

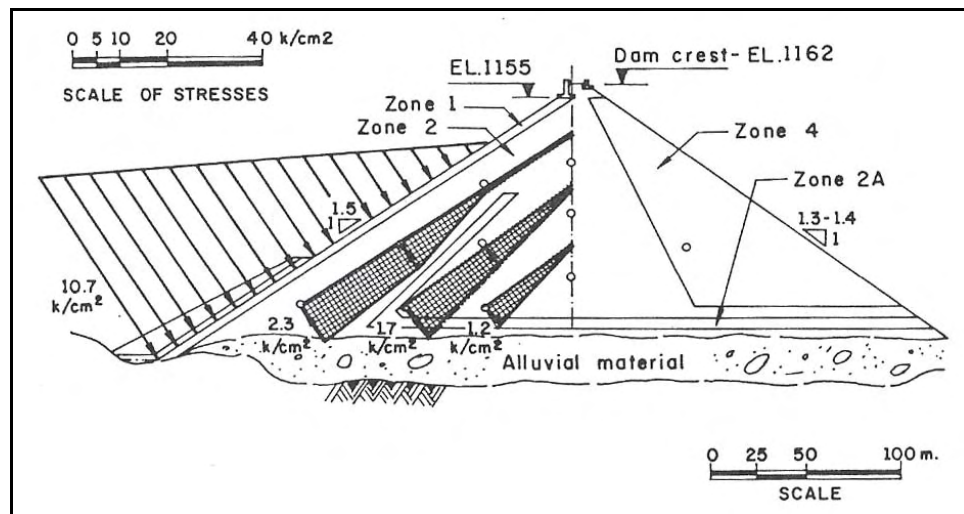


Figure 3.11 Salvajina dam, normal stress increment during filling
(Hacelas et al, 1985)

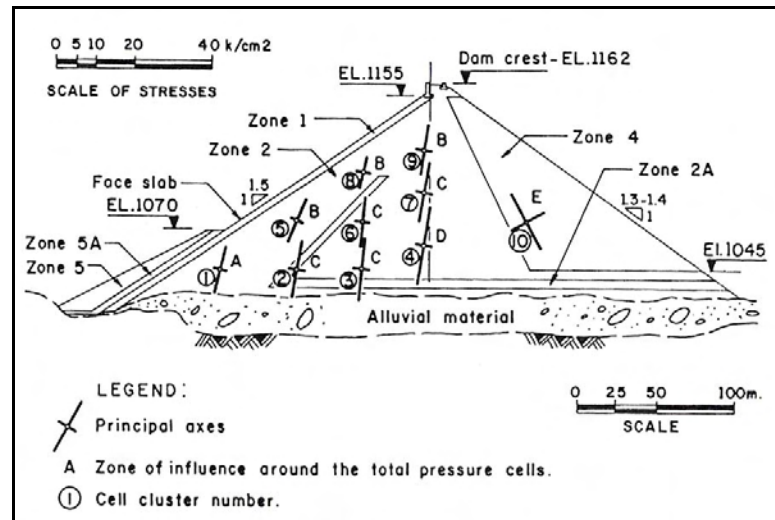


Figure 3.12 Salvajina dam, principal stresses (Hacelas et al., 1985)

In the literature there are many studies about post-construction behaviour. In 1964, Lawton et al. suggested the following relationship to determine the post-construction crest settlements.

$$S = 0.001H^{3/2} \quad (3.1)$$

where S represents settlements and H represents the dam height which are both in meters. They also indicated that, 85% of the settlement took place in the first year after the first filling in CFRDs. In 1975, Sowers et al. studied settlement behaviour of 14 of the earlier rockfill dams and found that the settlements ranged between 0.25% and 1% of the dam height in ten years. They concluded that, sluicing during construction was an important parameter to reduce settlements (Singh et al., 1995).

Another remarkable study was the one carried out by Clements in 1984 in which he studied post-construction crest settlements and deflections of 68 rockfill dams in order to assess the usefulness and accuracy of prediction of such deformations using empirical equations. He presented time versus deformation relationships per unit height for membrane faced, sloping and central core dams as shown in Figure 3.13.

After comparisons of predicted and observed movements Clements indicated that, the use of empirical equations can lead to large errors. He suggested that,

available deformation curves of existing dams with similar characteristics can be used for the dam under consideration. The enveloping curves, related with post-construction crest settlements and crest deflections are shown in Figures 3.14 and 3.15, respectively.

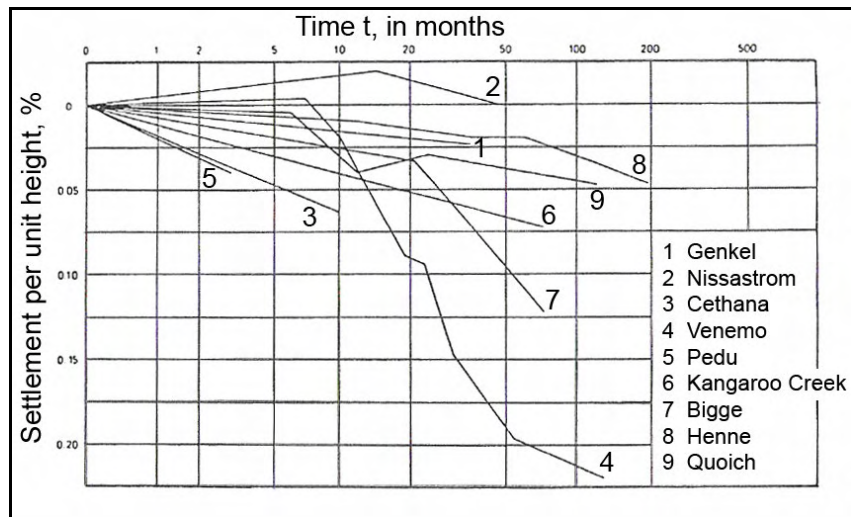


Figure 3.13 Crest settlements of CFRDs (Clements, 1984)

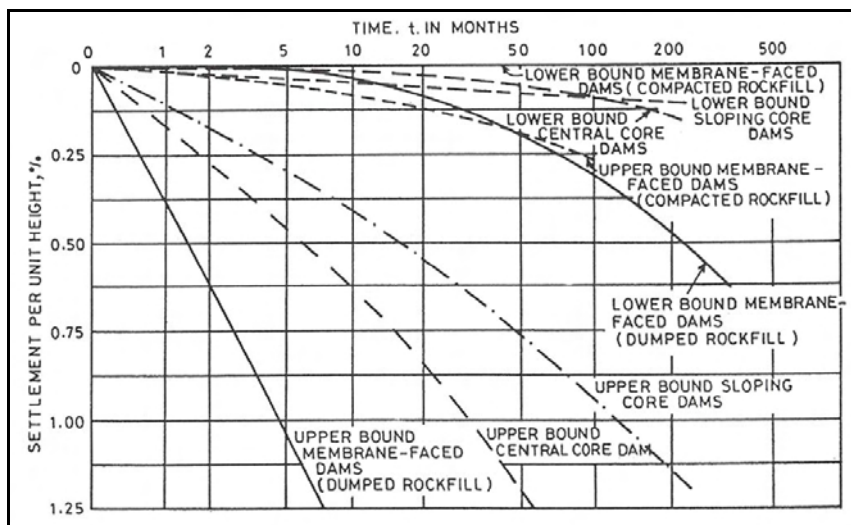


Figure 3.14 Envelopes of settlements curves (Clements, 1984)

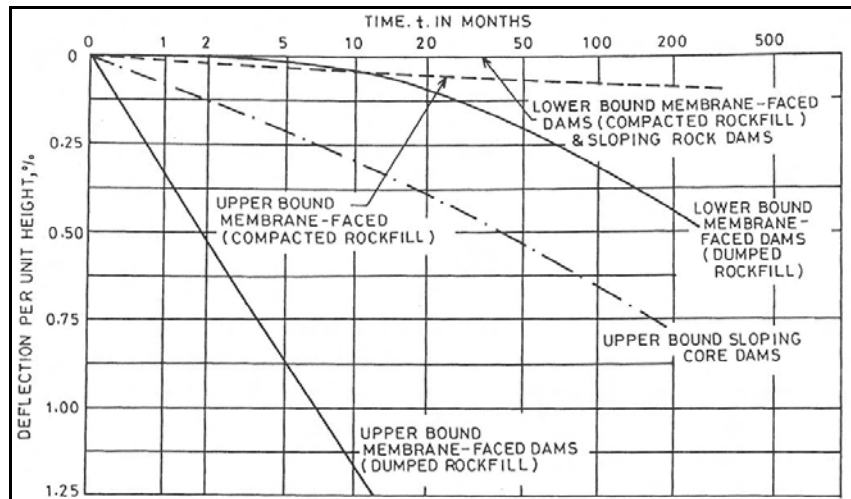


Figure 3.15 Envelopes of deflection curves (Clements, 1984)

3.2.2 Settlement Analyses of Earth and Rockfill Dams

3.2.2.1 Assessment of Behaviour of Fill Dams by Finite Element Method

As mentioned earlier, finite element method is first used in geotechnical engineering by Clough et al. in 1967. A 30.5 m high homogeneous earth dam was selected for analysis. They studied the effect of foundation elasticity and incremental construction on the stresses and deformations in the dam.

In their study, plane strain principles are used with the constant values of elastic modulus E and Poisson's ratio ν . To study the effect of incremental construction on the settlement behaviour, they compared the results of single stage construction with a 10 staged construction using 3m layers.

When the results were compared, they found that single stage construction gives information with sufficient accuracy if the stresses are concerned. From the horizontal displacements point of view, the results were similar too, but significant differences were observed when vertical displacements are compared.

As expected, the max settlement is found at the crest in the single stage analysis, however in the staged construction analysis, max. settlement is found at about the mid-height of the dam and a relatively small settlement is found at the crest (See Figure 3.16).

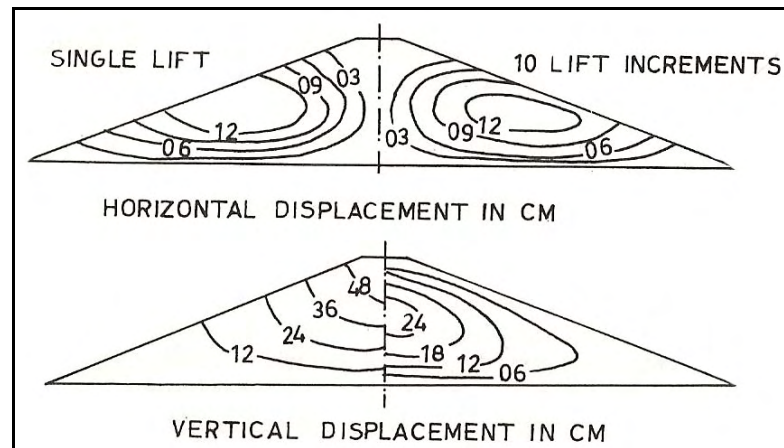


Figure 3.16 Displacements in standard dam (Clough et al., 1967)

In this study, the foundation was assumed to be rigid. Later, Clough et al. included the foundation in the analysis in order to study the effect of foundation elasticity on dam behaviour. Different values of E were used, where the lowest value was taken as equal to the embankment E and the highest was taken as infinite. At the end, it was observed that, the vertical stress σ_z was independent of the foundation elasticity, while the horizontal normal stress σ_x and the shear stress τ_{xy} varied significantly with it. In general, the stresses were reduced as the foundation become softer. However, the displacements of the dam were very sensitive to the foundation elasticity.

In 1973, Lefebvre et al. presented a valuable study where they compared the results of two dimensional and three dimensional analyses. Dams on different valley shapes having slopes of 1:1, 3:1, 6:1 (H:V) were analyzed in this study. The fill slopes was kept constant as 2.5:1 and the embankment fill was thought as a linear

elastic material. The dams were 49 m in height constructed in eight layers of uniform thicknesses. (See Figure 3.17) Two dimensional plane strain analyses were conducted on the transverse sections and both plain strain and plane stress analyses were conducted on the longitudinal sections.

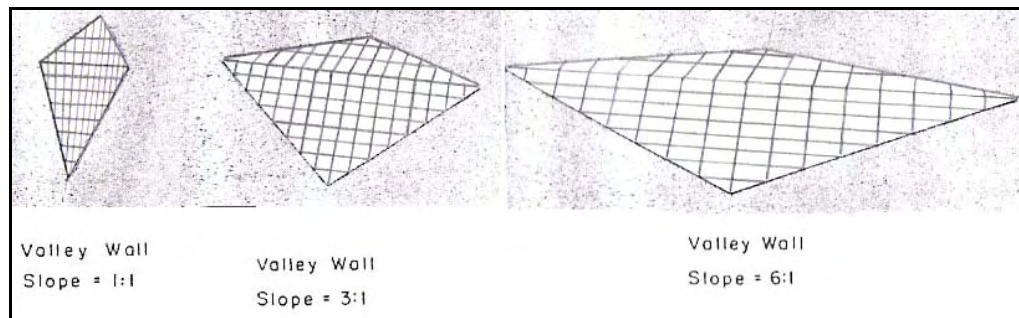


Figure 3.17 Analyzed dams in the study of Lefebvre et al., 1973

For purposes of comparing the results, Lefebvre et al. expressed the results of two dimensional analyses as percentages of three dimensional ones. They indicated that plane strain analyses provide an acceptable degree of accuracy for most purposes when transverse sections of dams in valleys with valley wall slopes of 3:1 or flatter are considered. However, significant errors were observed for dams in steeper valleys. The results are given Table 3.1. Here σ_1 , σ_3 , τ_{\max} , u_v and u_x represents major and minor principal stresses, max shear stress, vertical and horizontal displacements respectively.

In the longitudinal section, it is seen that plane stress analyses were not in very good agreement with three dimensional analyses and were unaffected with the valley slopes (Table 3.2). From plane strain analysis point of view, it was seen that the results were in good agreement with all types of valley slopes (Table 3.3). Lefebvre et al. also indicated that, arching is a significant parameter and reduces both the vertical and horizontal deformations in both transverse and longitudinal sections in valley slopes steeper than 3:1.

Table 3.1 Comparison of results of two dimensional plane strain and three dimensional analyses for transverse sections (Lefebvre et al., 1973)

	Plane strain values / three dimensional values (in %)					
	Valley slope 1:1		Valley slope 3:1		Valley slope 6:1	
	Average	Variation	Average	Variation	Average	Variation
σ_1	113	100-129	102	100-113	101	98-109
σ_3	98	79-125	96	81-111	97	88-100
τ_{\max}	138	108-225	112	100-150	108	100-150
u_v	136	91-156	106	85-114	100	85-105
u_x	268	75-435	120	80-149	105	85-120

Table 3.2 Comparison of results of two dimensional plane stress and three dimensional analyses for longitudinal sections (Lefebvre et al., 1973)

	Plane stress values / three dimensional values (in %)					
	Valley slope 1:1		Valley slope 3:1		Valley slope 6:1	
	Average	Variation	Average	Variation	Average	Variation
σ_1	109	80-127	110	102-115	111	100-115
σ_3	77	20-109	84	60-109	85	63-100
τ_{\max}	149	107-185	149	111-179	149	126-181
u_v	160	122-196	173	138-217	173	140-224
u_x	220	130-1300	228	139-400	224	139-400

Table 3.3 Comparison of results of two dimensional plane strain and three dimensional analyses for longitudinal sections (Lefebvre et al., 1973)

	Plane strain values / three dimensional values (in %)					
	Valley slope 1:1		Valley slope 3:1		Valley slope 6:1	
	Average	Variation	Average	Average	Variation	Average
σ_1	111	91-115	110	98-115	110	93-115
σ_3	122	85-130	124	100-136	123	100-135
τ_{max}	94	70-117	91	74-105	90	83-107
u_v	97	78-113	98	75-120	97	80-124
u_x	117	72-166	118	75-233	115	71-200

Linear elastic material models was utilized in both of the two studies outlined in this section up to here. However as mentioned in the previous chapter, especially in rockfill dams, the behaviour is seriously affected by confining stress conditions thus using non-linear material models will be more realistic. One of the first studies where non-linear material models were used, was carried out in 1972 by Kulhawy et al. They used Duncan and Chang's hyperbolic model and conducted two dimensional finite element analyses of Oroville dam which is located in Northern California. The dam was the world's highest embankment dam in those years having the dimensions of 1680 m crest length, 1050 m base width and 230 m height. The cross section of the dam and the hyperbolic parameters used in the study are shown in Figures 3.18 and Table 3.4 respectively. As mentioned earlier, the tangent Poisson's ratio concept was developed during this study by Kulhawy et al.

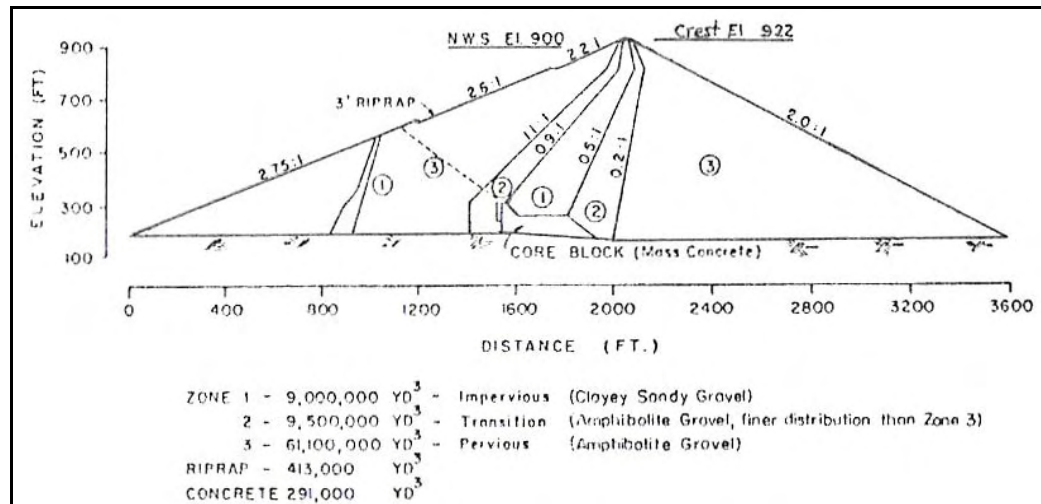


Figure 3.18 Oroville dam max section (Kulhawy et al., 1972)

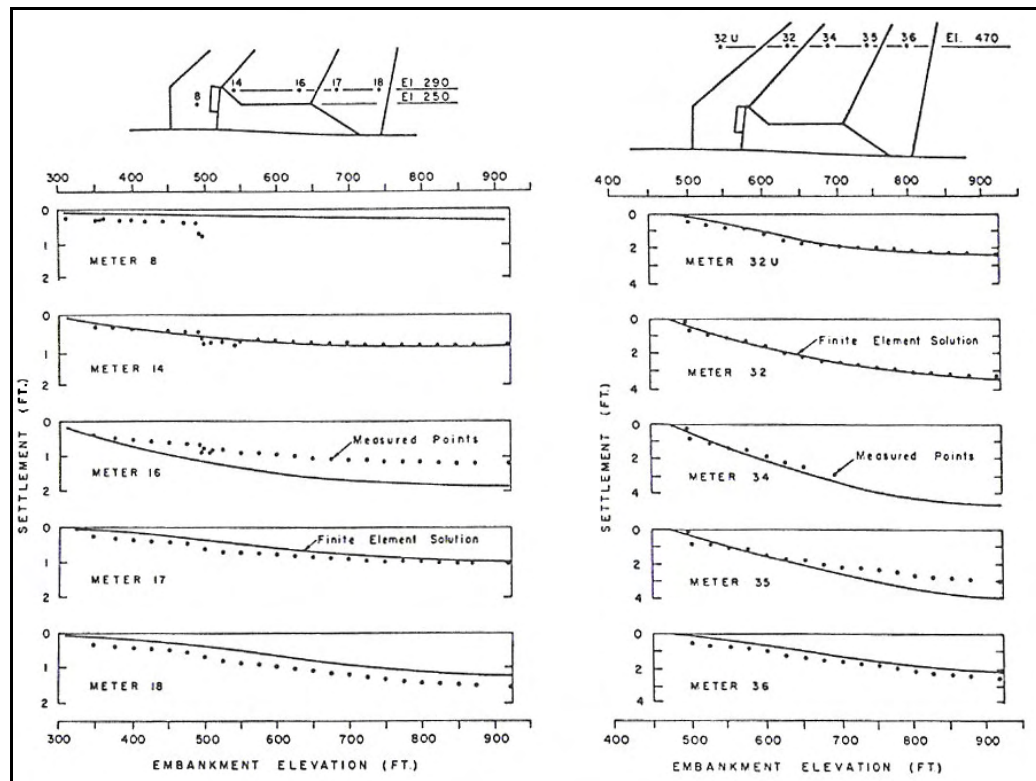
Table 3.4 Hyperbolic parameters used in their study by Kulhawy et al., 1972

Parameter	Values employed in the analyses				
	Shell	Transitio	Core	Soft Clay	Concrete
Unit weight, γ , lb/ft ³	150	150	150	125	162
Cohesion, c , t/ft ²	0	0	1.32	0.3	216
Friction angle, ϕ (°)	43.5	43.5	25.1	13.0	0
Modulus number, K	3780	3350	345	150	137500
Modulus exponent, n	0.19	0.19	0.76	1.0	0
Failure ratio, R_f	0.76	0.76	0.88	0.9	1.0
Poisson's ratio prm., G	0.43	0.43	0.30	0.49	0.15
Poisson's ratio prm., F	0.19	0.19	-0.05	0	0
Poisson's ratio prm., d	14.8	14.8	3.83	0	0

In Figures 3.19 and 3.20, the calculated vertical and horizontal displacements are compared with the observed values and in Figures 3.21 and 3.22 the contours of vertical and horizontal displacements are shown for the end of construction stage. In general, the results were consistent.

Kulhawy et al. also calculated the stresses in the dam and compared these with the observed values as shown in Table 3.5. However the consistency was not

good in this case. There were certain inconsistencies in the readings and according to the researchers, finite element calculations provided more reasonable values. Finally, Kulhawy et al. concluded that non-linear finite element analyses indicated a consistent behaviour with the actual behaviour of Oroville dam.



**Figure 3.19 Comparison of measured and calculated settlements
in Oroville dam (Kulhawy et al., 1972)**

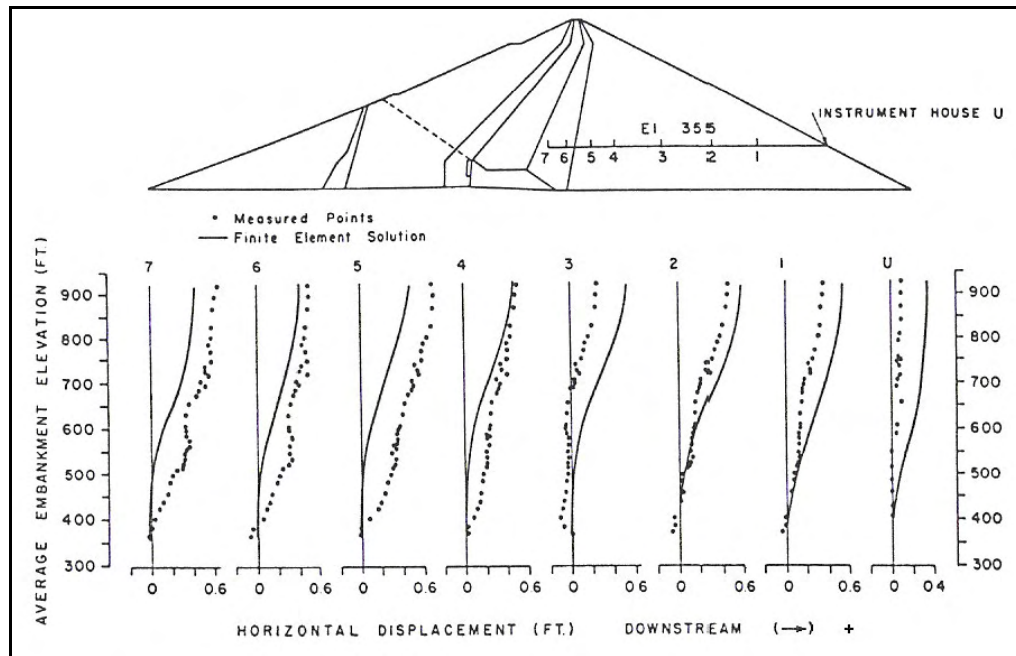


Figure 3.20 Comparison of measured and calculated horizontal displacements in Oroville dam (Kulhawy et al., 1972)

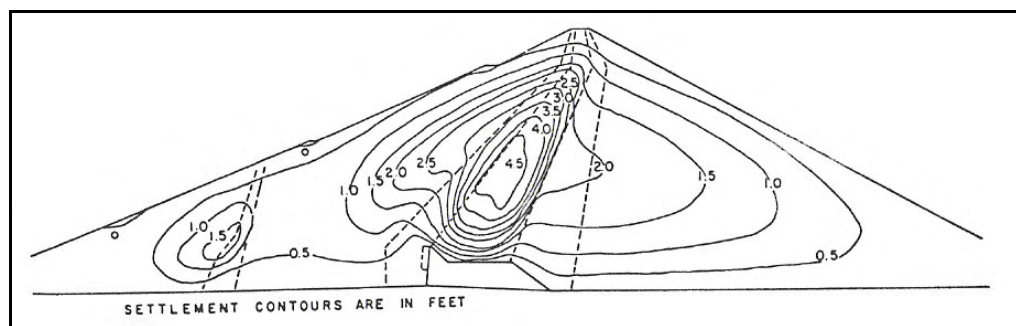


Figure 3.21 Contours of calculated settlements in Oroville dam (Kulhawy et al, 1972)

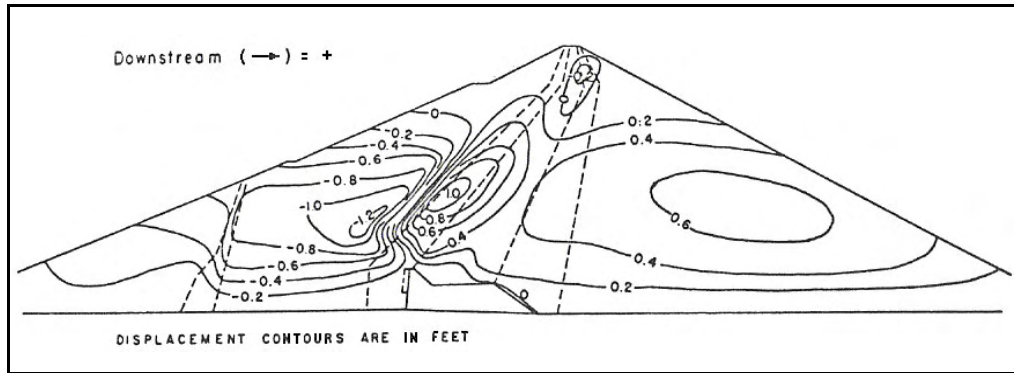


Figure 3.22 Contours of calculated horizontal displacements in Oroville dam (Kulhawy et al, 1972)

Table 3.5 Comparison of measured and calculated stresses at stress meter locations in Oroville dam (Kulhawy et al., 1972)

Stress meter	Elev (ft)	Location of stress meters	Measured		Calculated	
			$\sigma_1/\gamma h$	$\sigma_3/\gamma h$	$\sigma_1/\gamma h$	$\sigma_3/\gamma h$
A	280	Downstream transition, 20 ft upstream from shell	0.46	0.16	0.91	0.36
D	400	Upstream transition, 30 ft upstream from core	1.05	0.09	1.18	0.68
			$\sigma_y/\gamma h$		$\sigma_y/\gamma h$	
V	460	Downstream shell, 150 ft downstream from transition	1.01		0.93	
W	460	Downstream shell, 300 ft downstream from transition	1.27		1.00	
X	460	Downstream shell, 450 ft downstream from transition	1.18		1.01	
Y	580	Downstream shell, directly above group V	1.20		0.95	
Z	580	Downstream shell, directly above group W	1.11		1.03	

In the majority of dams, the impounding period is the most critical one since large displacements in the dam bodies and even sometimes cracks are observed during this period. This situation has been taken into consideration by Nobari et al. in 1972. They indicated that the complex displacements may be explained by two counteracting effects; (1) the water loads on the dam and (2) the softening and weakening of the embankment fill material due to wetting. They illustrated the effects of reservoir filling on a zoned dam as shown in Figure 3.23.

The first three of the effects illustrated in Figure 3.23 result directly from the water loading: (1) the water load on the core causes downstream and downward displacements, (2) the water load on the upstream foundation causes upstream and downwards displacements, (3) the buoyant uplift forces in the upstream shell cause upward displacements within this zone. The fourth effect is due to the softening and weakening caused by wetting the upstream shell material. As shown in Figure 3.24, even well compacted clean granular materials like the Oroville dam shell material undergo softening and strength loss due to wetting. The greater the difference between the stress-strain curves for the material in dry and wet conditions, the greater the calculated stress reduction due to softening (Nobari et al., 1972).

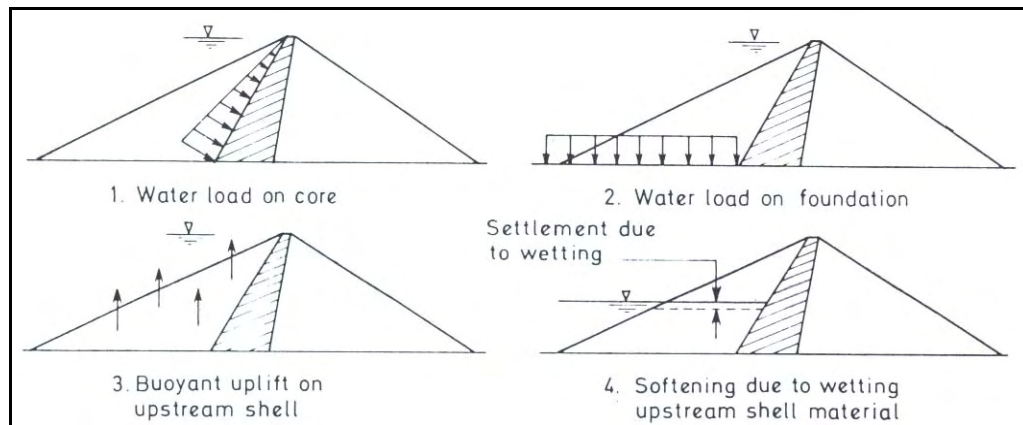


Figure 3.23 Effects of reservoir filling on a zoned dam (Nobari et al., 1972)

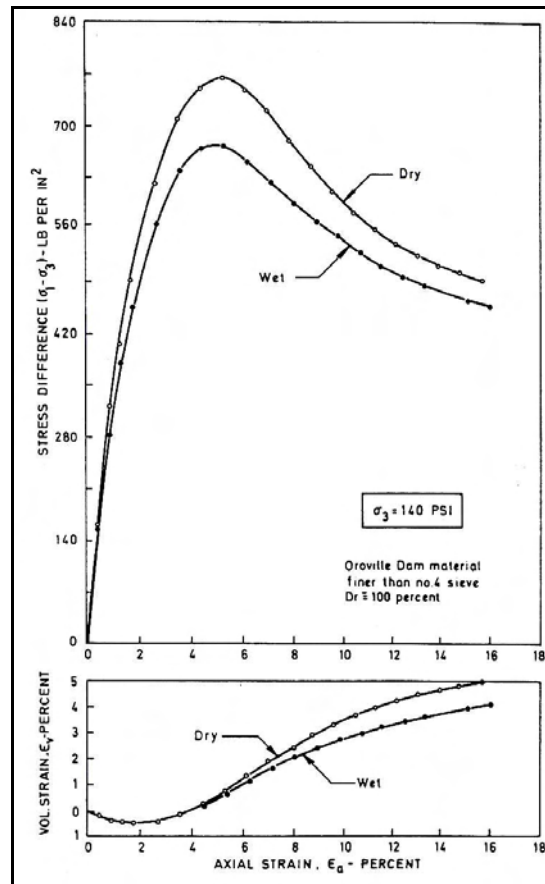


Figure 3.24 Triaxial test results for dry and wet specimens, Oroville dam material (Nobari et al., 1972)

In their study, Nobari et al. analyzed the displacements of El Infiernillo dam in which, during reservoir impounding, the displacements first occurred towards upstream and later occurred towards downstream, as shown in Figure 3.25. It may be seen that, the first part of the rise in reservoir water level, from about 80 m to 120 m, caused the core of the dam to deflect upstream. Continued rise of the water level to 160 m caused a slight downstream deflection, and the final rise from 160m to 170 m caused a large downstream movement (Nobari et al., 1972).

According to the researchers, in the first stages of impounding, the softening of the fill dominates the behaviour of the dam because in this stage the amount of compression is greatest since the overburden pressure is large and as a result

upstream movements occurred. However in the later stages of impounding water loads dominate the behaviour because the water load on the core increases as the square of the depth of the impounded water.

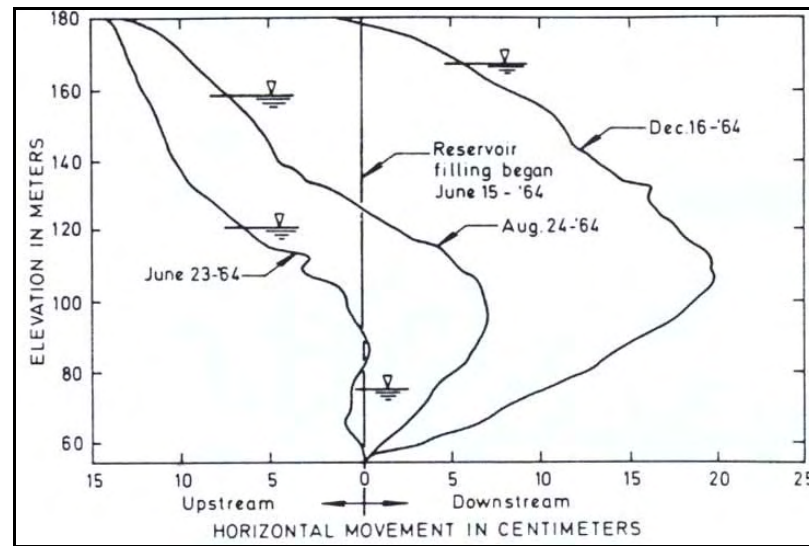


Figure 3.25 Upstream and downstream movements during impounding in El Infiernillo dam (Nobari et al, 1972)

Later, Nobari et al. analyzed the displacements during reservoir impounding of Oroville dam with the finite element method taking into account the effect of softening of the shell material due to wetting as well as the effects of water loads. Two dimensional plane strain analyses were carried out where the same mesh was used which was previously used by Kulhawy et al. Initial stresses are taken from the previous analyses by Kulhawy et al. The calculated and measured downstream displacements were compared as shown in Figure 3.26. The consistency was quite good and encouraging although the calculated settlements were larger than the observed values. Nobari et al. considered this difference was due to the effects of creep and secondary compression.

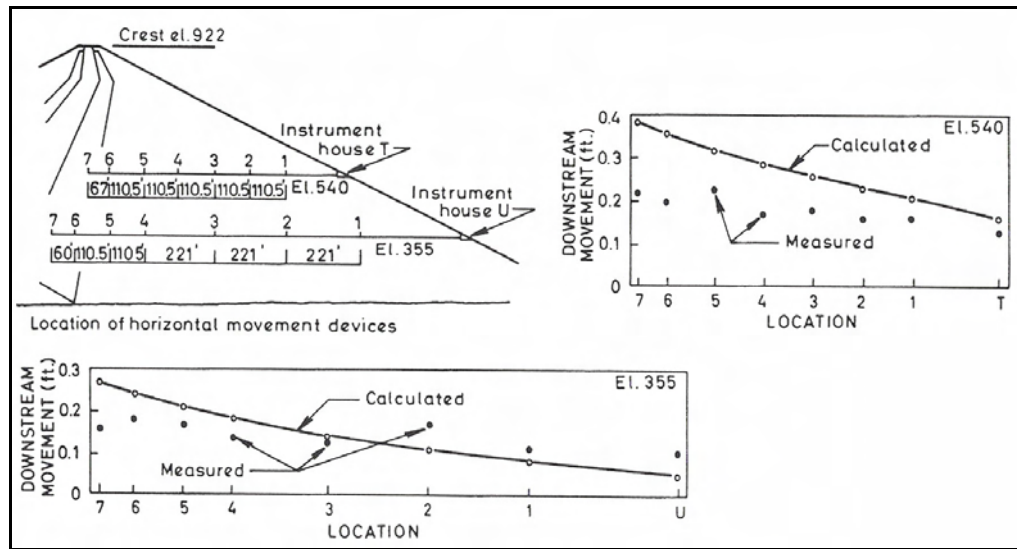


Figure 3.26 Comparison of calculated and measured downstream displacements in Oroville dam during reservoir filling (Nobari et al., 1972)

3.2.2.2 Empirical Approaches on Determining Deformation Moduli of CFRDs

At the 1985 ASCE Symposium on CFRDs, Fitzpatrick et al., presented a valuable paper about the general behaviour of CFRDs. They analyzed performances of nine CFRDs which were built in past-1965 period in Tasmania, Australia. In Table 3.6, the general characteristics of the dams are given.

In their study, Fitzpatrick et al. measured the rockfill deformation modulus in construction condition (E_{rc}) and in reservoir filling condition (E_{rf}) from measured settlements recorded in the rockfill embankments and measured displacements recorded normal to the upstream face respectively. They used the relationship which is given in Figure 3.27 in their calculations which have some shortcomings, such as: E_{rc} values should be taken as indicative at the center of the dam and E_{rf} values should be taken as indicative under the 60% portion of the upstream face which does not give accurate results near the crest and near the upstream toe level (Fitzpatrick et al., 1985).

Table 3.6 Concrete face rockfill dams examined by Fitzpatrick et al., 1985

Name of dam	Year compltd.	Max. height	Crest length	Face slopes		Rockfill volume	Rockfill type
		(m)	(m)	Upstr	Dnstr	(m ³)	
Wilmot	1970	35	138	1.33	1.33	171000	Greywacke
Cethana	1971	110	215	1.3	1.3	1610000	Quartzite
Paloona	1971	38	159	1.33	1.33	184000	Arg. Chert
Serpentine	1972	39	127	1.5	1.5	132000	Quartzite
Mackintosh	1981	75	465	1.3	1.3	980000	Greywacke
Tullabardine	1982	26	200	1.3	1.3	120000	Greywacke
Murchison	1982	94	200	1.3	1.3	906000	Rhyolite
Bastyan	1983	75	430	1.3	1.3	580000	Rhyolite
LowerPieman	1986	122	360	1.3	1.3	2720000	Dolerite

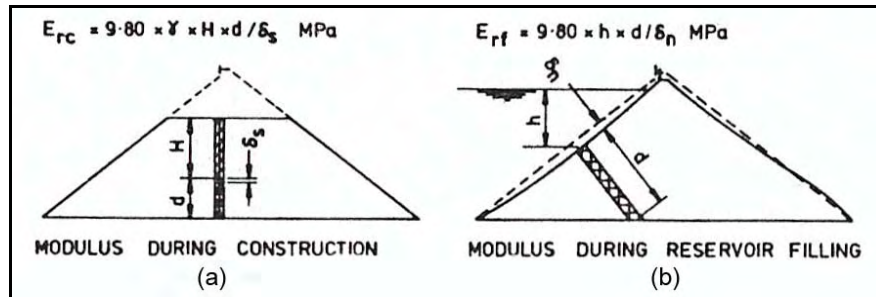


Figure 3.27 Determination of rockfill modulus (Fitzpatrick et al., 1985)

The calculated deformation moduli are shown in Table 3.7. It can be seen from the table that, in general reservoir filling modulus (E_{rf}) is considerably greater than construction modulus (E_{rc}), particularly when the filling period for the reservoir is short. When a long period is required to fill the reservoir, as in the case of Serpentine dam where reservoir filling completed in three years, creep within the rockfill during this period considerably reduces the value of the deformation modulus (Fitzpatrick et al., 1985).

Table 3.7 Dam embankment performance data (Fitzpatrick et al., 1985)

Name of dam	Rockfill data			
	Rock type	Rockfill	Modulus	Modulus Erf
		t/m ³	MPa	MPa
Wilmot	Greywacke	2.2	115	160
Cethana	Quartzite	2.1	145	310
Palooka	Chert	2.0	75	115
Serpentine	Quartzite	2.1	115	95
Mackintosh	Greywacke	2.2	40	95
Tullabardine	Greywacke	2.2	90	170
Murchison	Rhyolite	2.3	225	650
Bastyan	Rhyolite	2.2	160	300
Lower Pieman	Dolerite	2.3	160	-

Another valuable study about rockfill deformation moduli and settlement of CFRDs is the one carried out by Hunter et al., in 2003. They developed a database which consists of 35 CFRDs' and one ECRD (earth core rockfill dam) performances. Seven of the CFRDs were constructed of dumped rockfill and four of them were constructed using gravel in Zone 3A. (For a typical zoning of CFRDs, see Figure 2.2)

Hunter et al. conducted a two dimensional finite difference analysis to predict the effect of valley shape on the dam's behaviour, since it was indicated from several researchers that the valley shape has a significant effect on the vertical stresses within the dam because of the arching effect across the abutments. They analysed the behaviour of a 100 m high prototype rockfill dam. Linear elastic model was used where the parameters were taken as 100 MPa for elastic modulus and 0.27 for Poisson's ratio. Different rivers widths were used such as 20, 50 and 100 m with abutment slopes of 0°, 26.5°, 45° and 70°. They used a modulus of 50 GPa for linear elastic modeling of foundation. Embankment was assumed to be constructed first in 5m layers and later in a 100 m single layer.

After the analysis, Hunter et al. concluded that cross-valley arching is a significant parameter especially in narrow valleys where river width is less than 30 to 40% of the dam height and abutment slopes are greater than 50°. As a result, they suggested that stress reduction factors can be used in evaluation of vertical stresses. The stress reduction factors vary with river width to height ratio and valley slopes by the researchers as shown in Table 3.8.

Table 3.8 Approximate stress reduction factors suggested by Hunter et al.,2003

W_r/H ratio (river width to height)	Average abutment slope (°)	Stress reduction factor (embankment location)			
		Base (0 to 20%)	Mid to low (20 to 40%)	Mid (40 to 65%)	Upper (65% to crest)
0.2	10 to 20	0.93	0.95	0.97	1.0
	20 to 30	0.88	0.92	0.96	0.98
	30 to 40	0.82	0.88	0.94	0.97
	40 to 50	0.74	0.83	0.91	0.96
	50 to 60	0.66	0.76	0.86	0.94
	60 to 70	0.57	0.69	0.82	0.92
0.5	<25	1.0	1.0	1.0	1.0
	25 to 40	0.93	0.95	0.97	1.0
	40 to 50	0.91	0.92	0.95	0.05-1.0
	50 to 60	0.87	0.88	0.93	0.05-1.0
	60 to 70	0.83	0.85	0.90	0.05-1.0
1.0	All slopes	0.95-1.0	0.95-1.0	1.0	1.0

In the second part of their study, Hunter et al. suggested a relationship to estimate secant modulus of rockfill corresponding to the end of construction stage as a function of unconfined compressive strength (UCS) and D₈₀ particle size of rockfill using internal vertical deformation records close proximity to the dam centerline and from the lower half of the embankment. The relationship is shown in Figure 3.28.

It was indicated by Hunter et al. that, the representative secant modulus at the end of construction (E_{rc}) represent Zone 3B rockfill (see Figure 2.2) placed in 0.9 to 1.2 m layers, sluiced and compacted with a 10 t smooth drum vibratory roller by four to six passes and is applicable to average vertical stresses of 1400 kPa for high strength rockfill having an UCS in the range 70 to 240 MPa. For Zone 3C, a reduction factor of 0.5-0.75 should be used. To account for the nonlinearity of the stress-strain relationship of, Hunter et al. suggested the following correction:

For very high strength rockfills, a correction of $\pm 7.5\%$ is applied per 200 kPa to the E_{rc} value estimated from Figure 3.28 for a vertical stress of 1400 kPa. Positive corrections are applied for decreasing stresses and negative corrections are applied for increasing stresses. The applicable range is 400 to 1600 kPa. For medium to high strength rockfills, a correction factor of $\pm 7.5\%$ is applied for a vertical stress of 800 kPa. The applicable range is 200 to 1200 kPa (Hunter et al., 2003).

For evaluation of rockfill deformation modulus in reservoir filling stage (E_{rf}), Hunter et al. suggested the relationship shown in Figure 3.29. In this figure E_{rc} represents the rockfill modulus uncorrected for valley shape due to arching effects by dividing the E_{rc} estimations by stress correction factors given in Table 3.8. E_{rf} is determined from E_{rf}/E_{rc} ratio which vary with embankment height and embankment upstream slopes. Hunter et al., concluded that, the method shown in Figure 3.29, is approximate and applicable for CFRDs with relatively simple zoning geometries comprising a significant Zone 3B component (greater than 50 to 60%).

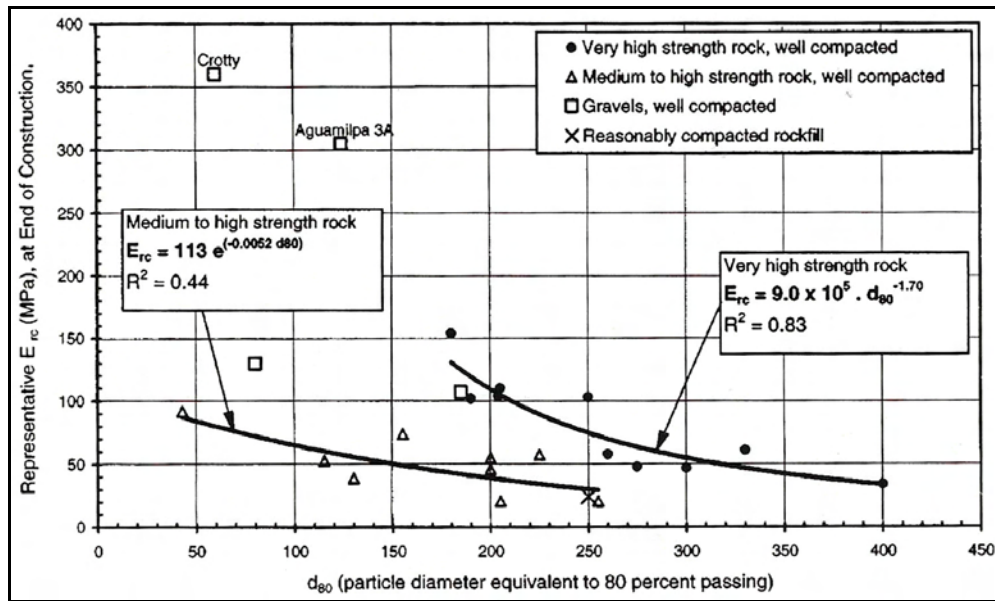


Figure 3.28 Representative secant modulus of compacted rockfill an the end of construction (Hunter et al., 2003)

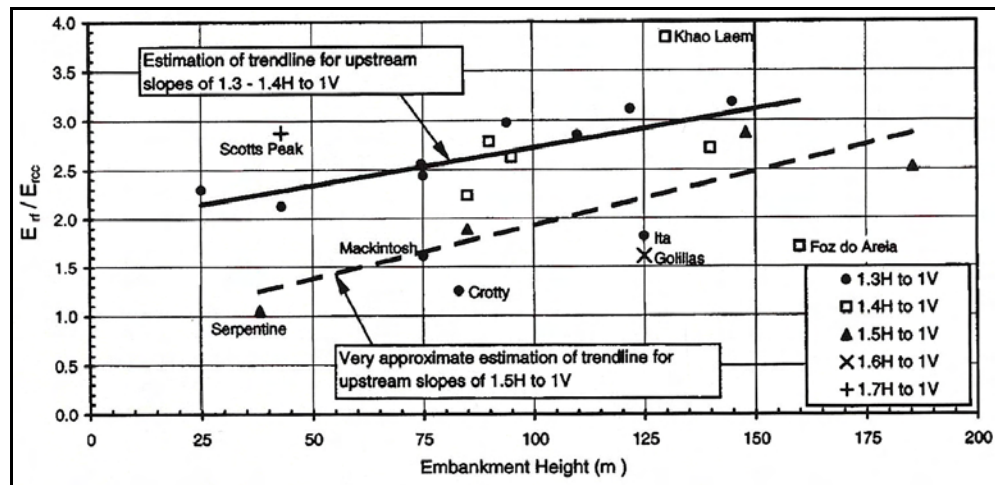


Figure 3.29 E_{rf} / E_{rc} ratio vs embankment height (Hunter et al., 2003)

3.2.3 Assessment of Settlement Behaviour of CFRDs by Finite Element Method

One of the valuable studies among the finite element analysis of CFRDs, is the one which was carried out by Khalid et al. in 1990. Cethana dam was selected in their study which is located in Australia.

For modeling of rockfill material, Duncan and Chang's hyperbolic model was used. Hyperbolic material model parameters are selected from appropriate studies since no available test results found representing the stress strain characteristics of rockfill material of Cethana dam. The hyperbolic parameters given in Table 3.9 which were derived by Sharma et al. (1976) for the 260.5 m high Tehri dam were used in the study.

Table 3.9 Hyperbolic parameters used in rockfill modeling by Khalid et al,1990

Parameters	Rockfill Material
Unit weight, kN/m^3	20
Cohesion c , kN/m^2	-
Friction angle, ($^\circ$)	38
Modulus number, K	2500
Modulus exponent, n	0.25
Failure ratio, R_f	0.76
Poisson's ratio parameter, G	0.43
Poisson's ratio parameter, F	0.19
Poisson's ratio parameter, d	14.80

In the analysis, the effect of intermediate principal stress is allowed where it was taken as average of major and minor principal stresses. The Poisson's ratio kept within the limits of 0.18 and 0.485. Sequential construction and incremental reservoir loading are used in order to simulate the behaviour more realistically. The concrete

membrane was thought to be constructed after the rockfill embankment was finished. The finite element mesh is shown in Figure 3.30.

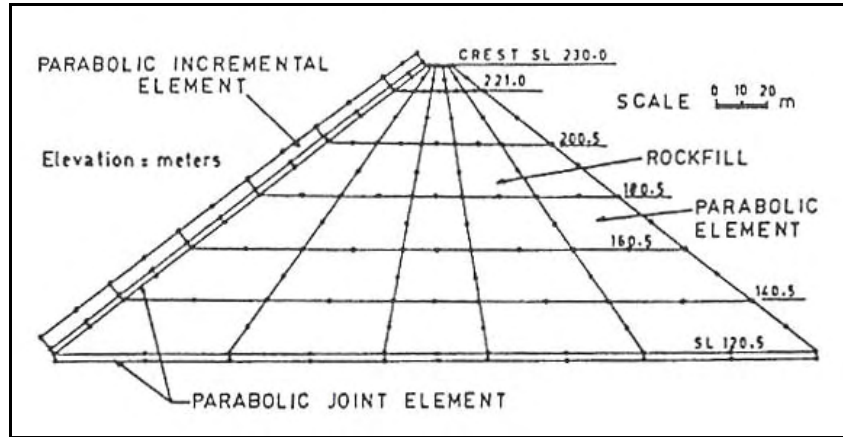


Figure 3.30 Finite element mesh used in the study of Khalid et al., 1990

In Figure 3.31, the calculated stress distributions are shown both for construction and reservoir full conditions where contours of calculated horizontal and vertical displacements (settlements) are given in Figure 3.32. In these figures, Khalid et al. calculated horizontal and vertical displacements separately in reservoir full condition. However, the stresses calculated at the reservoir full condition include the stresses at the end of construction condition as initial stresses.

It was indicated by Khalid et al. that for the end of construction case, the stresses in the upstream half mirror those of the downstream half, as expected. For corresponding points at the same horizontal elevation, the ratio of vertical stress to the depth of overburden rock is less in central region and increases for points near the two dam faces indicating part of the weight of embankment material coming over to the central portion is thrown to the sides (Khalid et al., 1990).

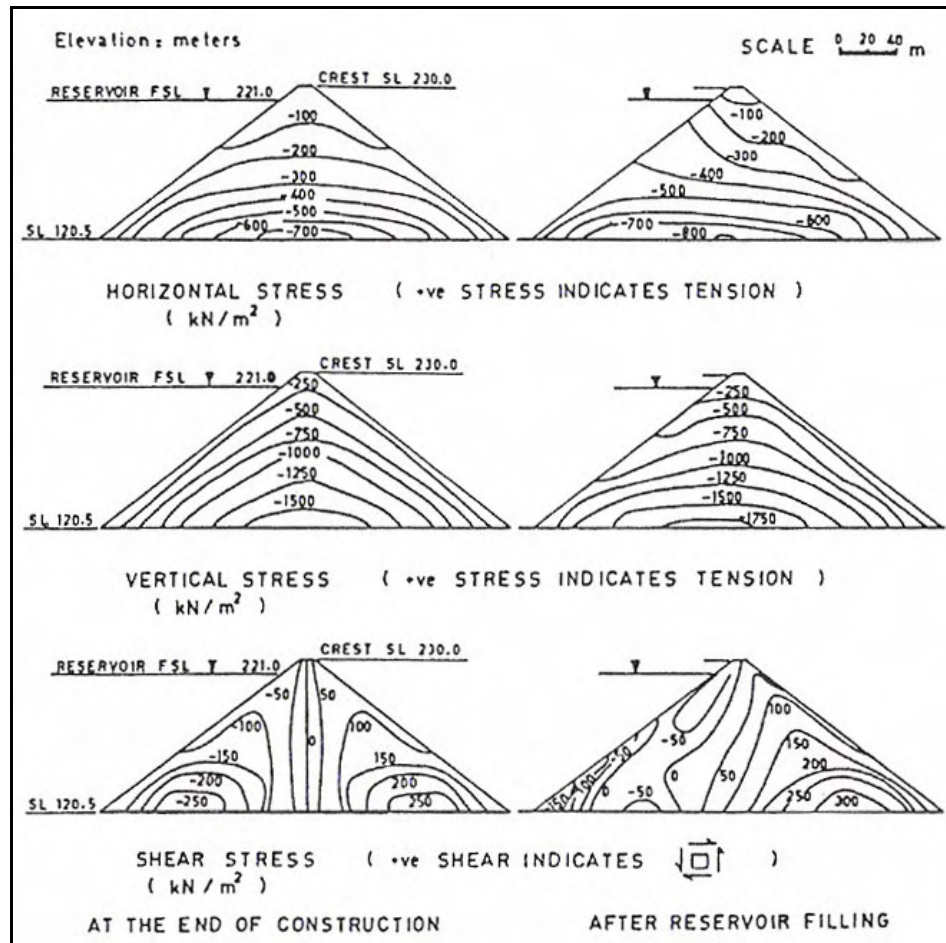


Figure 3.31 Contours of calculated stresses in Cethana dam (Khalid et al., 1990)

When the reservoir water load was applied on the membrane, both the horizontal and vertical stresses in the upstream half of rockfill embankment increased considerably. But in the downstream part, the increase in stresses is very little. This difference in stresses is one of the major behavioral differences of CFRDs from the conventional earth core rockfill dams where the reservoir water load causes reduction of both the horizontal and vertical stresses in the upstream shell and increases the stresses in the downstream shell. However in the case of membrane faced dams, the total force exerted by the reservoir on the dam is directed downwards with a much greater inclination, thereby increasing the stresses in the upstream portion with only marginal effect in the downstream portion of the dam. The difference in the shear

stresses are significant also. In the reservoir full condition, water force pushes the dam towards downstream thus stresses in the upstream portion were increased (Khalid et al., 1990).

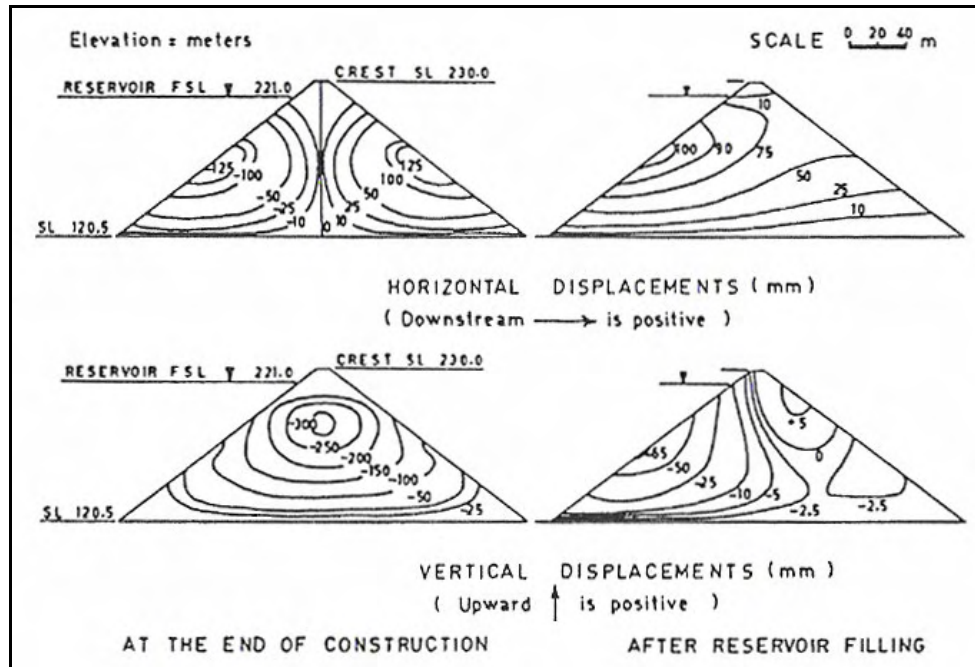


Figure 3.32 Contours of calc. displacements in Cethana dam (Khalid et al, 1990)

When the displacements for the end of construction were analyzed, it is seen that horizontal displacements is zero along the dam centerline and increases towards upstream and downstream faces. The max. horizontal displacement was calculated at the dam faces, at about $0.45H$ above the base where H is the dam height. The calculated max. vertical settlement was about 0.275% of the height which was occurred at $0.65H$ level. For the reservoir full condition, both of the max. horizontal and vertical displacements occurred at the upstream face at about $0.50H$ level.

For the analysis in the cross valley transverse direction, Khalid et al considered vertical sections that intersects the concrete membrane and parallel to dam axis as the one shown in Figure 3.33 where it is indicated that, movement of

rockfill along an inclined path from the abutment towards the center of the valley. The horizontal displacements indicate compression in the central portion of the membrane and tension along the entire perimeter of the contact of the face slab with sloping abutments. (Khalid et al., 1990)

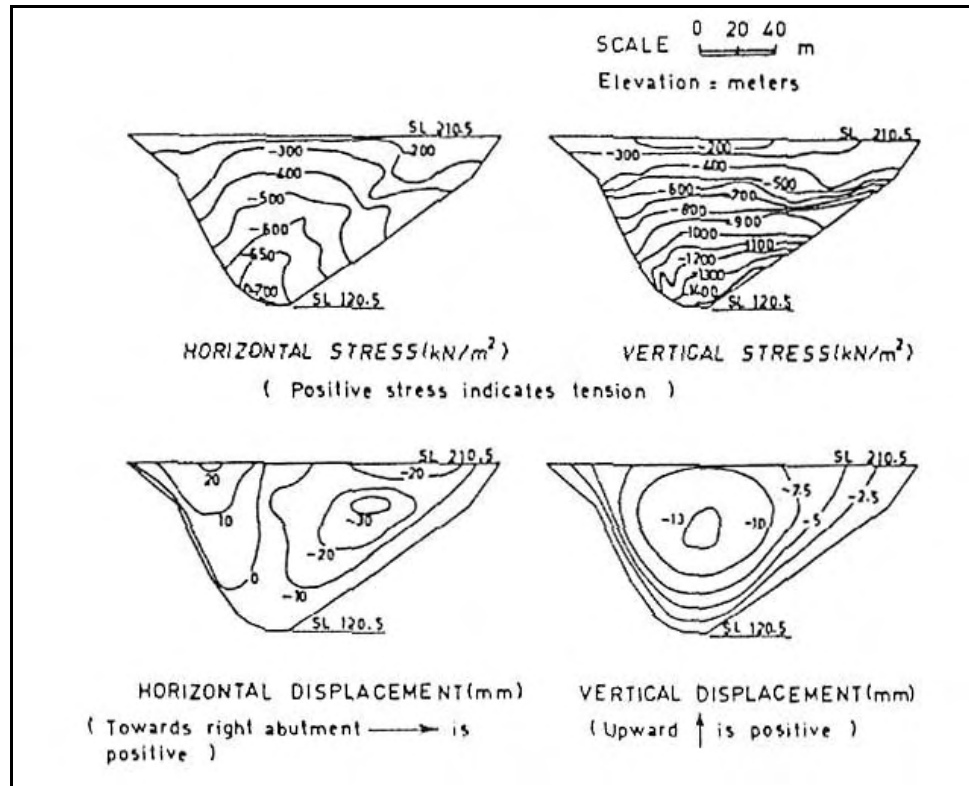


Figure 3.33 Contours of stresses and displacements for reservoir filling in cross-valley transverse dam section (Khalid et al., 1990)

In the next part of their study, Khalid et al. analyzed the deflection of concrete membrane due to reservoir filling. Two kind of deflections were calculated; (1) slope deflection defining the deflection from crest to the toe in the plane of membrane and normal to dam axis and (2) the normal deflection which defining the deflection in the direction normal to the plane of the face. In Figures 3.34 and 3.35, the calculated slope deflection and normal deflection distributions are depicted due to varying levels of reservoir, respectively.

Despite its success in certain points, the non-linear analyses of Khalid et al. failed in predicting downstream face and crest displacements due to reservoir filling. One of the shortcomings of the study was in predicting the stresses in the concrete membrane since it was concluded from Figure 3.36 that, the non-linear analyses resulted tensile stresses all along the membrane length in slope direction, which was contrary to observations in Cethana dam, where compression was observed in the central portion of the membrane (Khalid et al., 1990).

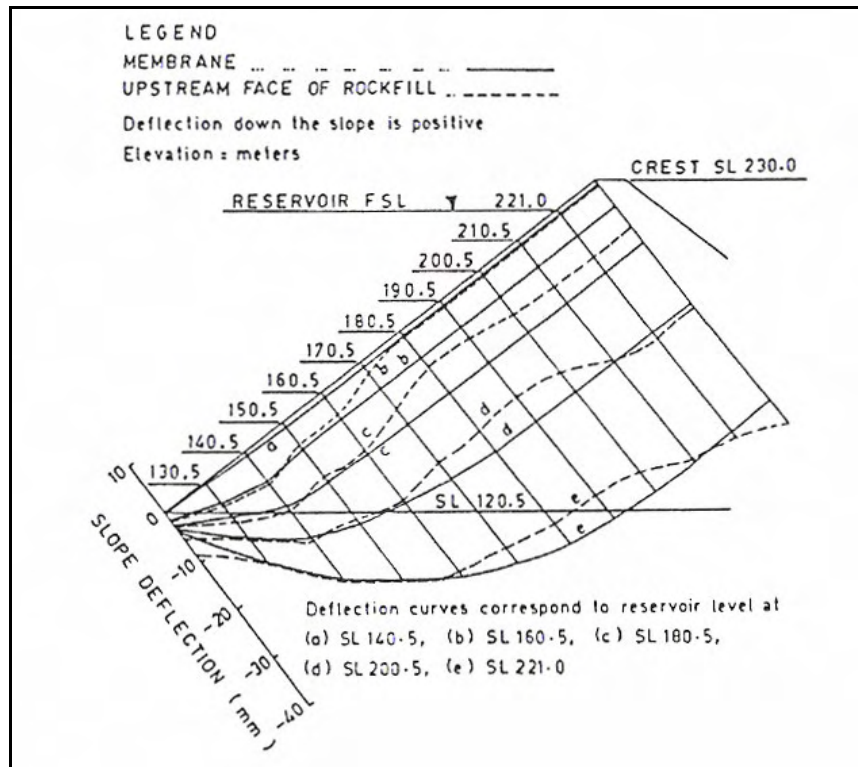


Figure 3.34 Slope deflection of concrete membrane and upstream face of rockfill for different stages of reservoir filling in Cethana dam (Khalid et al., 1990)

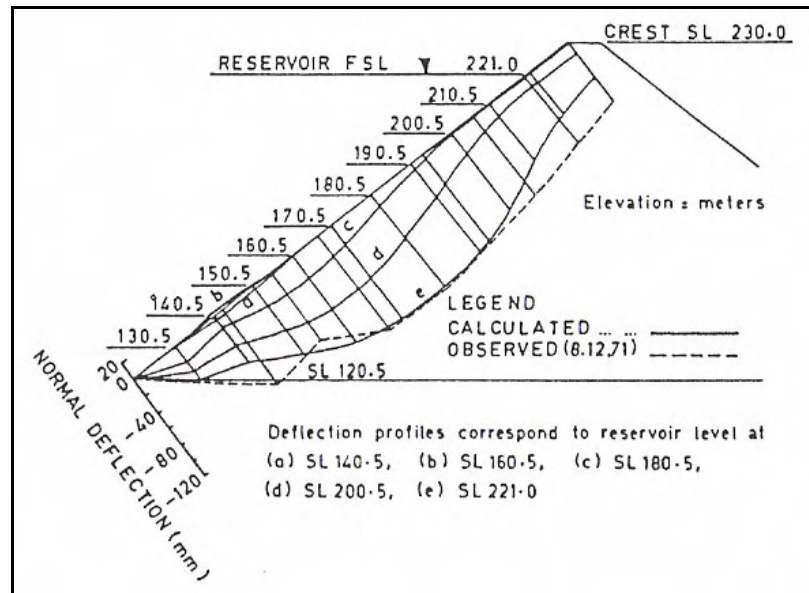


Figure 3.35 Normal deflection of concrete membrane for different stages of reservoir filling in Cethana dam (Khalid et al., 1990)

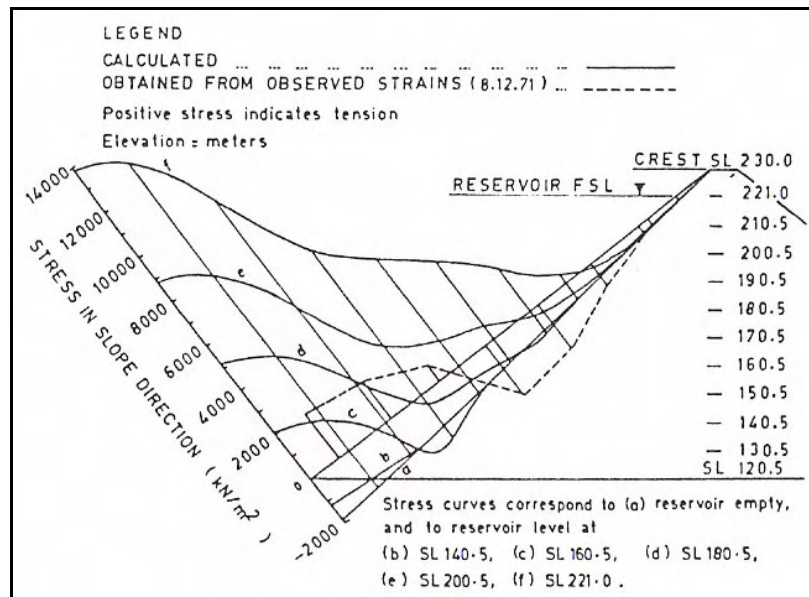


Figure 3.36 Slope stress in concrete membrane for different stages of reservoir filling in Cethana dam (Khalid et al., 1990)

In 1993, Saboya et al. analyzed the behaviour of 160 m high Foz de Areia dam which is located in Brazil. As mentioned in Chapter 2, when it was completed, Areia dam was the world's highest CFRD.

In Figure 3.37 the simplified cross section of Areia dam is shown. As it can be seen from this figure Saboya et al. did not include the transition zone materials beneath the concrete face and downstream face material since they thought that these materials would not significantly affect the predicted dam response (for zoning of Areia dam, see Figure 3.1).

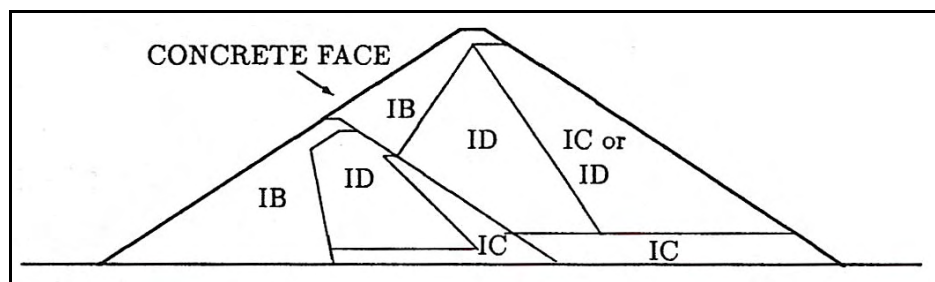


Figure 3.37 Simplified cross section used in the analysis by Saboya et. al, 1993

Areia dam comprises 75% massive basalt and 25% basalt breccia in the rockfill embankment. In Figure 3.38, the grading curves of these materials is shown with the measured mechanical properties of the materials. Zones IB and ID was compacted in 0.8 m layers whereas zone IC in 1.6 m layers.

In the finite element analyses, Duncan and Chang's hyperbolic model was used to evaluate the tangent elastic modulus and bulk modulus concept was used for the volume change characteristics which was developed by Duncan et al., 1980. The hyperbolic parameters were selected from the available parameters in the literature which are listed in Table 3.10, since Saboya et al. did not conducted triaxial tests. A special computer program called FEADAM84 developed by Duncan et al. (1984) was used in the finite element calculations.

As mentioned earlier, some elements in the embankment fill behave as in unloading condition in the reservoir impounding stage (See Duncan et al., 1980 and Fitzpatrick et al., 1985 for more details). In this program two different criteria were

used to verify an element is being loaded or unloaded; (1) stress level and (2) stress state. The first criteria can be defined as follows:

$$SL = \frac{(\sigma_1 - \sigma_3)}{(\sigma_1 - \sigma_3)_f} \quad (3.1)$$

If $SL \geq SL_{\max}$, where SL_{\max} is the previous max. stress level ever experienced by the element, the element is in loading condition and tangent elastic modulus (E_t) is used; otherwise unloading modulus (E_{ur}) is used. The second criteria is defined as follows:

$$SS = SL \left(\frac{\sigma_3}{p_a} \right)^{1/4} \quad (3.2)$$

The second criteria was used in the analyses with the following modification (Saboya et al., 1993).

$$SL_{crit} = \frac{SS_{\max}}{\left(\frac{\sigma_3}{p_a} \right)^{1/4}} \quad (3.3)$$

where SL_{crit} is the critical stress level above which the primary loading behaviour is assumed (Saboya et al., 1993).

The finite element analyses was carried out for end of construction and for reservoir impounding stages. The embankment considered to be built in 14 layers. In Figure 3.39 the finite element mesh is shown. In Figure 3.40 calculated settlements beneath the dam axis are shown with the observed settlements for the end of construction case. Here, the predicted behaviour was in very close to the observed values beneath the dam axis. The first stage dam axis is shown in Figure 3.1.

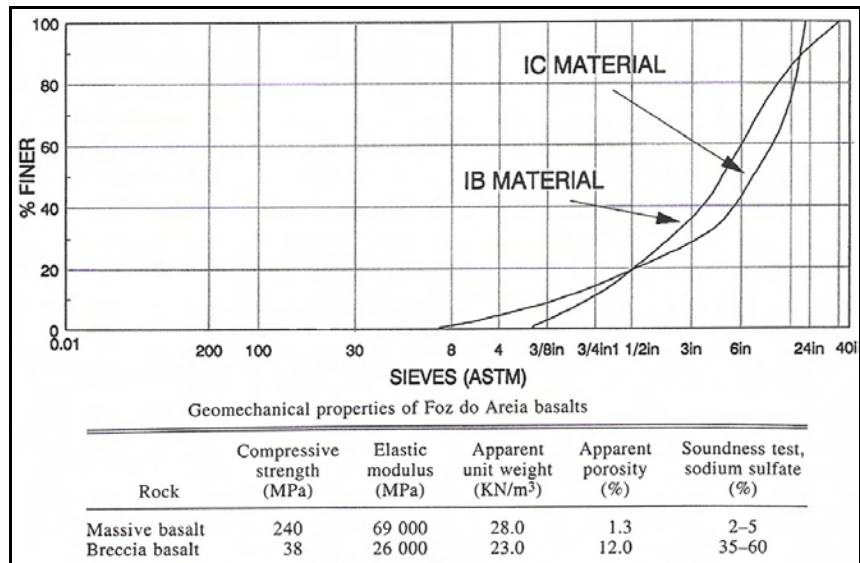


Figure 3.38 Areia dam rockfill grading curves and rockfill material properties
(Saboya et. al, 1993)

Table 3.10 Typical hyperbolic parameters (Saboya et. al, 1993)
(* references are given in Duncan et al., 1980)

Reference	C _u	K _E	n	m	K _B	D _r (%)	D ₆₀ (cm)	Particle type
Marsal 1973	18.0	534	0.37	0.14	283	-	20.0	Sound basalt, sub-angular
Signer, 1973	4.7	450	0.35	-	-	82	5.0	Sound basalt, sub-angular
Signer, 1973	5.0	400	0.51	-	-	100	2.0	Basalt, sub-angular
Marsal et al*	52.0	540	0.43	0.34	135	70	4.7	Conglomerate, sub-angular
Marsal et al*	84.0	690	0.45	0.22	170	85	2.1	Gravel, sub-rounded
Marsal et al*	5.5	340	0.28	0.18	52	90	9.3	Diorite, angular
Marsal et al*	19.0	450	0.37	0.18	255	95	1.9	Basalt, angular
Shannon*	2.5	410	0.21	0.00	175	90	1.5	Crushed basalt, angular

Saboya et al. indicated that, it has been found that during impounding CFRDs respond in a stiffer manner than during construction and measured deflections are smaller from the construction measurements (Saboya et al, 1993). Under unload-reload conditions, Duncan et al (1980) found that the unload-reload moduli E_{ur} , are similar and 1.2-3.0 times the primary modulus, E . Byrne et al. (1987), based on tests on granular soils, and Marsal (1973), based on rockfill found E_{ur}/E ratio in the range 2-4. (Saboya et al, 1993) For linear elastic analysis, it has been a common practice to increase the elastic moduli by a factor of two or three in order to achieve unloading behaviour in reservoir impounding stage (Fitzpatrick et al., 1985).

In Figure 3.41, the calculated settlements of Areia dam are compared with the observed values. The results indicated that K_{ur}/K_E ratios in the range 3-4 gives a good agreement with the measured values (Saboya et al., 1993).

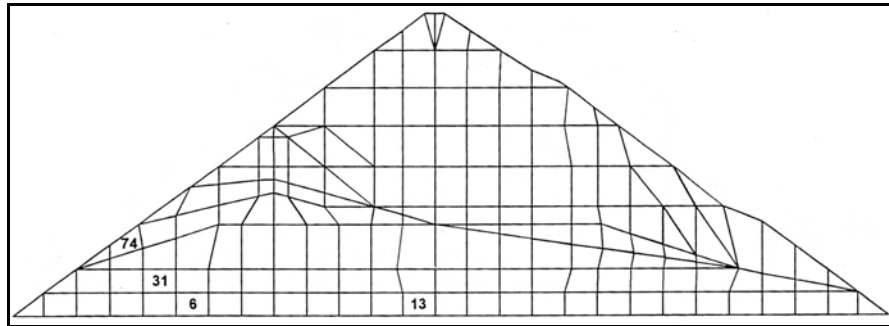


Figure 3.39 Finite element mesh used in the analysis by Saboya et. al, 1993

In Figure 3.42, the effect of reservoir water level on the elastic modulus are shown on the selected elements by Saboya et al., 1993. They concluded that, if the water level is less than 100 m, the material adjacent to the upstream membrane responds in unloading manner and when the water level exceeds 100 m, the material behave in first-time loading manner. This finding could explain the poor behaviour of a number of un-compacted rockfill dams constructed in 1950s when their heights and hence water levels exceeded about 100 m such as Salt Springs and Paradela dams (Saboya et al., 1993).

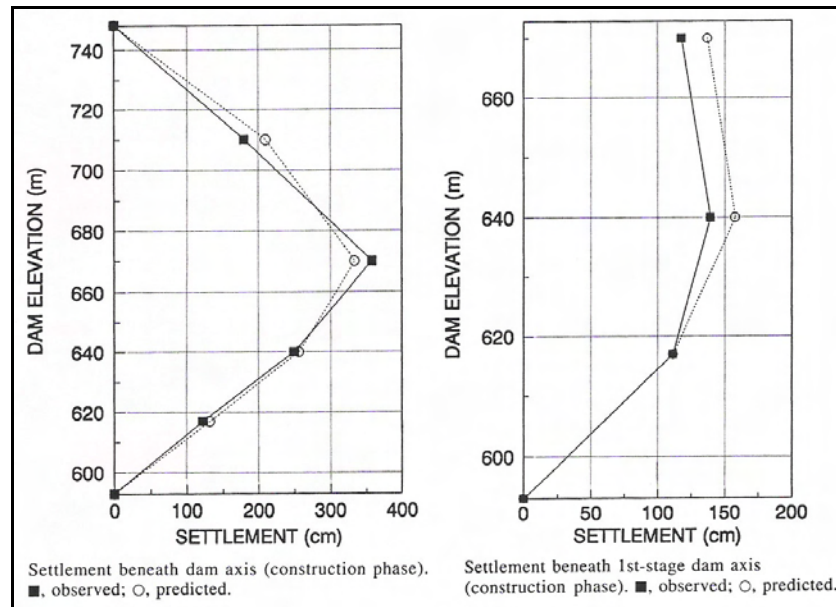


Figure 3.40 Calculated and observed settlements for end of construction condition in Areia dam (Saboya et. al, 1993)

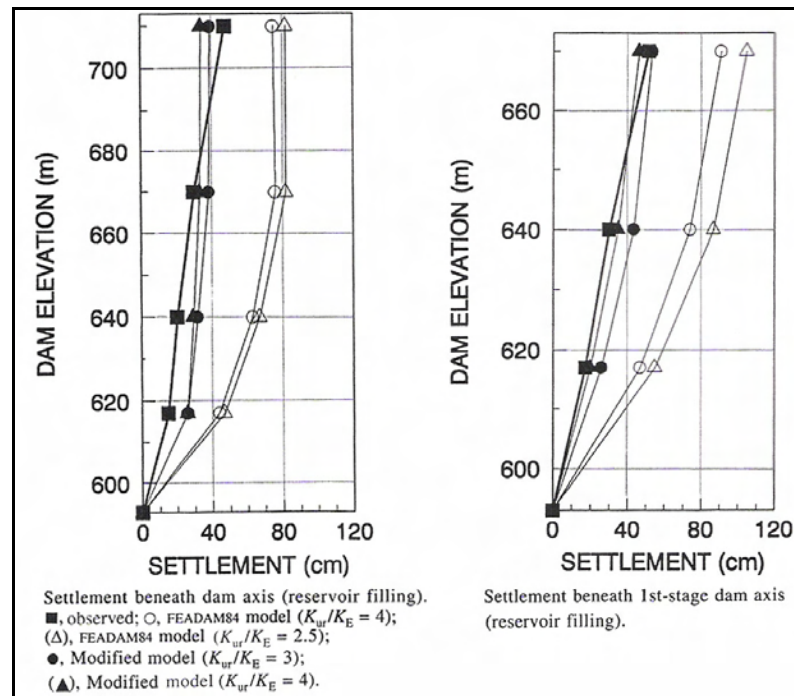


Figure 3.41 Calculated and observed settlements for reservoir full condition in Areia dam (Saboya et. al, 1993)

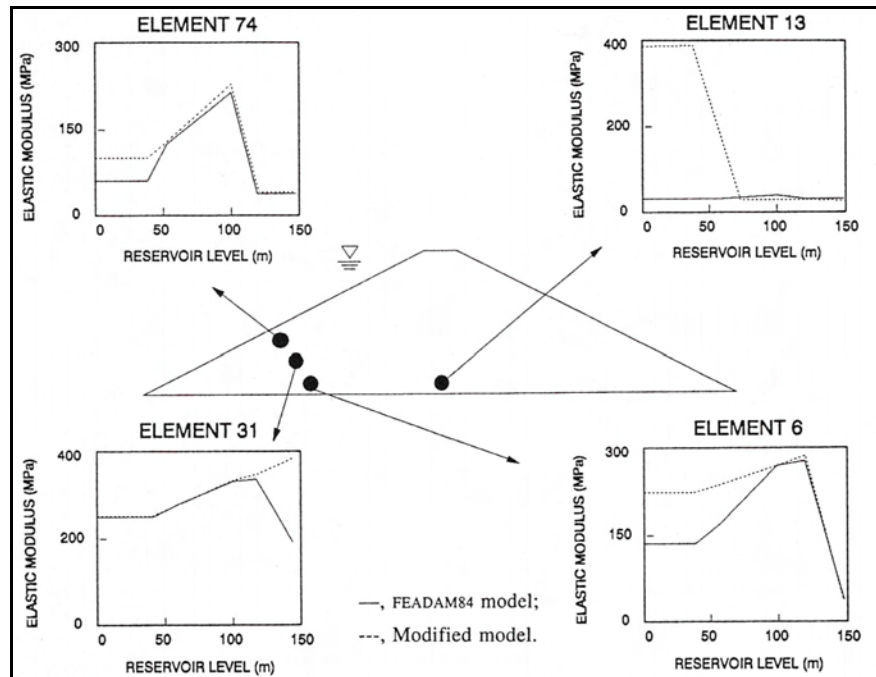


Figure 3.42 Change in elastic modulus in reservoir filling (Saboya et. al, 1993)

One of the recent studies is carried out by Liu et al. in 2002. They performed three-dimensional finite element analysis of Yutiao dam located in China. The dam is 110 m high and built in a asymmetric valley having 35° - 50° and 55° - 70° slopes at the left and right abutments respectively. The crest length is 204 m. Three dimensional finite element mesh and max cross section are shown in Figure 3.43 where positive X direction corresponds to the direction from left abutment to right abutment, the one of Y axis is the direction from upstream to downstream and the one of Z axis is the direction from bottom to top (Liu et al., 2002).

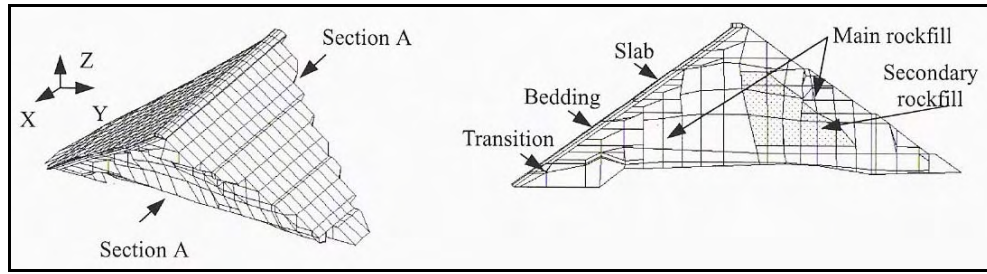


Figure 3.43 Finite element mesh and max section of Yutiao dam (Liu et al.,2002)

In their analyses, Duncan and Chang's hyperbolic model was used with the hyperbolic material model parameters listed in Table 3.11. (for information about hyperbolic parameters, see Section 2.4) In the calculations, FEADAM84 computer program was used. The dam was thought to be constructed in 13 steps where the last one was for concrete membrane casting. The 14th step was the beginning of reservoir filling and 17th step was the end of reservoir filling where reservoir level achieved 108 m in height.

Table 3.11 Hyperbolic model parameters used in analysis by Liu et al., 2002

Material Type	K_E	ϕ (°)	$\Delta\phi$ (°)	n	R_f	K_b	m
Slab	190000	0	0	0	0	120000	0
Main rockfill	800	46	0	0.34	0.75	400	0.40
Bedding	910	45	0	0.37	0.65	455	0.40
Transition	850	46	0	0.37	0.65	425	0.48
Secondary rockfill	300	42	5.7	0.17	0.82	166	0.28

The calculated horizontal and vertical displacements for construction and reservoir filling conditions are shown in Figure 3.44. It was indicated that, horizontal deformation of upstream part during reservoir filling is less than that of end of construction condition where horizontal deformations of downstream under two

loading conditions were the same. When the settlements were compared, it was seen that the settlements were slightly increased during reservoir filling (Liu et al., 2002).

Contours of calculated major and minor principle stresses for the end of construction and reservoir filling conditions are shown in Figure 3.45. It can be seen from this figure that, reservoir filling increased both of the principle stresses significantly where the increase mostly occurred in the vicinity of concrete membrane, as expected.

Contours of calculated displacements in the other two directions and stresses of the concrete membrane for the reservoir filling stage are given in Figure 3.46. It was seen that, the major horizontal displacement in the x-direction was 0.035 m which occurred at 0.7-0.8H level (for the directions see Figure 3.41). Major vertical displacement occurred in the middle of the slab whose value was 0.169 m. When the stresses are examined, it is seen that major portion of the slab was under compression except the vicinity of abutments where tension stresses occurred at those points (Liu et al., 2002).

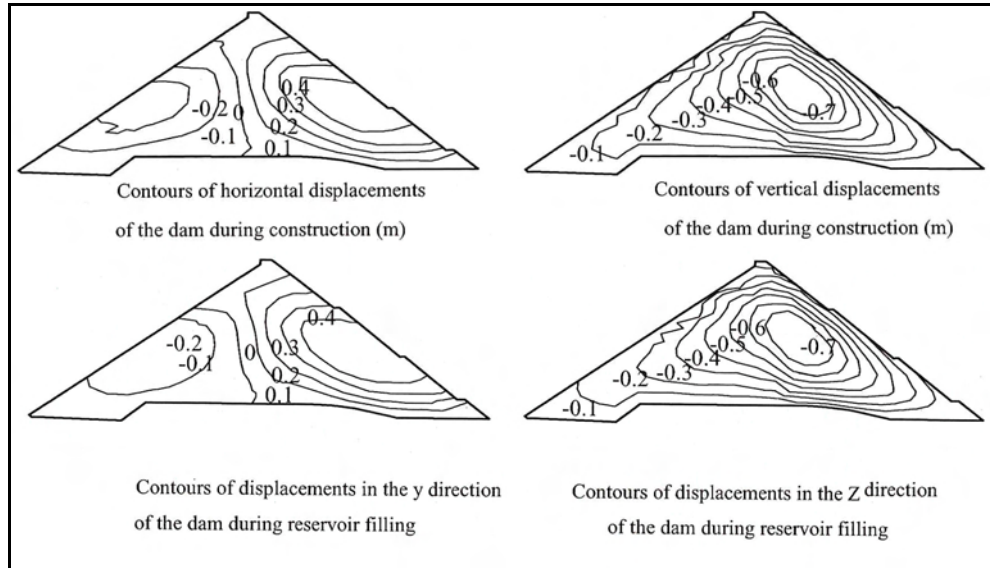


Figure 3.44 Contours of displacements in Yutiao dam (Liu et al., 2002)

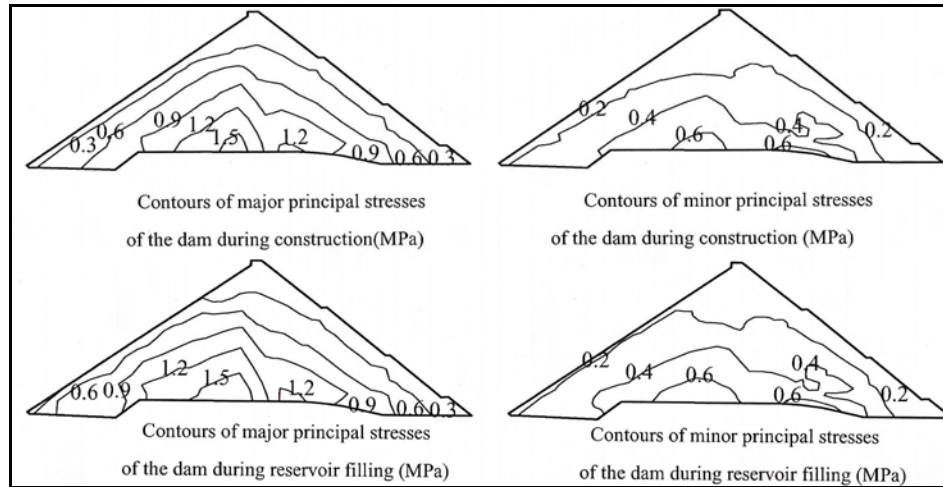


Figure 3.45 Contours of calculated stresses in Yutiao dam (Liu et al., 2002)

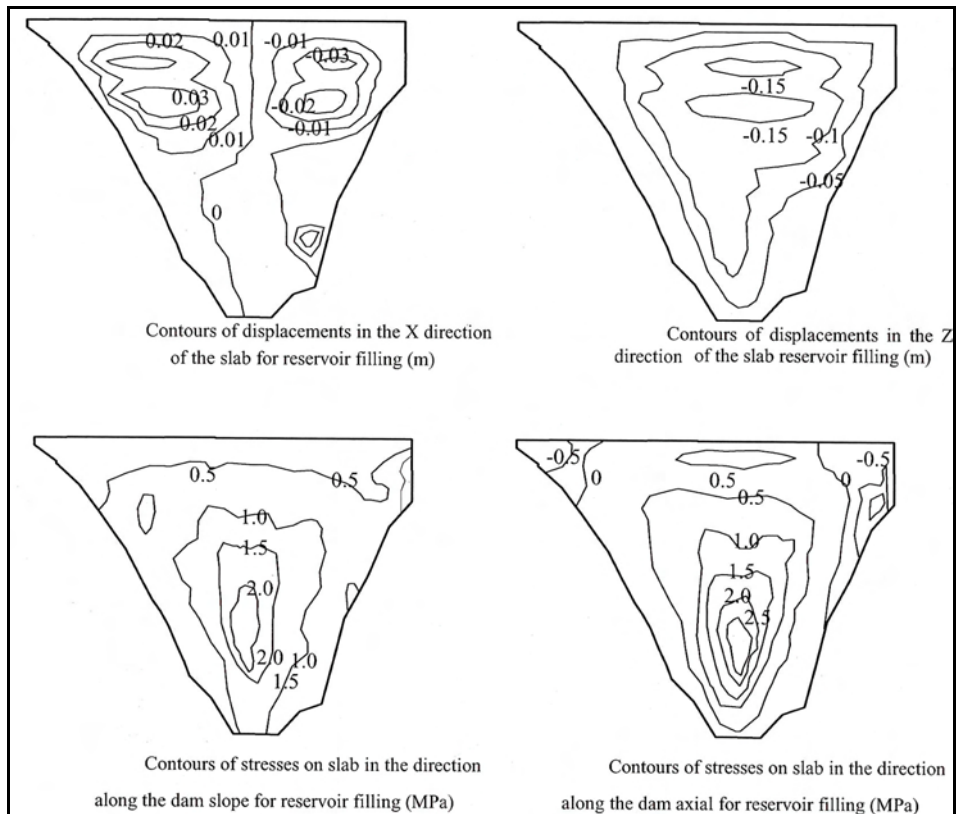


Figure 3.46 Contours of calculated displacements and stresses of the slab for reservoir filling in Yutiao dam (Liu et al., 2002)

CHAPTER 4

SETTLEMENT ANALYSES OF KÜRTÜN DAM BY FINITE ELEMENT METHOD

4.1 Kürtün Dam

Kürtün dam is the first CFRD in Turkey and it is located in East Black Sea Region, 27 km northwest of Torul, of Gümüşhane province and built on Harşit river. The main purpose of the project is energy production. It has a capacity and annual generation of 85 MW and 198 GWh, respectively. In the preliminary project, Kürtün dam was designed as an ECRD, however due to heavy rainy weather conditions and difficulties in obtaining impervious soils, the dam was redesigned as a CFRD. In Figure 4.1 a view of the completed dam from the upstream is given.

Construction of the rockfill embankment was started in 1997 and completed on 28.04.1999. After the completion of rockfill embankment, the construction process paused for about 1.5 years until the start of construction of concrete membrane. This time period was for the completion of the major portion of the rockfill embankment settlement and to protect the membrane from these settlements.

After the completion of concrete membrane, the parapet wall at the crest and the fill behind it are constructed. The reservoir impounding process started on 08.02.2002 and reservoir level achieved 630 m elevation on 28.05.2002.

Kürtün dam is 133 m high from the river bed having slopes of 1.4:1 and 1.5:1 (H:V) for upstream and downstream embankment faces, respectively. The slope of the concrete membrane is 1.4055:1. The crest length is 300 m.

The dam is constructed on a narrow and steep valley. The river width is 40 m and average abutment slopes are 61° and 52° for the left and right abutments respectively.

The max. cross section of the dam is given in Figure 4.2 with material zoning. Detailed information about the materials shown in Figure 4.2 is given, in Table 4.1, together with construction methods.

The basic geologic formations at the dam site are granodiorite, diabase, andesite and limestones. Among these formations, granodiorite is the most common one where the dam settled on. During foundation explorations, it was observed that weathering was high at the right abutment.



Figure 4.1 View of Kürtün dam from the upstream (DSİ, 2003)

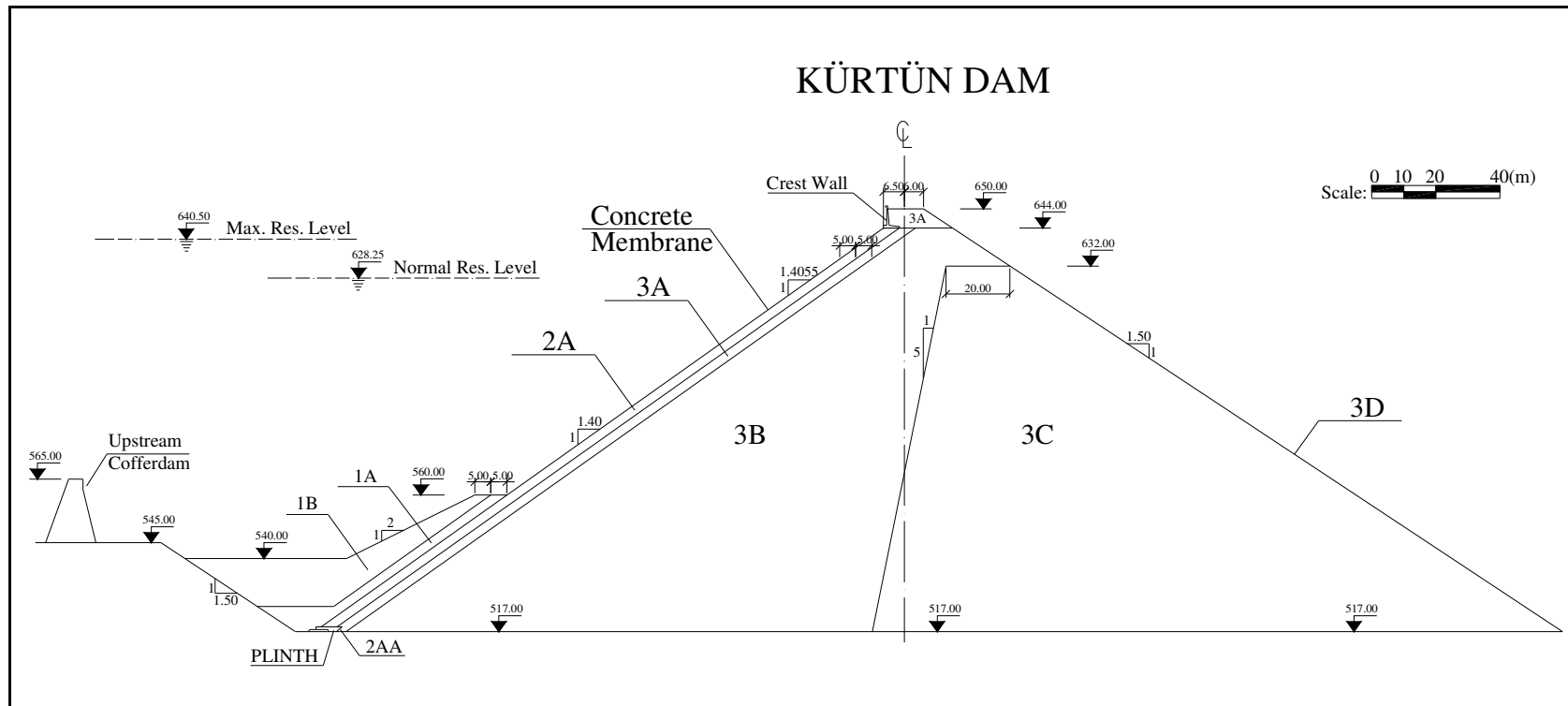


Figure 4.2 Max cross section and zoning of Kürtün dam (dimensions are in meters)

Table 4.1 Materials and Construction Techniques used in Kürtün dam

Zone	Material				Construction Techniques	
	Type	Particle Sizes			Layers (m)	Compaction with a 10 t. vibratory roller
		D _{max} (mm)	Sand Limit (%)	Fines Limit (%)		
1A	Impervious Fill	50	>70	>35	0.60	4 passes (static)
1B	Tuvenan Alluvium	400	-	<20	0.60	4 passes
2A	Sieved Rock (or alluvium)	150	30-55	2-10	0.40	6 passes (surface: 4 static + 6 dynamic)
2AA	Filter	20	70-100 40%<0.5	<5	-	-
3A	Selected Rock	300	15-45	<5	0.40	6 passes
3B	Quarry Rock Fill	600	<20	<5	0.80	4 passes + 150 lt/m ³ water
3C	Quarry Rock Fill	1000	-	<2	1.20	4 passes
3D	Selected Rock	2000	-	-	Surface placed rocks	

4.2 Instrumentation

Kürtün dam was extensively instrumented in order to observe the behaviour of the dam. Four type of instruments are used for monitoring the behaviour. These are:

- Hydraulic settlement devices, located in the rockfill embankment (ZDÖ)
- Hydraulic pressure cells, located in the rockfill embankment (BÖ)
- Strainmeters, located in the concrete membrane (GÖ)
- Surface-mount jointmeters, located in the concrete membrane (DDÖ)

In Kürtün dam, a total of 33 hydraulic settlement devices (ZDÖ) and 21 earth pressure cells (BÖ) are installed in the rockfill embankment, in three cross sections (0+120, 0+180 and 0+240) and at four different elevations. In Figures 4.3, 4.4 and 4.5, locations of these devices are shown. The cross-sections are indicated in Figure 4.6 together with the locations of instruments installed at the concrete face. As it is shown in Figure 4.6, 16 surface-mount jointmeters (DDÖ) and 6 strainmeters (GÖ) are installed in the membrane whose locations are given in Table 4.2. The properties of the instrumentation devices are briefly outlined in this section.

Table 4.2 Locations of concrete membrane instruments

Instrument	Elevation (m)	Location (Km)	Instrument	Elevation (m)	Location (Km)
DDÖ-1	603.11	0+258.54	DDÖ-12	626.29	0+018.54
DDÖ-2	589.61	0+243.54	DDÖ-13	575.00	0+161.04
DDÖ-3	576.12	0+236.04	DDÖ-14	600.00	0+101.04
DDÖ-4	544.56	0+198.54	DDÖ-15	600.00	0+206.04
DDÖ-5	521.41	0+161.20	DDÖ-16	625.00	0+161.04
DDÖ-6	560.00	0+108.54	GÖ-1	540.00	0+153.54
DDÖ-7	566.83	0+093.54	GÖ-2	565.00	0+168.54
DDÖ-8	575.22	0+078.54	GÖ-3	585.00	0+108.54
DDÖ-9	583.71	0+063.54	GÖ-4	585.00	0+153.54
DDÖ-10	592.20	0+048.54	GÖ-5	615.00	0+168.54
DDÖ-11	606.57	0+033.54	GÖ-6	615.00	0+228.54

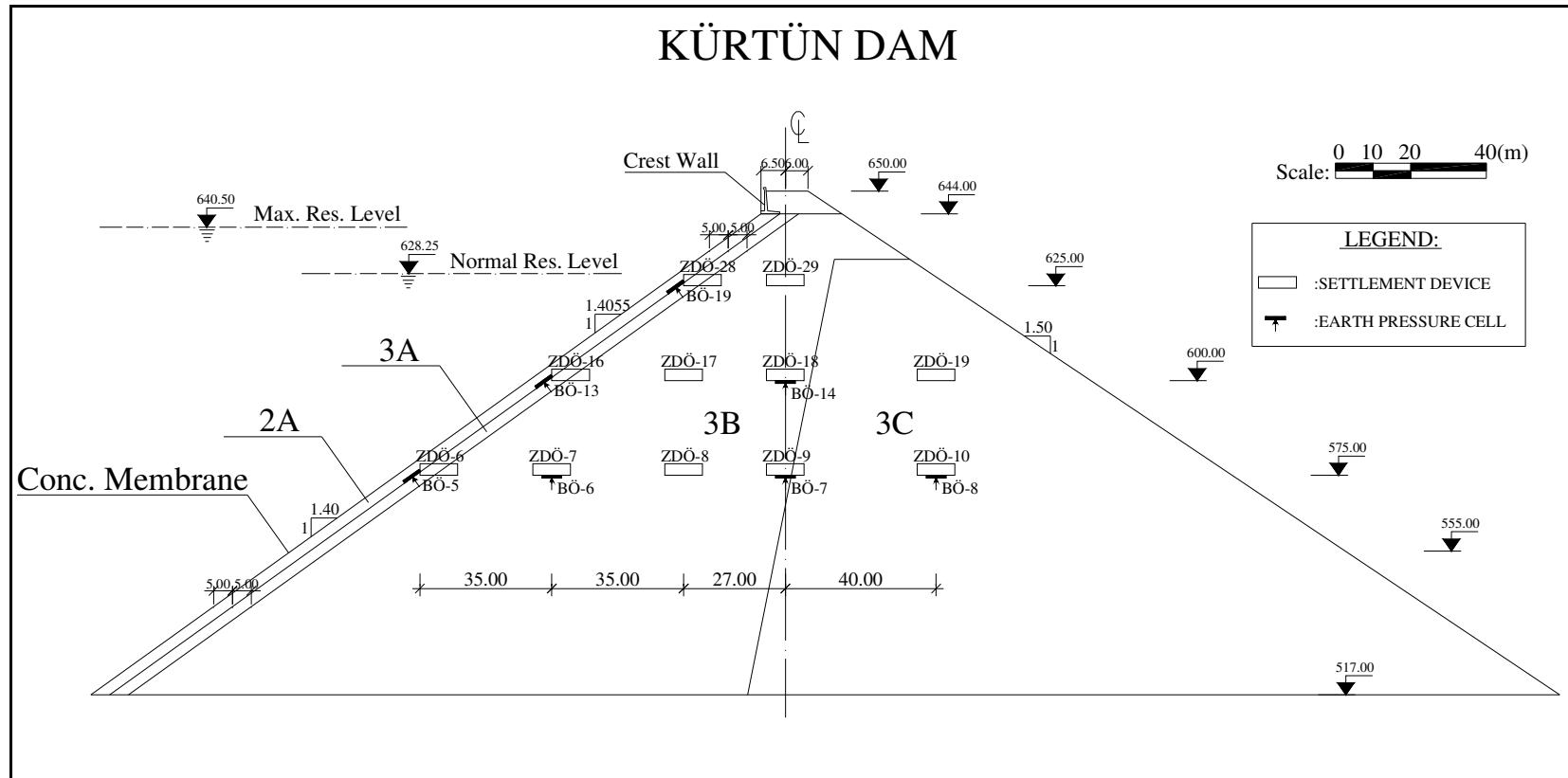


Figure 4.3 Location of settlement devices and pressure cells in cross section KM :0+120.00 of Kürtün dam

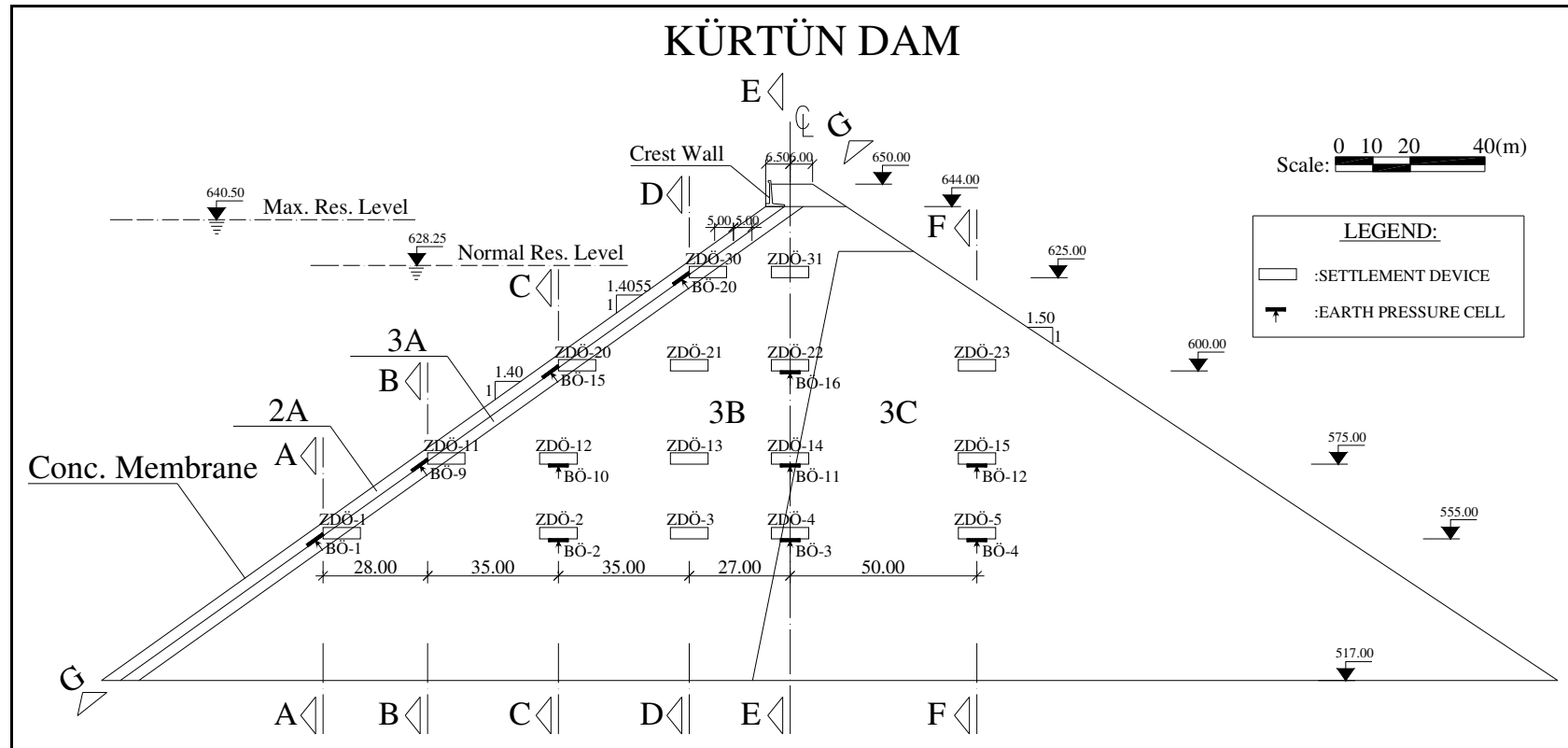


Figure 4.4 Location of settlement devices and pressure cells in max cross section (KM:0+180.00) of Kürtün dam

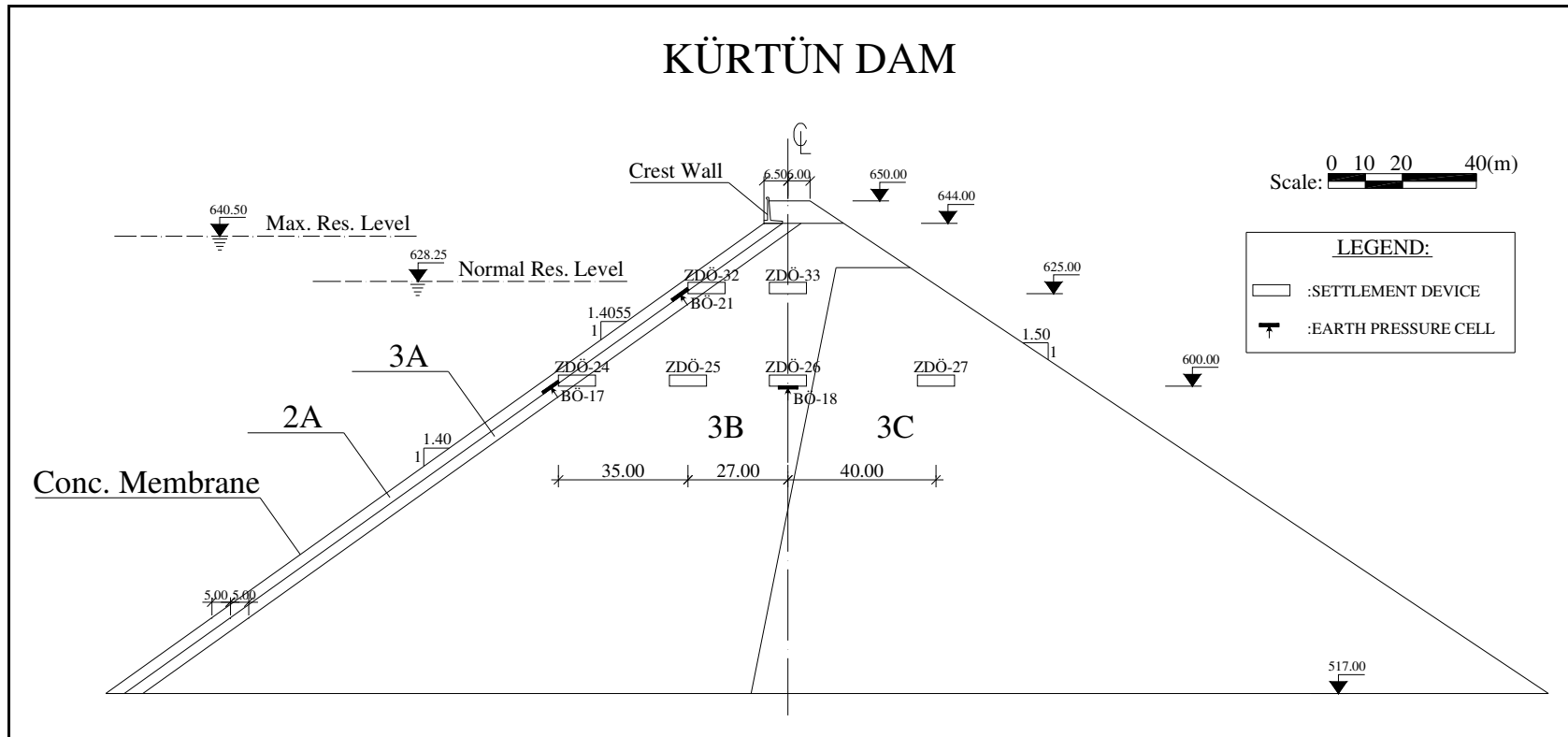


Figure 4.5 Location of settlement devices and pressure cells in cross section KM:0+240.00 of Kürtün dam

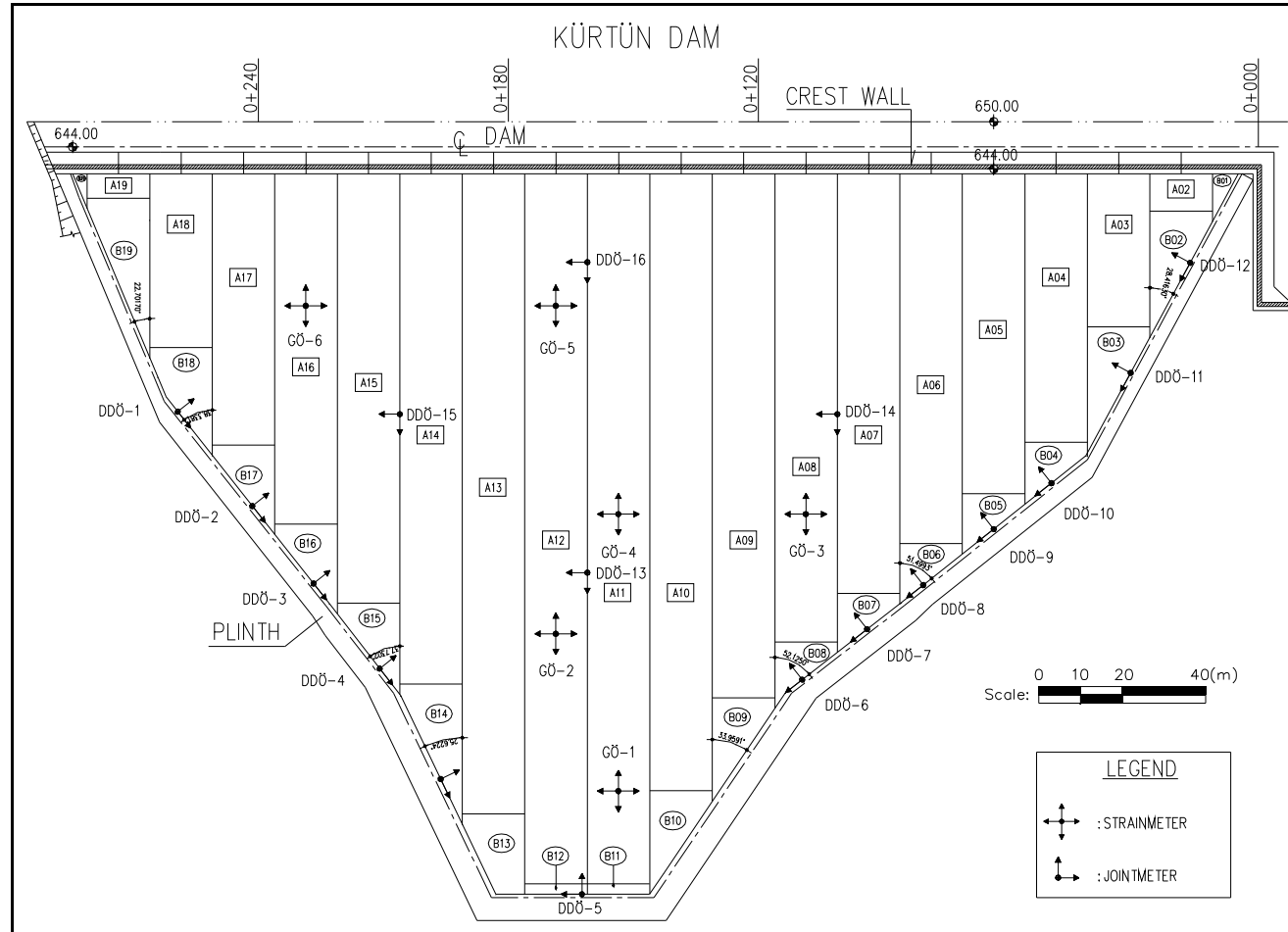


Figure 4.6 Locations of jointmeters and strainmeters at concrete membrane of Kürtün dam

4.2.1 Hydraulic Settlement Devices

These devices consist of the measuring sensors with temperature compensated pressure transducers linked to one another by a liquid line and a data line. They are designed for monitoring settlement in embankments by measuring the difference in pressure created by the column of liquid in the tubing. As the transducer settles with the surrounding ground the height of the column increases and the pressure changes. Later the pressures are converted to settlements with the relation of “1 bar = 10 m.” The device has a measuring range of 5 m. with a system accuracy of ± 20 cm. In Figure 4.7 a hydraulic settlement device is shown.

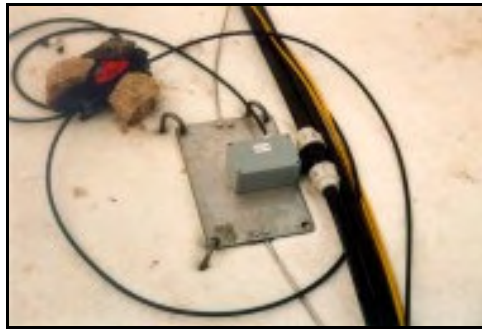


Figure 4.7 Hydraulic Settlement Device

4.2.2 Hydraulic Pressure Cells

These devices are used to measure the total stresses; namely the sum of effective stresses and pore water pressures. The total pressure cells are formed from two circular plates of stainless steel. The edges of the plates are welded together to form a sealed cavity, which is filled with fluid. Then a pressure transducer is attached to the cell. The cell is installed with its sensitive surface in direct contact with the soil. The total pressure acting on that surface is transmitted to the fluid inside the cell and then measured by the pressure transducer. In Figure 4.8 a hydraulic pressure cell is shown.

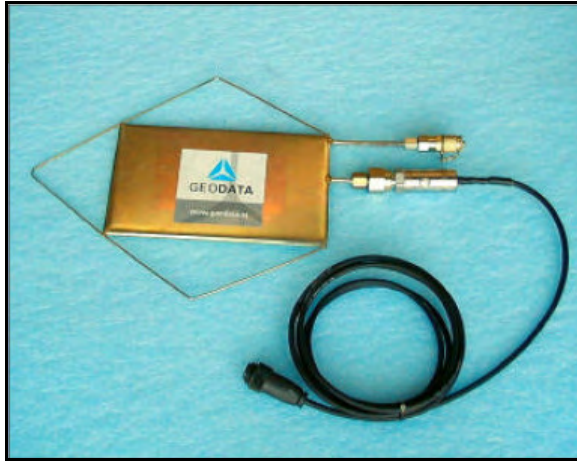


Figure 4.8 Hydraulic Pressure Cell

4.2.3 Strainmeters

Strainmeters are used in measuring the strains in concrete in order to detect the compression and tension zones. The strainmeters consist of a central tube and two parallel bars embedded in concrete which induce a displacement on the central tube. This is proportional to the displacement of concrete and is measured by the use of applied strain gauges. In Figure 4.9 a strainmeter is shown.



Figure 4.9 Strainmeter

4.2.4 Surface-Mount Jointmeters

These devices are used to monitor movement at joints and cracks which consist of two half-gauge fixtures, one mounted on each side of the joint. The jointmeters used at Kürtün dam are designed to measure the relative movements in three directions where each distance indicator is supported with one displacement transducer. In Figure 4.10, an example of the jointmeters is shown.

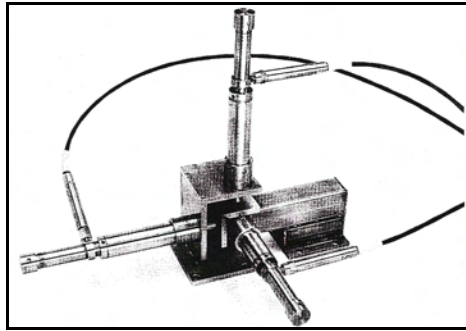


Figure 4.10 Surface-mount jointmeter

4.3 Observed Settlement Behaviour of Kürtün Dam

As mentioned in the previous sections, the embankment construction of Kürtün dam has started in 1997 and finished on 28.04.1999. During this period the performance of the dam has been inspected by hydraulic settlement devices installed at different locations in the rockfill embankment where the location of instruments are given in Figures 4.3, 4.4 and 4.5 (Cross section places are indicated in Figure 4.6). The observed settlements recorded at three cross sections by settlement devices are given in Tables 4.3, 4.4 and 4.5 where in these tables, 28.4.99 represents the end of construction (EoC), 08.2.02 represents the beginning of reservoir impounding and 28.5.02 represents the reservoir full condition (RFC, reservoir water level at 630.00). 23.9.03 is the last date of available observations.

As mentioned in the previous sections, construction of the concrete membrane started about 1.5 years after than the construction of the rockfill embankment completed up to El 644.00. The parapet wall and the fill behind it (between El's 644.00 and 650.00) has constructed after the completion of concrete membrane between 23.1.01 and 10.4.01.

4.3.1 Construction Period

When the Tables 4.3, 4.4 and 4.5 are examined, it is seen that, EoC settlements measured at corresponding elevations are higher at Km 0+180 than the other two cross sections, as expected. Min settlement values are recorded at Km 0+240 because it is the nearest section to the abutments. At the same cross section, settlement values are largest at the dam centerline and decrease in upstream and downstream directions as indicated in Figure 4.11. Max settlement value is 2155 mm which is recorded at ZDÖ 14 located at El 575 where settlement values reduce towards the crest and foundation along the centerline. This is due to the fact that, as the embankment construction continues rockfill material at lower elevations become relatively incompressible when compared with the newly constructed upper layers. Whereas the upper elevations continue to settle with a decreasing amount under their own weight.

Between 28.4.99 and 08.2.02, the embankment settled under its own weight. During this period, no significant settlement occurred at cross-sections 0+120 and 0+240 due to the support of the abutments except the instruments installed at El 625. However relatively significant settlements occurred at section 0+180. This indicates the effect of the newly constructed fill behind the parapet wall between El's 644.00 and 650.00. Also creep and secondary compression of rockfill material have an effect on the settlements recorded between 28.4.99 and 08.2.02.

4.3.2 Impoundment Period

During impoundment (08.2.02 – 28.5.02) significant settlements are observed at the instruments located close to upstream face (ZDÖ's 1, 11, 20, 30, 6, 16, 28, 24 and 32) due to reservoir water load, as expected. At the instruments under the concrete membrane, settlements are high in lower elevations and decrease towards upper elevations due to decreasing reservoir water load. Between the instruments located at the same cross section and same elevations, settlements in impoundment period are higher close to upstream face and decreases considerably towards downstream. When the instruments located at the same elevations but in different cross sections are considered, higher settlement values are observed in max cross section, as in the case of EoC settlements.

4.3.3 Operation Period

At the operation period (28.5.02 -) the rockfill embankment continue to settle due to creep and secondary compression of rockfill material, as it was indicated by Cooke (1984) and Clements (1984). The settlements are nearly at order of magnitude for the three cross-sections (See Figure 4.11).

Table 4.3 Recorded settlements at cross section 0+120 (settlements are in mm)

Instrument	Elevation (m)	28.4.99	23.1.01	10.4.01	08.2.02	28.5.02	31.3.03	29.3.03	28.4.99- 08.2.02	08.2.02- 28.5.02	28.5.02- 23.9.03
ZDÖ – 6	575	405	410	401	399	679	717	779	-6	280	100
ZDÖ – 7	575	1084	1136	1126	1124	1216	1228	1262	40	92	46
ZDÖ – 8	575	1522	1601	1600	1601	1646	1661	1705	79	45	59
ZDÖ – 9	575	1538	1636	1636	1640	1670	1712	1761	102	30	91
ZDÖ – 10	575	1016	1027	1027	1032	1067	1081	1103	16	35	36
ZDÖ – 16	600	674	667	682	651	826	824	859	-23	175	33
ZDÖ – 17	600	1380	1499	1513	1487	1567	1583	1638	107	80	71
ZDÖ – 18	600	1535	1579	1589	1558	1610	1646	1716	23	52	106
ZDÖ – 19	600	1256	1309	1317	1298	1342	1347	1391	42	44	49
ZDÖ – 28	625	538	689	709	725	854	872	927	187	129	73
ZDÖ – 29	625	650	792	822	839	935	974	1020	189	96	85

Table 4.4 Settlements at cross section 0+240 (settlements are in mm)

Instrument	Elevation (m)	28.4.99	23.1.01	10.4.01	08.2.02	28.5.02	31.3.03	29.3.03	28.4.99- 08.2.02	08.2.02- 28.5.02	28.5.02- 23.9.03
ZDÖ – 24	575	112	113	128	59	153	133	191	-53	94	38
ZDÖ – 25	575	486	499	510	491	538	527	578	5	47	40
ZDÖ – 26	575	835	923	947	953	994	993	1035	118	41	41
ZDÖ – 27	575	902	918	923	902	927	912	959	0	25	32
ZDÖ – 32	575	167	330	346	343	429	455	497	176	86	68
ZDÖ – 33	600	439	554	564	560	620	638	673	121	60	53

Table 4.5 Recorded settlements at cross section 0+180 (max cross section) (settlements are in mm)

Instrument	Elevation(m)	28.4.99	23.1.01	10.4.01	08.2.02	28.5.02	31.3.03	29.3.03	28.4.99- 08.2.02	08.2.02- 28.5.02	28.5.02- 23.9.03
ZDÖ – 1	555	311	292	292	285	648	654	699	-26	363	51
ZDÖ – 2	555	1113	1196	1198	1197	1236	1244	1287	84	39	51
ZDÖ – 3	555	1460	1585	1586	1591	1634	1663	1708	131	43	74
ZDÖ – 4	555	1607	1720	1724	1723	1749	1772	1804	116	26	55
ZDÖ – 5	555	1313	1422	1428	1434	1443	1463	1488	121	9	45
ZDÖ – 11	575	609	664	678	671	1036	1043	1101	62	365	65
ZDÖ – 12	575	1417	1560	1557	1560	1715	1743	1794	143	155	79
ZDÖ – 13	575	2019	2125	2123	2129	2198	2228	2272	110	69	74
ZDÖ – 14	575	2155	2305	2306	2315	2379	2441	2500	160	64	121
ZDÖ – 15	575	1682	1785	1790	1800	1849	1883	1932	118	49	83
ZDÖ – 20	600	836	913	927	911	1135	1155	1230	75	224	95
ZDÖ – 21	600	1592	1722	1738	1777	1884	1913	1991	185	107	107
ZDÖ – 22	600	1861	1997	2011	2024	2093	2118	2168	163	69	75
ZDÖ – 23	600	1462	1498	1511	1508	1550	1566	1623	46	42	73
ZDÖ – 30	625	621	724	739	744	879	904	974	123	153	95
ZDÖ – 31	625	717	926	982	1007	1127	-	-	290	120	-

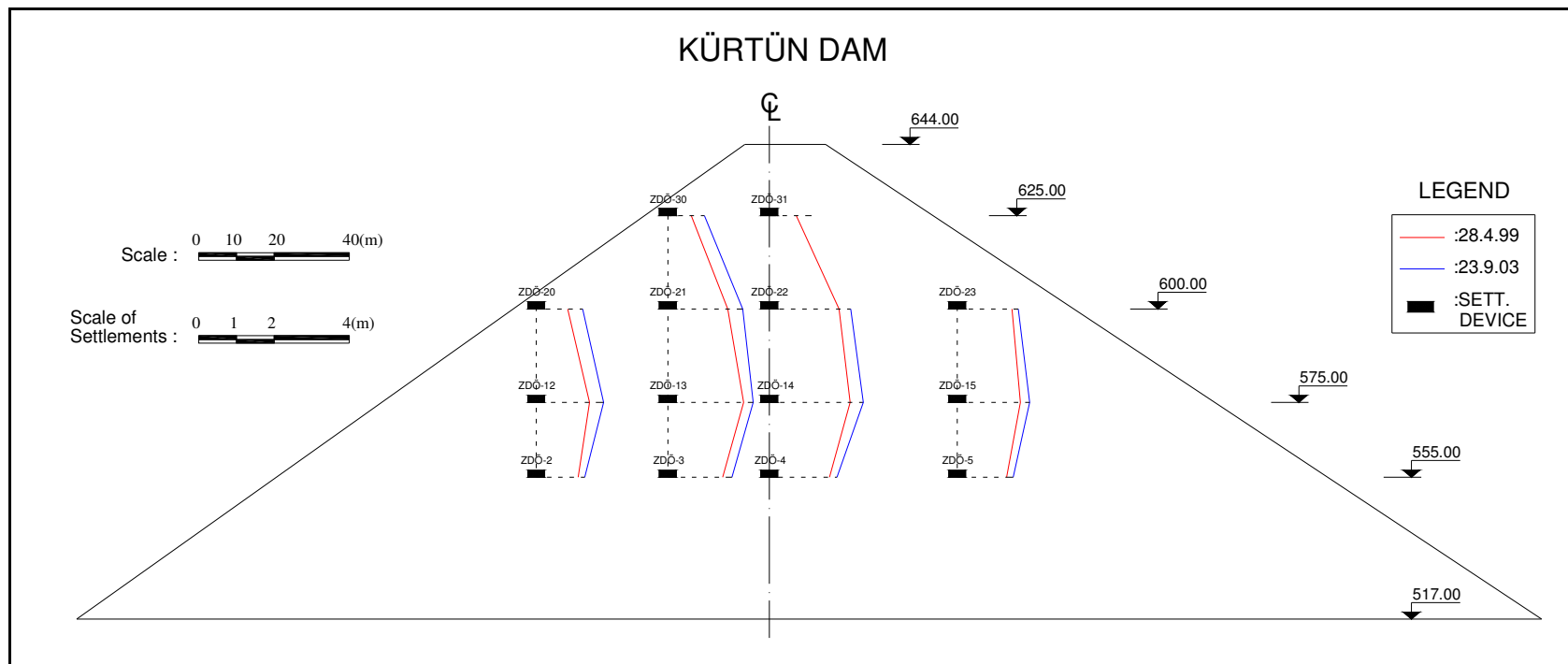


Figure 4.11 Development of settlements recorded in max cross section (KM:0+180) of Kürtün dam

4.4 Preliminary Finite Element Analyses of Kürtün Dam

4.4.1 Material Model and Material Parameters

For the finite element analysis, first of all a suitable material model is needed in order to model the stress-strain behaviour of the materials realistically. As mentioned earlier, triaxial tests have shown that the behaviour of rockfill is highly stress dependent, non-linear and inelastic (Saboya et al., 1993). In the literature, mostly hyperbolic model is used to represent the rockfill behaviour which was developed by Duncan and Chang in 1970 and updated by Kulhawy et al. in 1972 (Details of hyperbolic model were given in Section 2.4).

Hyperbolic model assumes incrementally elastic behaviour and does not include the plastic behaviour of rockfill. In this study, finite element program PLAXIS is selected with the hardening soil model which was developed on the basis of hyperbolic model.

As mentioned in the Chapter 2, determination of shear strength characteristics of rockfill materials in the laboratory by using the triaxial apparatus is a difficult subject since the rockfill material can contain particles up to 1.2 m diameter particle sizes. So it is decided to determine the material parameters from the previous studies.

When the observed settlement values of Kürtün dam are examined, it is seen that max settlement was recorded as 2155 mm for the end of construction condition (EoC). The recorded max settlements of similar dams such as 140 m high Alto Anchicaya dam, 110 m high Cethana dam and 160 m high Foz de Areia dam were 630 mm, 450 mm and 3580 mm respectively for EoC condition.

Thus, the 160 m high Foz de Areia dam is selected for the determination of material model parameters. As mentioned in the previous chapter, Saboya et al. presented a valuable paper about finite element analysis of Areia dam in 1993. In their study, the hyperbolic material parameters were determined from the appropriate test results in the literature. In Table 4.6, the range of hyperbolic parameters for preliminary analysis of Saboya et al., is presented.

Table 4.6 Range of laboratory hyperbolic parameters for preliminary analysis of Saboya et al., 1993

Material	C_u	K_E	n	R_f	K_B	m	ϕ (°)	$\Delta\phi$ (°)
IB	6	250-400	0.25-0.50	0.60	100-200	0-0.30	45	5.5
IC	14	250-400	0.25-0.50	0.80	150-200	0-0.30	42	2.0
ID	-	300-350	0-0.25	0.65	100-200	0-0.30	38	2.0

Since there are not sufficient hardening soil parameters which can be used to model the rockfill material, it is determined to use a similar range of hyperbolic parameters for this study as the ones used by Saboya et al. assuming $E_{50}^{ref} \approx 50K_E$. E_{oed}^{ref} is taken as the same as E_{50}^{ref} and R_f is taken as 0.75. The hardening soil model parameters used in the preliminary analysis are listed in the following table where ψ represents the dilatation angle (Detailed information about Hardening soil model and its parameters is given in Section 2.4).

Table 4.7 Range of hardening soil model parameters for preliminary analysis

Mat	γ kN/m ³	E_{50}^{ref} (kPa)	E_{oed}^{ref} (kPa)	m	R_f	c_{ref} (kPa)	ϕ (°)	ψ (°)
3B	21.00	12500-25000	12500-25000	0-0.35	0.75	1.0	45	10
3C	21.00	12500-25000	12500-25000	0-0.35	0.75	1.0	42	10

Transition zones 2A, 3A and Zone 3D are not included in the finite element analysis. These zones are not expected to have a significant effect on the dam behaviour (Saboya et al., 1993). It is observed that in the previous studies, the cohesion of rockfill material is generally taken as zero. However in this study,

cohesion is taken as 1 kPa, due to the recommendation of computer software, in order to improve calculation performance. Friction angle of Zone 3C material is taken as 3 degrees smaller than Zone 3B material due to its higher max particle diameter and layer thickness as indicated in Table 4.1.

For concrete membrane, special beam elements are used. Note that as mentioned earlier, the thickness of membrane increases with the height of the dam from top to bottom, which is 30 cm at the crest and 70 cm at the upstream toe. Due to its varying thickness, concrete membrane is divided into five sections in the analyses. Elastic material behaviour is selected for the concrete. Deformation characteristics are taken as suggested in TS 500 for C20 class concrete (i.e. $E = 28500$ MPa). The material parameters of membrane are listed in Table 4.8 per 1 m width of concrete membrane. In this table I represents moment of inertia, A represents cross section area, d represents thickness, E represents the elastic modulus and ν represents Poisson's ratio.

Table 4.8 Elastic material properties used in different sections of membrane

Elevation	EI (kNm²/m)	EA (kN/m)	d (m)	ν
517 – 545	682803	18810000	0.66	0.20
545 – 570	463391	16530000	0.58	0.20
570 – 595	296875	14250000	0.50	0.20
595 – 620	175959	11970000	0.42	0.20
620 - 644	93347	9690000	0.34	0.20

4.4.2 Elements and Finite Element Mesh Used in the Analyses

In Plaxis program, there are two choices for the elements. These are 6-noded triangular elements and 15-noded triangular elements. The displacements are calculated at the nodes however stresses are calculated at the stress points where 6-noded elements have 3 stress points and 15-noded elements have 12 stress points. In

this study 15-noded triangular elements are selected in order to achieve more accurate displacements and stresses. These elements are shown in Figure 4.12. Finite element mesh used in the analysis is shown in Figure 4.13. The mesh consists of 1984 elements with 16221 nodes and 23808 stress points.

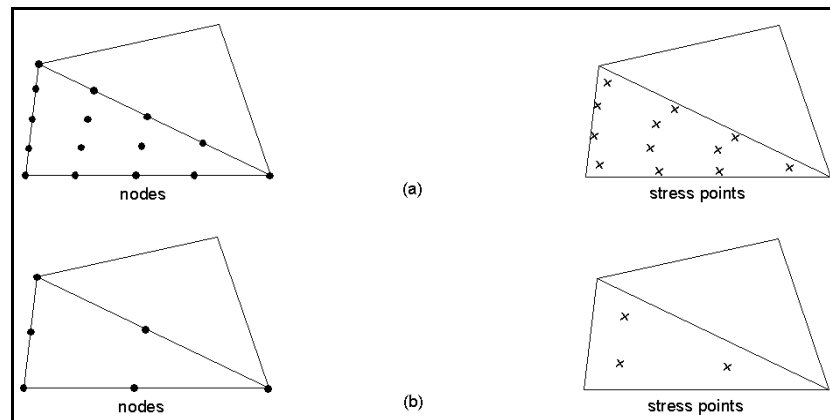


Figure 4.12 Elements used in computer software; a) 15-noded, b) 6-noded

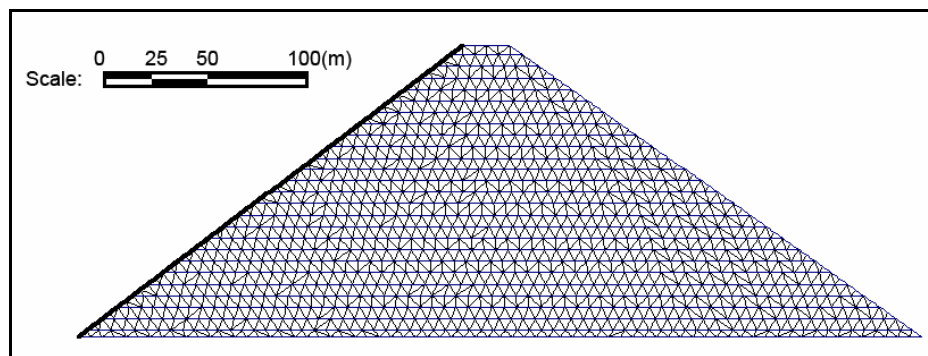


Figure 4.13 Finite element mesh used in the analysis

4.4.3 Analysis Technique

To predict the dam behaviour as realistically as possible, embankments are modeled to be constructed in layers. Here an important point is determination of layer thicknesses and it must be remembered that, the analysis becomes more accurate as the number of layers increases. Whereas as the layer thicknesses decrease, evaluation time and computation effort already increase. With keeping this valuable information in mind, “layered construction technique” is used in this study, as in the previous studies which are briefly outlined in Chapter 3.

The two important conditions contributing to settlements are analyzed which are the end-of-construction condition (EoC) and reservoir-impounding or reservoir-full-condition (RFC). In EoC condition, the rockfill material settles under its own weight whereas in RFC, displacements occur due to water loads. In the finite element calculations, two dimensional (2-D) plane strain criterion is utilized and, calculations are carried out for the max cross section (0+180).

To evaluate the EoC displacements, at the beginning of each computation phase (step), the displacements of previous phase are recorded and then reset to zero. At the end, the recorded displacements are superposed in order to get the EoC displacements.

The granodiorite foundation of dam is considered to be infinitely rigid. The bond between the concrete membrane and rockfill material was assumed to be totally perfect.

The parapet wall at the upstream of the crest and the 6 m high-fill behind it, are not included in the analyses in order to keep the finite element model as simple as possible. However the weight of them, are considered as a uniformly distributed surcharge load of 100 kPa, and applied to the model at the crest. This load is not included in EoC analyses and activated as a separate phase after the EoC condition, since the parapet wall and the fill were constructed after the completion of concrete membrane, as mentioned in Section 4.3.1.

4.4.4 Determination of Layer Thicknesses

In the preliminary analyses, 10 m thick layers are used. When the results are compared with the observed values, it is seen that there are significant differences especially for elevations of 600 and 625, as depicted in Figure 4.14. So it is decided to use 5 m layers in the following analyses.

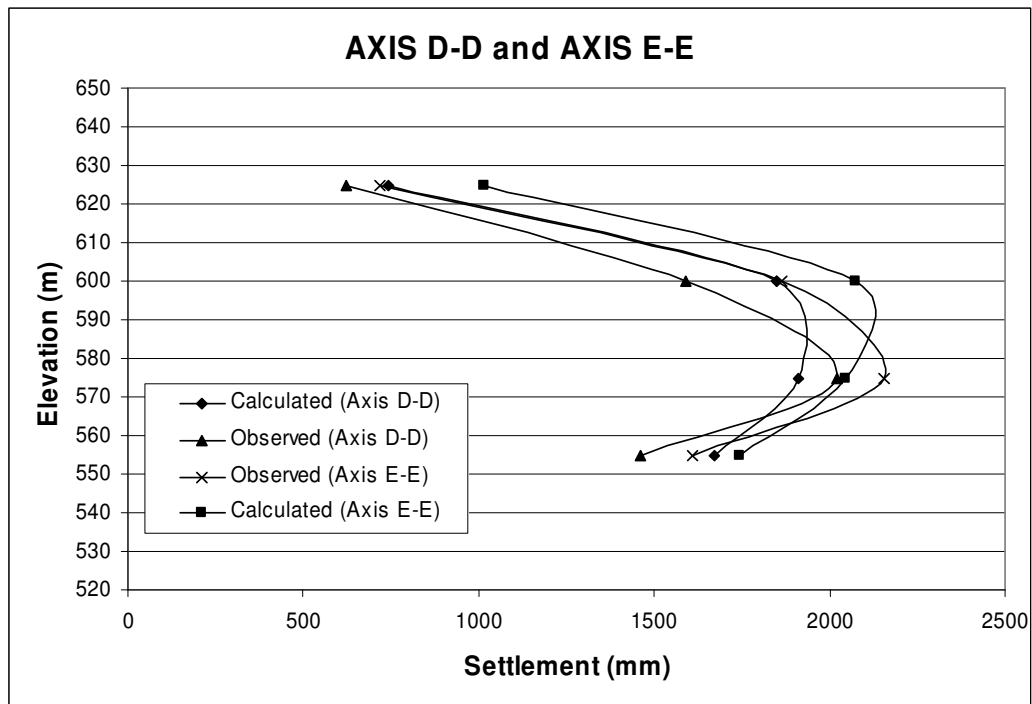


Figure 4.14 Comparison of calculated settlements using 10-m layers with observed values in Axis D-D and E-E for EoC

4.5 Analyses and Results

In the study, the following procedure is followed :

- a) Material parameters which give the best fit settlement distribution for the EoC condition are determined ignoring the effect of Zone 3C in order to simplify the analysis
- b) Effects of Zone 3C are examined for the EoC condition
- c) RFC is analyzed
- d) Calculated total stresses are compared with the observations
- e) Behaviour of concrete membrane upon reservoir impounding is examined
- f) Contours of stresses and displacements are depicted in order to indicate the general behaviour for the EoC and RFC conditions

4.5.1 Determination of Material Model Parameters and EoC Analyses

The examined hardening soil model parameters used for modeling of Zone 3B are listed in Table 4.9. Other parameters which are not given in Table 4.9, are the same with those given in Table 4.7 (Detailed information about Hardening soil model and its parameters is given in Section 2.4).

Table 4.9 Hardening soil model parameters used in Plaxis analysis

Loading	$E_{50}^{ref} = E_{oed}^{ref}$ (kPa)	m
1	22500	0.20
2	21000	0.25
3	19000	0.30
4	17000	0.35

Although the results of the analyses with the loading conditions given in Table 4.9 are close to each other, the parameters in Loading 2 gives the best-fit settlements when compared with the observed ones. In these analyses, the rockfill embankment is assumed to be constructed by only one type of material (Zone 3B type material). Calculated settlement curves using Loading 2 are given against the observed results through Figures 4.15 – 4.20 (The axes A-A, B-B, C-C etc are indicated in Figure 4.4). Calculated settlements and observed values are summarized in Table 4.10 for comparison.

When Figures 4.15 to 4.20 are examined, it can be said that the overall agreement is satisfactory when using only one type of material in the whole rockfill embankment. The differences between the calculations and the readings are significantly larger at the instruments located at El 555 and reduce towards upper elevations. This situation is attributed to cross-valley arching effects which are not included in the calculations.

At El 575 and El 600, the agreement is quite satisfactory but in case of El 625 the settlement difference is significantly high especially at the centerline. (ZDÖ-31) This difference may be attributed to the relative changes in the compaction effort or to instrument calibration error. In EoC condition, max calculated settlement at the centerline is 2033 mm at El 580, 5 m above ZDÖ-14.

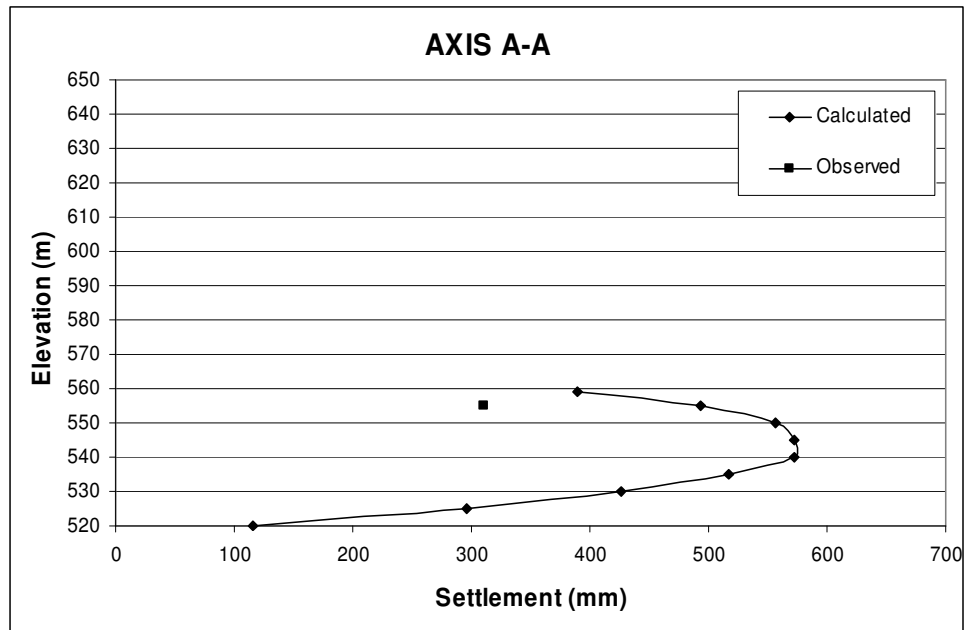


Figure 4.15 Comparison of settlements in Axis A-A for EoC

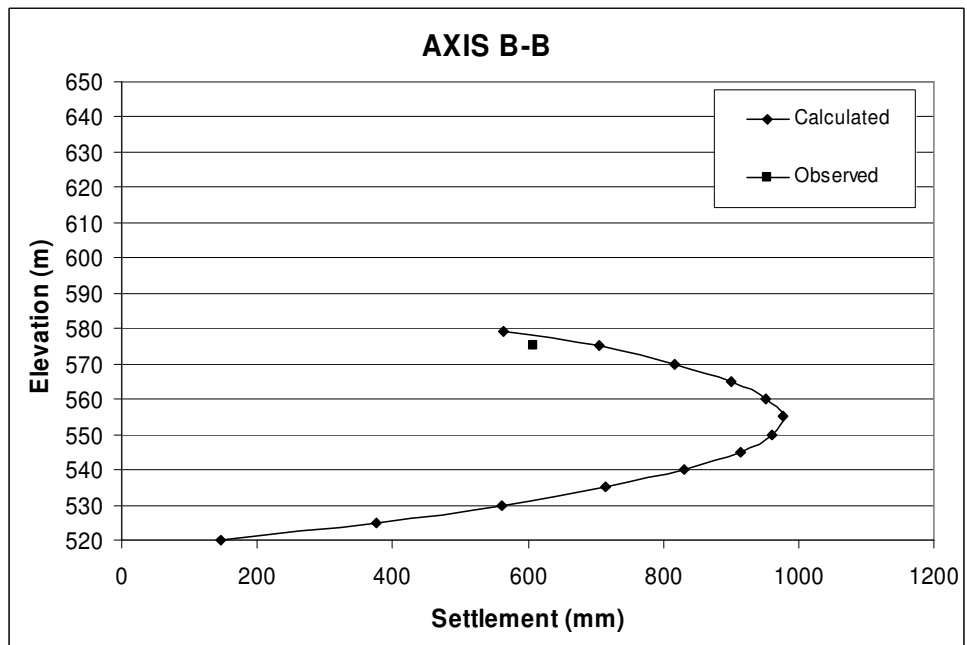


Figure 4.16 Comparison of settlements in Axis B-B for EoC

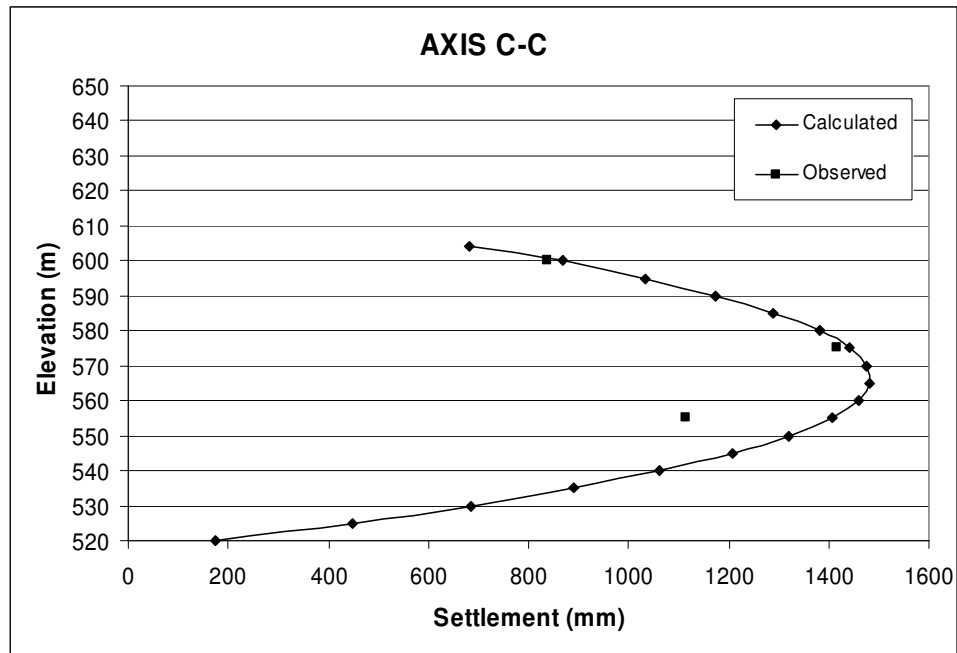


Figure 4.17 Comparison of settlements in Axis C-C for EoC

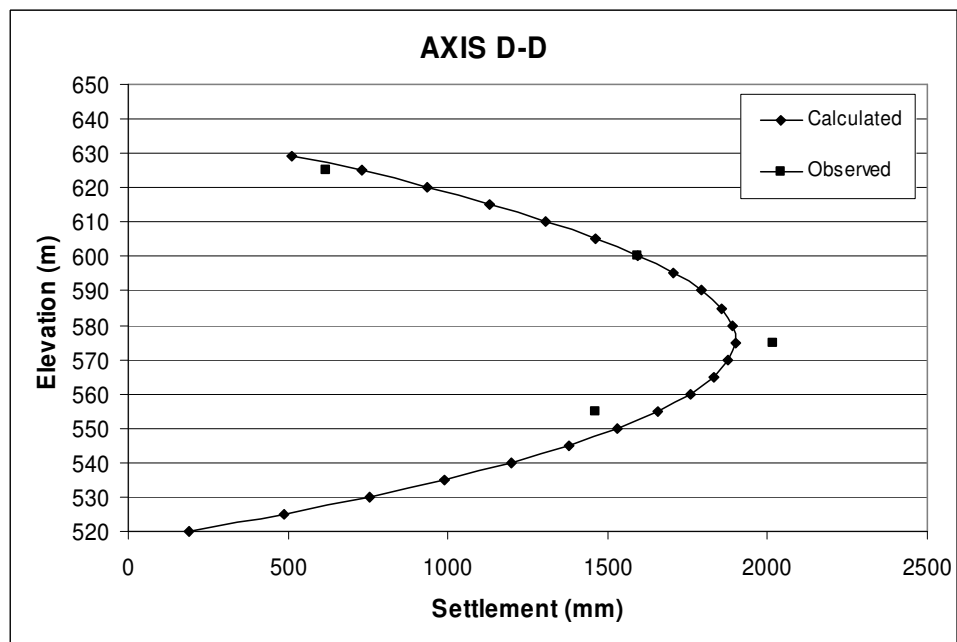


Figure 4.18 Comparison of settlements in Axis D-D for EoC

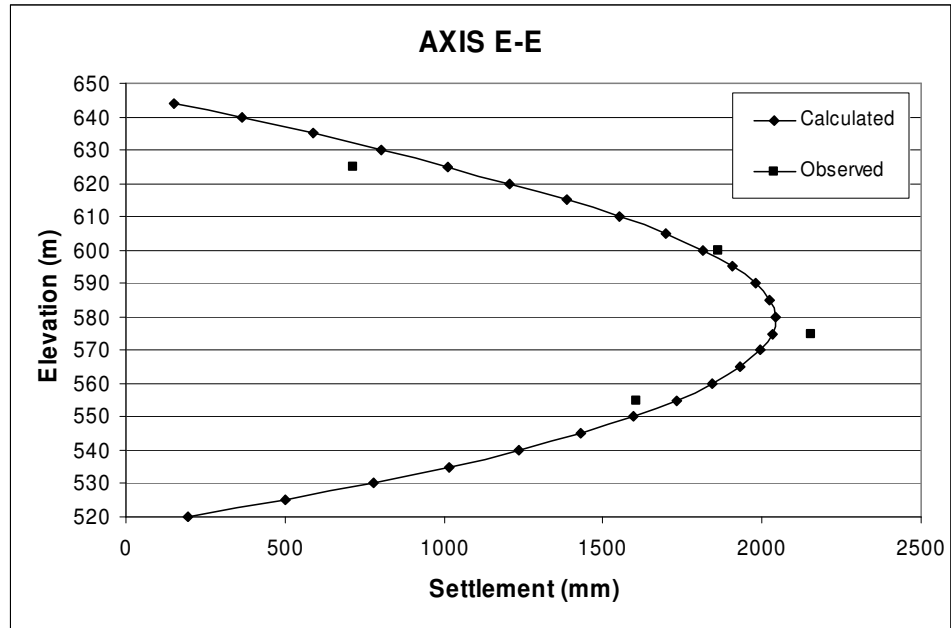


Figure 4.19 Comparison of settlements in Axis E-E for EoC

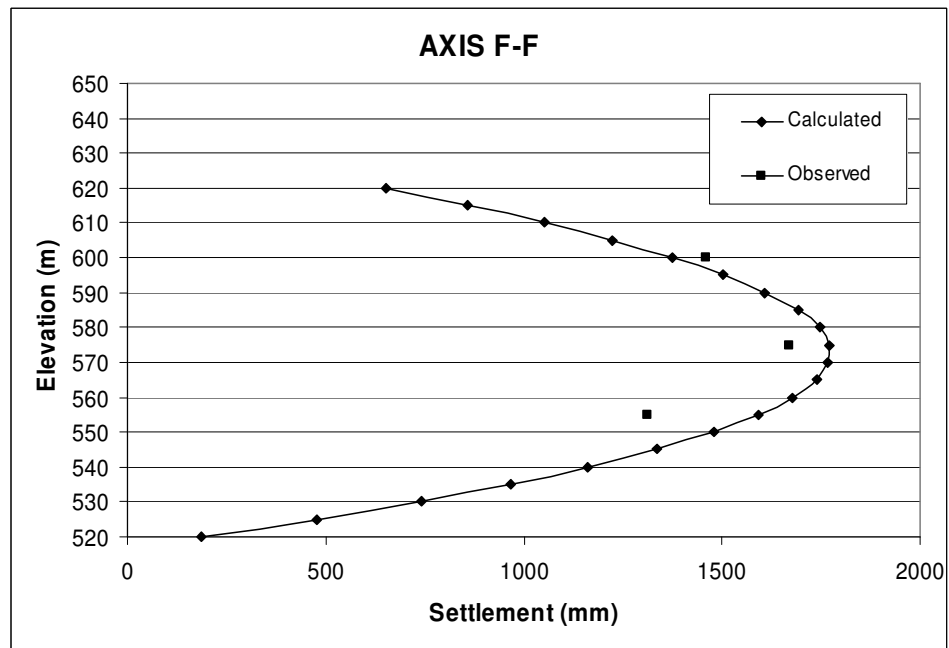


Figure 4.20 Comparison of settlements in Axis F-F for EoC

Table 4.10 Comparison of calculated and observed settlement values for EoC

Axis	Instrument	Elevation (m)	Observed Sett. (mm)	Calculated Sett. (mm)	Difference (mm)
A-A	ZDÖ-1	555.00	311	494	183
B-B	ZDÖ-11	575.00	609	706	97
C-C	ZDÖ-2	555.00	1113	1407	294
	ZDÖ-12	575.00	1417	1442	25
	ZDÖ-20	600.00	836	870	34
D-D	ZDÖ-3	555.00	1460	1658	198
	ZDÖ-13	575.00	2019	1899	-120
	ZDÖ-21	600.00	1592	1594	2
	ZDÖ-30	625.00	621	733	112
E-E	ZDÖ-4	555.00	1607	1732	125
	ZDÖ-14	575.00	2155	2033	-122
	ZDÖ-22	600.00	1861	1813	-48
	ZDÖ-31	625.00	717	1011	294
F-F	ZDÖ-5	555.00	1313	1592	279
	ZDÖ-15	575.00	1669	1772	103
	ZDÖ-23	600.00	1462	1373	-89

4.5.2 Effects of Zone 3C

In the further analyses, Zone 3C material is included in the model to see the effect of this material on the dam behaviour. The analyses are performed with the geometry which is shown in Figure 4.2.

As mentioned in Table 4.1, Zone 3C material has been compacted in 1.2 m layers with a max particle size of 1.0 m where these values are 0.8 m and 0.6 m respectively for Zone 3B.

In the analyses, the exponent m is kept as same for Zone 3C material ($m = 0.25$). However larger and smaller E_{50}^{ref} values than zone 3B material are used, 19000 and 23000 kN/m² for weaker and stiffer Zone 3C materials.

To clarify the effect of Zone 3C material, calculated settlements at the locations of instruments are given in Table 4.11, together with the settlements calculated assuming only one type of material, Zone 3B, was included. Here Analysis 2 and 3 represent the analyses where stiffer and weaker Zone 3C materials are included. Analysis 1 is the one where only Zone 3B material was included in the model. It is clearly seen from Table 4.11 that, Zone 3C has a significant effect on the behaviour. When Table 4.11 is examined, it is seen that, Analysis 2 shows a better agreement with the observed behaviour than Analysis 3 especially in Axis F-F.

When the results of Analyses 1 and 2 are compared, it is seen overall agreement is quite satisfactory in both cases where Analysis 2 gives a better agreement in lower elevations especially at the instruments ZDÖ-4 and ZDÖ-5. This is reasonable because cross valley arching effect reduces the settlements at the lower elevations and due to higher modulus of Zone 3C, Analysis 2 gives better agreement. However Analysis 1 gives more convenient results in the upper elevations especially at the instruments ZDÖ-13, ZDÖ-14, ZDÖ-22 and ZDÖ-23.

Considering the fact that, Analysis 1 and Analysis 2 gives satisfactory results for EoC condition, the rockfill embankment is modeled as in Analysis 1 where only one type of material is used, in further analyses for simplicity.

Table 4.11 Effect of Zone 3C on behaviour (settlements are in mm)

Axis	Instrument	Elevation (m)	Observed Settlement	Analysis 2 (stiffer Zone 3C)		Analysis 3 (weaker Zone 3C)		Analysis 1 (only Zone 3B)	
				Results	Difference	Results	Difference	Results	Difference
C – C	ZDÖ – 2	555	1113	1408	295	1411	298	1407	294
	ZDÖ – 12	575	1417	1437	20	1438	21	1442	25
	ZDÖ – 20	600	836	869	33	862	26	870	34
D – D	ZDÖ – 3	555	1460	1627	167	1677	217	1658	198
	ZDÖ – 13	575	2019	1850	-169	1915	-104	1899	-120
	ZDÖ – 21	600	1592	1549	- 43	1609	17	1594	2
	ZDÖ – 30	625	621	716	95	740	119	733	112
E – E	ZDÖ – 4	555	1607	1648	41	1855	248	1732	125
	ZDÖ – 14	575	2155	1949	-206	2156	1	2033	-122
	ZDÖ – 22	600	1861	1756	-105	1910	49	1813	-48
	ZDÖ – 31	625	717	993	276	1064	347	1011	294
F – F	ZDÖ – 5	555	1313	1463	150	1760	447	1592	279
	ZDÖ – 15	575	1669	1653	-16	1982	313	1772	103
	ZDÖ – 23	600	1462	1316	-146	1570	108	1373	-89

4.5.3 Reservoir Full Condition (RFC)

Reservoir impounding is an important stage in dam performances. Major amount of the post-construction settlements occur after impounding. As the reservoir level rises, horizontal and vertical displacements occur in the rockfill embankment. These displacements have a direct effect on the dam behaviour. Large displacements may indicate cracks in the concrete membrane, thus causing leakage problems which may cost expensive repairs. Here the impounding rate is important. If the impounding occurs rapidly, it causes larger settlements and horizontal displacements.

In Kürtün dam, reservoir water level reached El 630.00 at 28.5.2002. After this date, water level fluctuated a little. As mentioned in Chapter 3, the first impounding condition is critical in the behaviour thus reservoir El 630 at 28.05.2002 is considered as RFC in the study.

As mentioned in the literature by various researchers such as Fitzpatrick et al., 1985 and Saboya et al., 1993 that, during the first stages of reservoir impounding, rockfill material responds in a stiffer manner than construction condition (i.e. like unloading) where it is suggested that to determine the impounding displacements realistically, primary loading modulus has to be multiplied by a reasonable coefficient in order to get this unloading modulus. In most cases, this coefficient is taken between 2 and 4. (Saboya et al., 1993)

In the finite element analysis of CFRDs, it is a common practice to assume the concrete membrane as impervious and uncracked. This assumption is utilized in this study too and reservoir water load is taken as a uniformly distributed triangular load acting perpendicular on the membrane as shown in Figure 4.21.

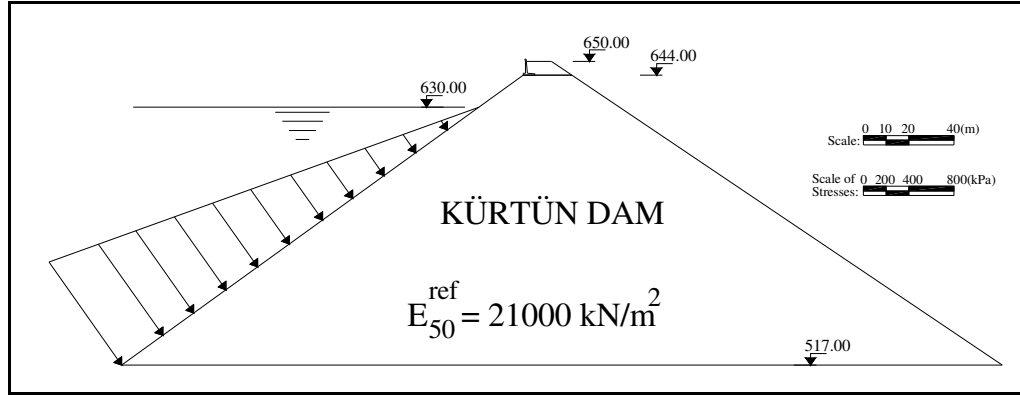


Figure 4.21 Reservoir water load applied on the concrete membrane

In Figure 4.21, reservoir water load is 1108.53 kN/m^2 at El 517.00. The results of reservoir full condition (RFC) analyses are depicted through Figures 4.22 - 4.27 for the axes shown in Figure 4.4. Note that these settlements calculated separately and do not include EoC settlements calculated in Sec 4.5.1 to indicate the impounding effect on the dam body. Thus the settlement values recorded at the beginning of impounding (08.2.02) are subtracted from the ones recorded at the end of impounding (water level at El 630.00 at 28.5.02) to indicate the observed settlements for RFC. As mentioned in Sec 4.5.1, only Zone 3B material was included in rockfill embankment for RFC analyses. The results are summarized in Table 4.12.

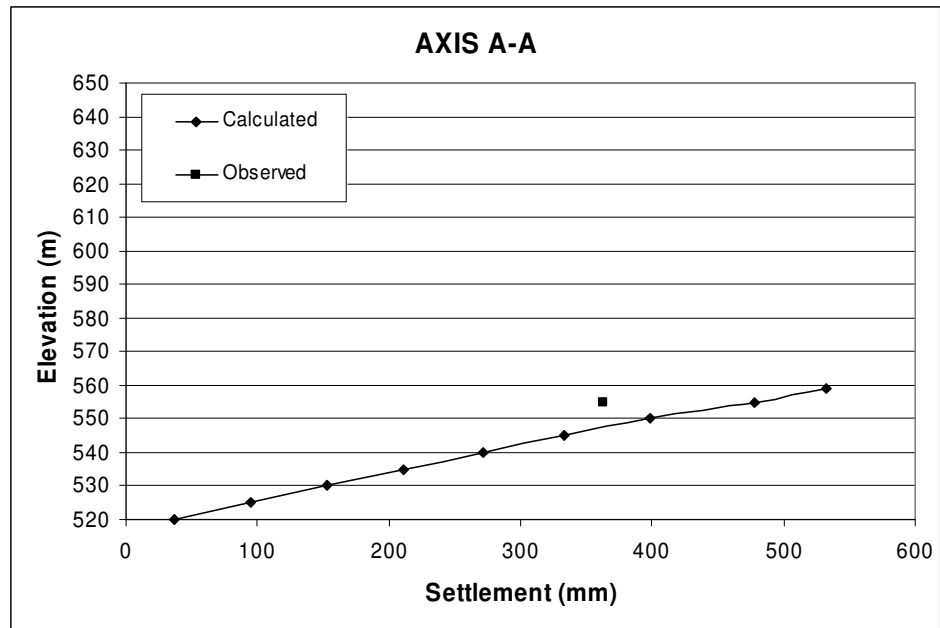


Figure 4.22 Comparison of settlements in Axis A-A for RFC

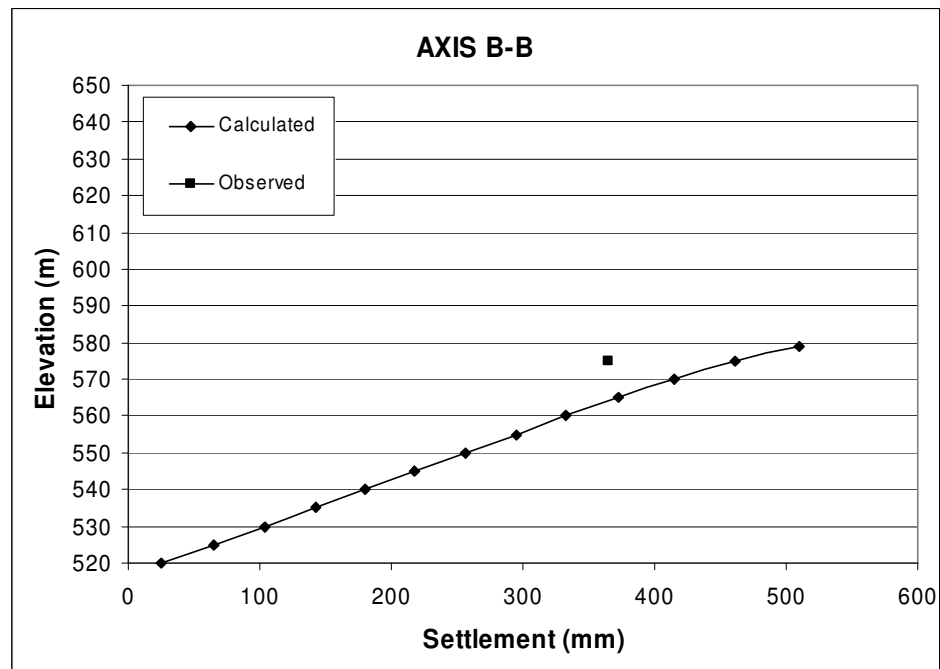


Figure 4.23 Comparison of settlements in Axis B-B for RFC

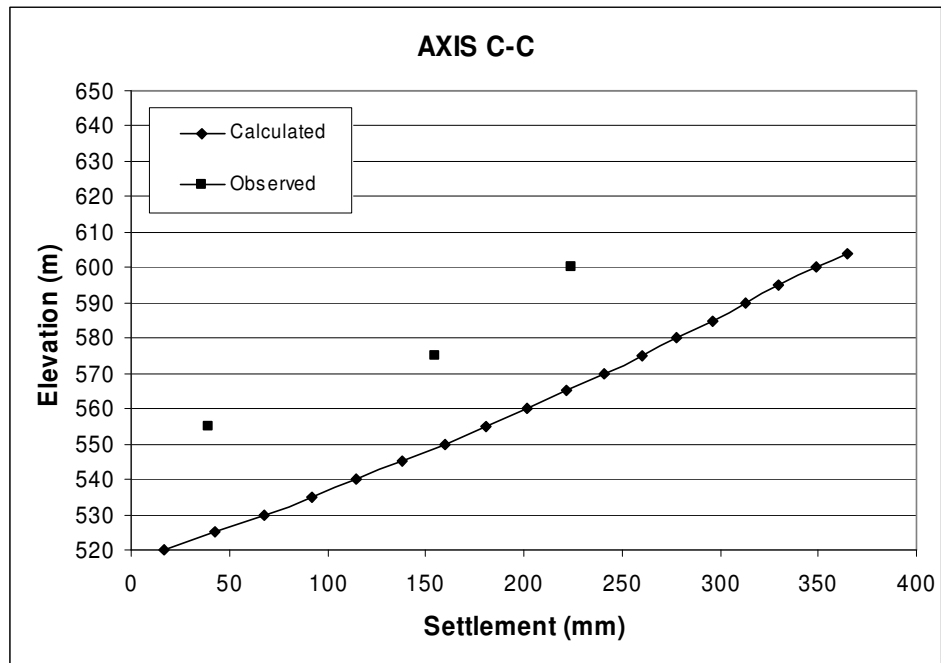


Figure 4.24 Comparison of settlements in Axis C-C for RFC

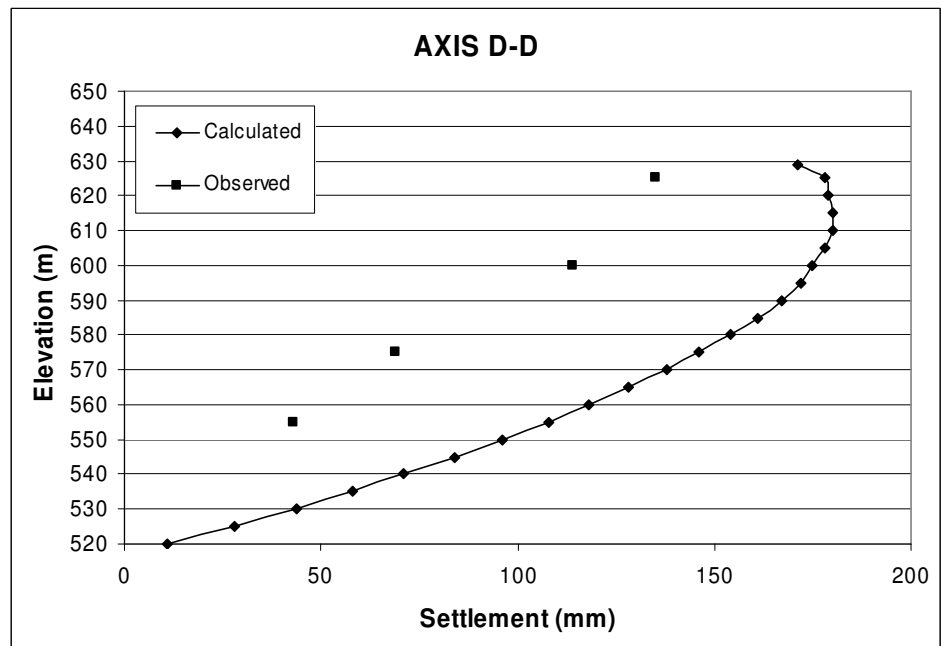


Figure 4.25 Comparison of settlements in Axis D-D for RFC

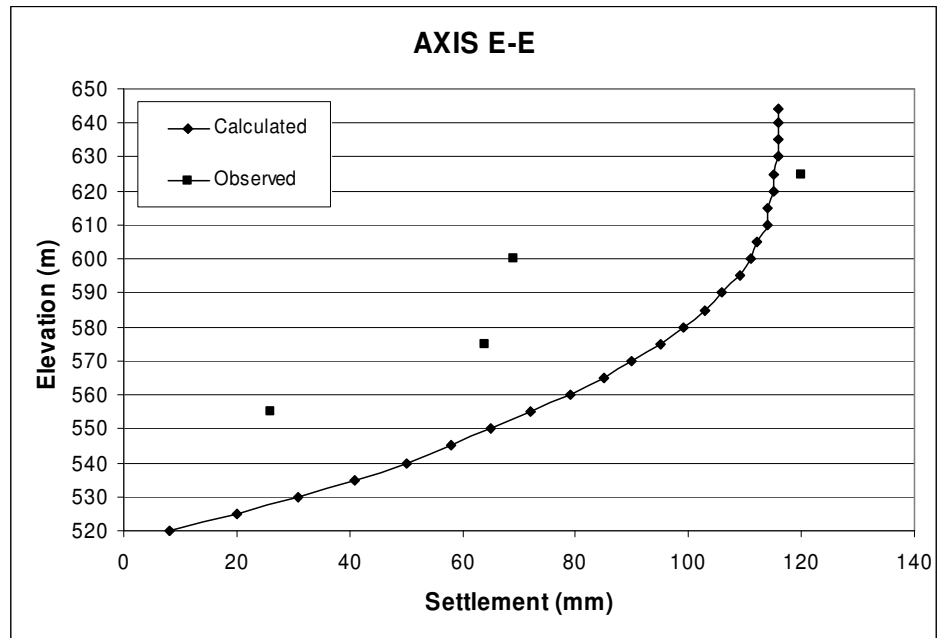


Figure 4.26 Comparison of settlements in Axis E-E for RFC

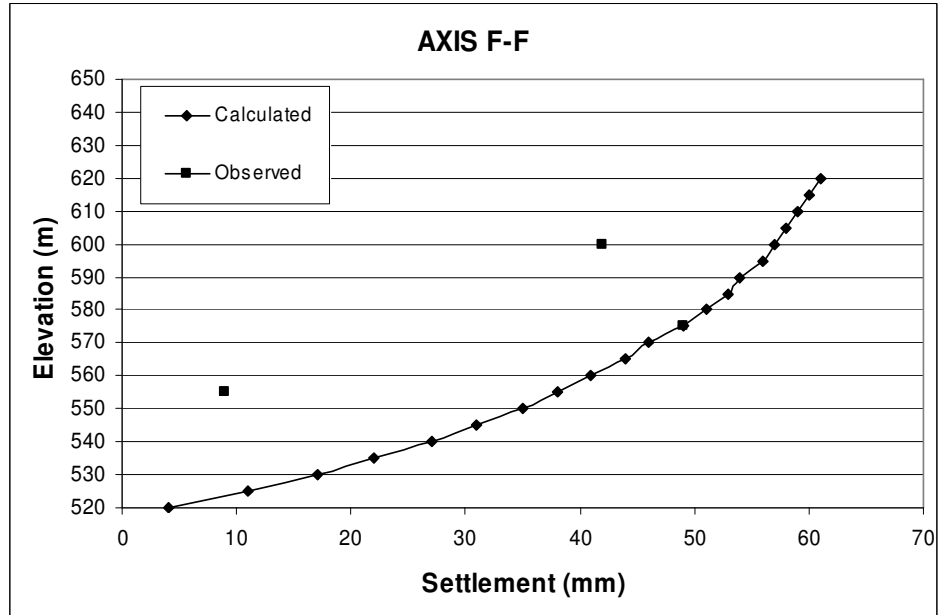


Figure 4.27 Comparison of settlements in Axis F-F for RFC

Table 4.12 Calculated and observed settlement values for RFC (in mm)

Axis	Instrument	Elev. (m)	Observed Sett.	Calculated Sett.	Difference
A-A	ZDÖ-1	555.00	363	478	115
B-B	ZDÖ-11	575.00	365	461	96
C-C	ZDÖ-2	555.00	39	181	142
	ZDÖ-12	575.00	155	260	105
	ZDÖ-20	600.00	224	349	125
D-D	ZDÖ-3	555.00	43	108	65
	ZDÖ-13	575.00	69	146	77
	ZDÖ-21	600.00	114	175	61
	ZDÖ-30	625.00	135	178	43
E-E	ZDÖ-4	555.00	26	72	46
	ZDÖ-14	575.00	64	95	31
	ZDÖ-22	600.00	69	111	42
	ZDÖ-31	625.00	120	115	-5
F-F	ZDÖ-5	555.00	9	38	29
	ZDÖ-15	575.00	49	49	0
	ZDÖ-23	600.00	42	57	15

When Figures 4.22 - 4.27 and Table 4.12 are examined, it is seen that larger settlements occur in the region close to upstream membrane which diminish towards the downstream face, as expected. Through axes D-D and E-E, observed settlements increase with a considerable amount from El 600 to 625, which indicates the settlement of the embankment continues due to creep and secondary settlement of rockfill material. Also it is believed that, newly constructed upper 6 m of the embankment has a slight effect on this difference. Since these kind of effects are not considered in the analyses, negligible increase occur in calculated values at El 600 and El 625 through axes D-D and E-E.

It is seen that the calculated settlements are larger than the observed values for RFC. As mentioned previously, in reservoir impounding rockfill material responds in a much stiffer manner than the construction condition. This condition is closely related with the direction of principal stresses. As shown in Figure 3.12, in the upstream half, the major principal stress direction is nearly parallel to the

concrete face. So the minor principal stress is close to normal to the concrete face which has to be perpendicular to the major principal stress. When the water load is applied on the concrete face which is normal to the face, it compresses the rockfill material and minor principal stresses increase because the water load and minor principal stress are nearly in the same direction. However the stress increase is not significant as the one for minor principal stresses. Thus the mean stress increases however the shear stress decreases because minor principal stress increases more than major principal stress. As a result, the rockfill material in the upstream part moves away from failure like being unloaded. This phenomena is also indicated by the previous researchers such as Saboya et al (1993) and Liu et al (2002). This condition is considered as the main reason for the differences between the calculated and the observed settlements summarized in Table 4.12 due to the fact that unloading response of the rockfill material is not represented realistically in the computer software for RFC.

To see the effect of unloading due to reservoir impounding effect, a region is assumed to be unloaded as shown in Figure 4.28. The primary deformation modulus of this region is multiplied by 1.5 and the analyses are performed again.. The results are given in Table 4.13 together with previous analysis. Here Analysis 4 represents the analysis where whole embankment is under primary loading condition and Analysis 5 represents the analysis shown in Figure 4.28.

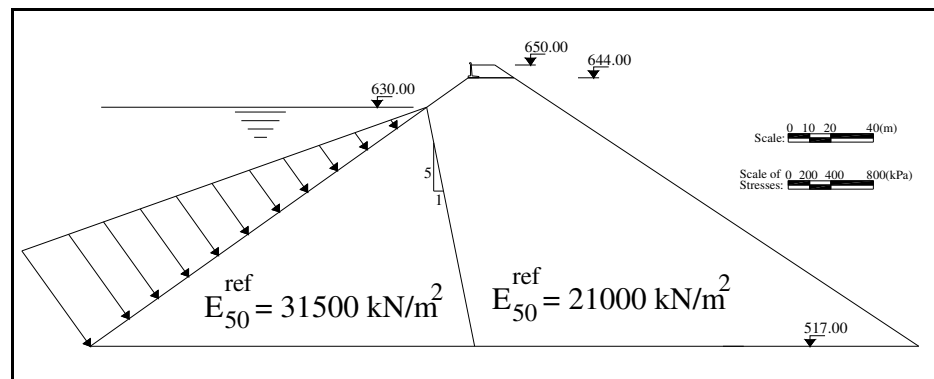


Figure 4.28 Assumed unloaded region of the embankment due to reservoir impounding

The results of Analysis 5 are more agreeable with the observed settlements. This indicates that, in reservoir impounding stage, upstream part of the embankment responds in unloading manner. Thus, the assumption is found reasonable.

Table 4.13 Comparison of results of RFC analyses (settlements are in mm)

Axis	Instrument	Elevation (m)	Observed Settlement	Analysis 4		Analysis 5	
				Results	Diff.	Results	Diff.
A-A	ZDÖ-1	555.00	363	478	115	297	-66
B-B	ZDÖ-11	575.00	365	461	96	294	-71
C-C	ZDÖ-2	555.00	39	181	142	105	66
	ZDÖ-12	575.00	155	260	105	155	0
	ZDÖ-20	600.00	224	349	125	217	-7
D-D	ZDÖ-3	555.00	43	108	65	64	21
	ZDÖ-13	575.00	69	146	77	89	20
	ZDÖ-21	600.00	114	175	61	111	-3
	ZDÖ-30	625.00	135	178	43	118	-17
E-E	ZDÖ-4	555.00	26	72	46	48	22
	ZDÖ-14	575.00	64	95	31	62	-2
	ZDÖ-22	600.00	69	111	42	72	3
	ZDÖ-31	625.00	120	115	-5	76	-44
F-F	ZDÖ-5	555.00	9	38	29	28	19
	ZDÖ-15	575.00	49	49	0	26	-23
	ZDÖ-23	600.00	42	57	15	42	0

4.5.4 Assessment of Total Stresses

In Kürtün dam, total stresses are measured by hydraulic pressure cells whose locations are shown in Figure 4.3, 4.4 and 4.5. The results of calculations both for EoC and RFC are given with the measured stress values in Table 4.14 together with the overburden stresses on the instruments. The values given in this table are the results of the analysis where only one type of material is included in the dam body.

Table 4.14 Comparison of total stresses for EoC and RFC (stresses are in kN/m²)

Axis	Instrument	Elevation (m)	Overburden Stresses	Observed Stresses		Calculated Stresses		Difference of observations and calculations		Stress Increase	
				EoC	RFC	EoC	RFC	EoC	RFC	Observed	Calculated
C – C	BÖ – 2	555.00	1029	931	1040	1126	1347	195	307	109	221
	BÖ – 10	575.00	609	623	690	716	890	93	200	67	174
E – E	BÖ – 3	555.00	1995	-	-	1563	1641	-	-	-	78
	BÖ – 11	575.00	1575	1123	1265	1226	1283	103	18	142	57
	BÖ – 16	600.00	1050	896	931	800	842	96	-89	35	42
F – F	BÖ – 4	555.00	1375	1024	996	1368	1410	344	414	-28	42
	BÖ – 12	575.00	955	927	934	994	1023	67	89	7	29
G – G	BÖ – 1	555.00	-	40	232	35	756	-5	524	192	721
	BÖ – 9	575.00	-	65	261	35	560	-30	299	196	525
	BÖ – 15	600.00	-	135	45	35	315	-100	270	-90	280
	BÖ – 20	625.00	-	27	33	35	75	8	42	6	40

As shown in Figure 4.4, instruments in Axis G-G, are located parallel to the concrete membrane in order to see the pressure changes in the impounding condition where others are located perpendicular to the dam centerline to record vertical stresses. Note that, the instrument BÖ-3 failed in recording during the construction.

As it is seen from Table 4.14, the measured stresses vary from each other along axis G-G for the EoC condition, where calculated values are all equal. This may be due to the placement of pressure cells at unequal distances from the membrane.

When Table 4.14 is examined it is seen that, for axes C-C, E-E and F-F, calculated stresses are larger than the readings except instrument BÖ-16 where the readings are slightly higher than the calculations. The difference is more significant in El 555 and reduces towards El 600.

In EoC, cross valley arching is a significant parameter in lower elevations, reducing the observed stress values. As the analysis is based on two dimensional plane strain analysis, arching effects could not be included in the calculations.

As mentioned in Chapter 3 by Hunter et al. (2003) that, arching effect is significant in the valleys having steep abutments on narrower rivers such as the one of Kürtün dam, where general information is given in Section 4.1. In order to see the effect of arching on calculated stresses, the correction factors suggested by Hunter et al. (2003) are applied to the calculated values for EoC. The results are shown in Table 4.15. In this table, average abutment slope and river width to height ratio are taken as 57° and 0.30, respectively. It is seen that, corrected values due to arching are more agreeable with the readings than the uncorrected ones.

For RFC, both observations and finite element analysis results indicate an increase in stresses, as expected. This increase is more evident from the readings of instruments closer to the upstream membrane and slight for the points closer to the downstream face.

For RFC, there are some inconsistencies in these instruments where observed total stress decreases 90 kN/m^2 in BÖ-15; however it increases 192, 196 and 6 kN/m^2 in BÖ-1, BÖ-9 and BÖ-20 respectively. This may be due to the calibration errors in the instruments.

Table 4.15 Corrected vertical stresses for EoC (stresses are in kPa)

Axis	Instrument	Elevation (m)	Observed Stresses	Calculated Stresses		Corrected Vertical Stresses due to Arching		
				Results	Diff.	Factor	Results	Diff.
C-C	BÖ-2	555.00	931	1126	195	0.79	890	-41
	BÖ-10	575.00	623	716	93	0.88	630	7
E-E	BÖ-3	555.00	-	1563	-	0.79	1235	-
	BÖ-11	575.00	1123	1226	103	0.88	1079	-44
	BÖ-16	600.00	896	800	-96	0.99	792	-104
F-F	BÖ-4	555.00	1024	1368	344	0.79	1081	57
	BÖ-12	575.00	927	994	67	0.88	875	-52

4.5.5 Behaviour of Concrete Membrane due to Reservoir Impounding

As mentioned in Section 4.2, the performance of concrete membrane in reservoir impounding and operation conditions is observed by strainmeters and jointmeters, whose locations are given in Figure 4.6 and Table 4.2.

Due to the variations in reservoir water level, three different analyses are carried out in order to predict the concrete membrane behavior realistically. The results of analyses are compared in Table 4.16 with the observed strain values taken from 2002 readings. Note that, the water level 630.00 m corresponds to RFC in the previous analyses. As the analyses based on two dimensional plane strain phenomena, jointmeter readings could not be included in Table 4.16.

The strainmeters used in Kürtün dam consist of four receivers where, first and third receivers were installed to record the strains parallel to the slope direction of concrete membrane (axial strains) and second and fourth ones were installed to record the strains perpendicular to the slope direction (shear strains). Also embedded distances of the receivers are different from each other. Third and fourth receivers

were embedded a quarter of thickness down from the axis of concrete membrane where first and second receivers were embedded a quarter of thickness up from the axis.

Calculated axial strain values (1-3) given in Table 4.16, are obtained by dividing the axial stress values given by the computer software to axial rigidity (EA) of the membrane given in Table 4.8. The negative values in the results indicate compressive strains in the membrane and positive values indicate tensile strains. Due to the assumption of totally perfect bond between the membrane and the rockfill material and hence continuous support of rockfill, computer program gives relatively lower shear stress values in the membrane elements thus calculated shear strains are not included in Table 4.16.

As mentioned in Table 4.2, strainmeters GÖ-3 and GÖ-4 were located at the same elevation (El 585) but different locations on the concrete membrane. This is valid for instruments GÖ-5 and GÖ-6 which were located at El 615.00. Thus calculated values are the same at these instruments due to 2-D analysis. Mean values of the receivers which records the strains in the same direction are also given in Table 4.16, since computer software computes the stresses only on the central axis of the membrane.

When Table 4.16 is examined, it is seen that observed strains are very sensitive to variations in reservoir water level. At the beginning of impounding tensile strains are observed at some instruments, but these are turned into compressive strains when the water level reached El 630 except receiver 1 of GÖ-2. The readings of the instruments located at the same elevation indicate that, strains are higher at the regions close to the abutments than the center of the concrete membrane. Max strains are observed at El 585, close to ZDÖ-11, where max RFC settlement was observed.

When the observed and calculated strains are compared, it is seen that, calculated values give compressive axial strains however tensile strains are observed at some instruments especially at the beginning of impounding. In the finite element analysis, water load is applied in a separate phase as a surcharge load after the construction and completion of majority of settlements of rockfill embankment. The bond between concrete membrane and rockfill material was assumed to be totally

perfect. Thus no relative displacements occur in the membrane with respect to the embankment. However in the real case, this bond is not perfect and as a result tensile strains could be observed in early stages of reservoir impounding. This is thought to be the main cause of difference. Also the settlements in the third direction has some effects on the observations.

Table 4.16 Comparison of strains due to varying water level (10^{-6} m/m)

Date	Water level (m)	Instr.	Observed Strains						Calculated Strains (Mean 1-3)
			Rec 1	Rec 2	Rec 3	Rec 4	Mean 1-3	Mean 2-4	
14.02	581	GÖ-1	-42	-	-38	-96	-40	-110	-149
01.04	600		-45	-	-68	-	-57	-204	-181
28.05	630		-	-51	-	-	-215	-243	-177
14.02	581	GÖ-2	88	-7	-18	-53	35	-30	-121
01.04	600		147	-	-	-86	17	-98	-238
28.05	630		40	415	-	-	-77	-93	-365
14.02	581	GÖ-3	16	4	-28	-4	-6	0	-43
01.04	600		-1	-67	-	42	-84	-13	-173
28.05	630		-	-66	-	-23	-842	-45	-390
14.02	581	GÖ-4	34	21	-19	-22	8	-1	-43
01.04	600		80	-22	-	-	-147	-93	-173
28.05	630		-	-	-	-	-609	-322	-390
14.02	581	GÖ-5	33	63	-1	-6	16	29	-15
01.04	600		53	-34	31	-14	42	-24	-33
28.05	630		-31	-	-15	-	-23	-176	-187
14.02	581	GÖ-6	54	40	1	3	28	22	-15
01.04	600		-10	-	12	19	1	-151	-33
28.05	630		-	-	-	-	-338	-350	-187

4.5.6 Displacement and Total Stress Contours

The calculated equal stress and equal displacement contours both for EoC and for RFC are given through Figures 4.29 - 4.34 and 4.35 – 4.38 respectively. In the figures RFL indicates the reservoir full level. In stress contours, negative values indicate compression.

When contours are examined, it is seen that the contours are symmetrical about the central axis for the EoC condition. When EoC and RFC stress contours are compared, it is seen that impounding increases both the horizontal and vertical stresses with a considerable amount in the regions close to concrete membrane, however for the downstream part the increase is relatively small (Figures 4.29-4.32).

Max horizontal stress and max vertical stress are calculated as 641.9 kPa and 2189.6 kPa respectively at the foundation level of the dam at EoC condition. These values are calculated as 682.2 kPa and 2317.9 kPa, respectively for RFC (Figures 4.29-4.32).

When shear stress contours are examined, it is seen that, for EoC condition shear stresses are zero at the dam centerline and increase towards dam faces. At the upstream part max shear stresses are slightly higher than downstream part which may be attributed to different upstream and downstream slopes (Figure 4.33).

As water load is applied on the concrete membrane, positive shear stresses develop in the whole embankment due to impounding and as a result negative shear stresses turn to positive in the upstream part. Like the horizontal and vertical stresses, shear stresses in the downstream part are not significantly affected by reservoir impounding (Figure 4.34).

In EoC, max positive shear stress is 300.0 kPa at the downstream half and max negative shear stress is 312.8 kPa at the upstream half. In RFC, max positive shear stress is calculated as 325.7 kPa (Figures 4.33-4.34).

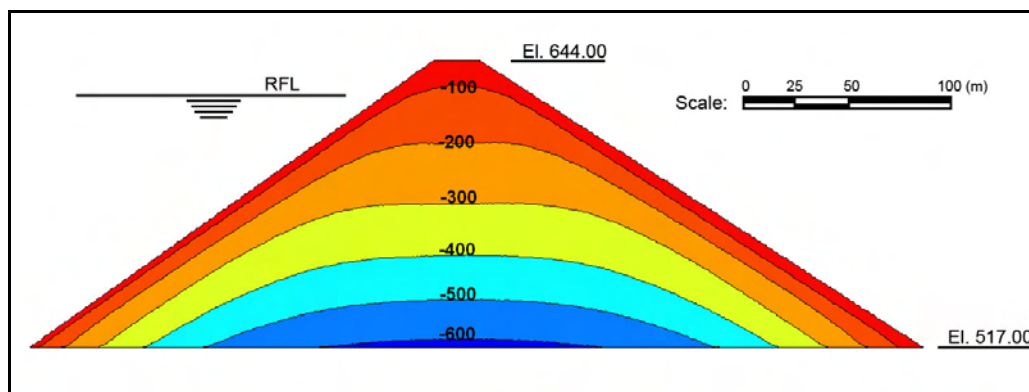


Figure 4.29 Horizontal stresses for EoC (stresses are in kPa)

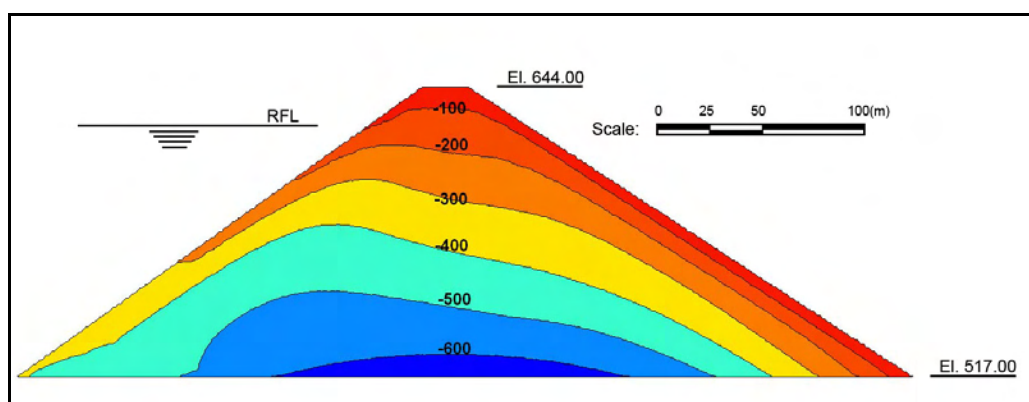


Figure 4.30 Horizontal stresses for RFC (stresses are in kPa)

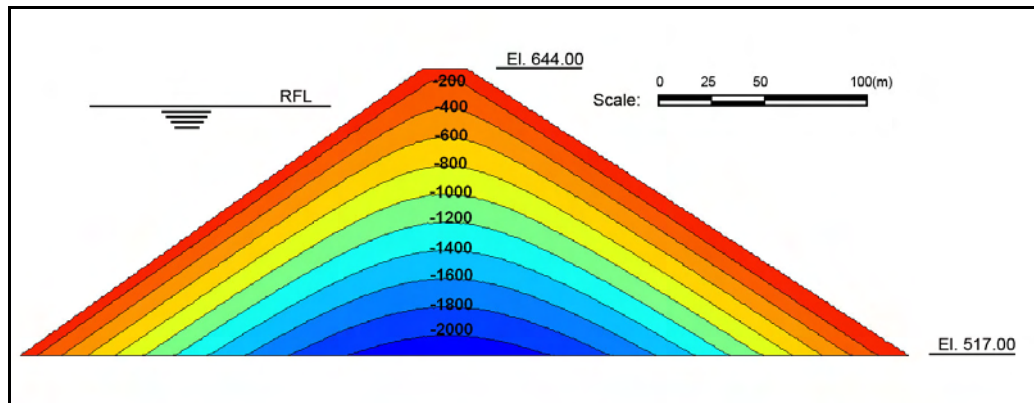


Figure 4.31 Vertical stresses for EoC (stresses are in kPa)

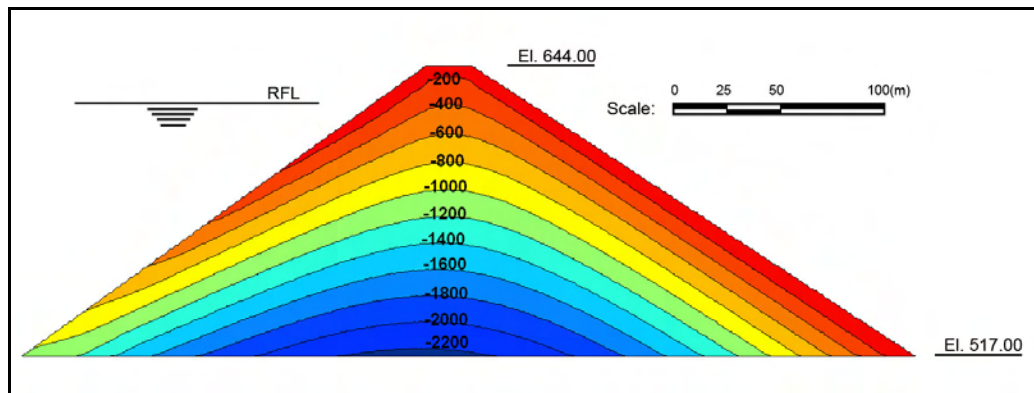


Figure 4.32 Vertical stresses for RFC (stresses are in kPa)

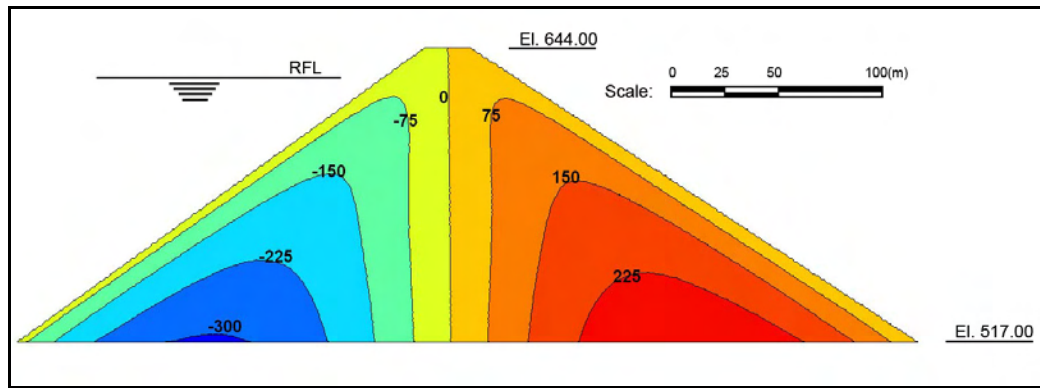



Figure 4.33 Shear stresses for EoC (stresses are in kPa)
 (positive values indicate )

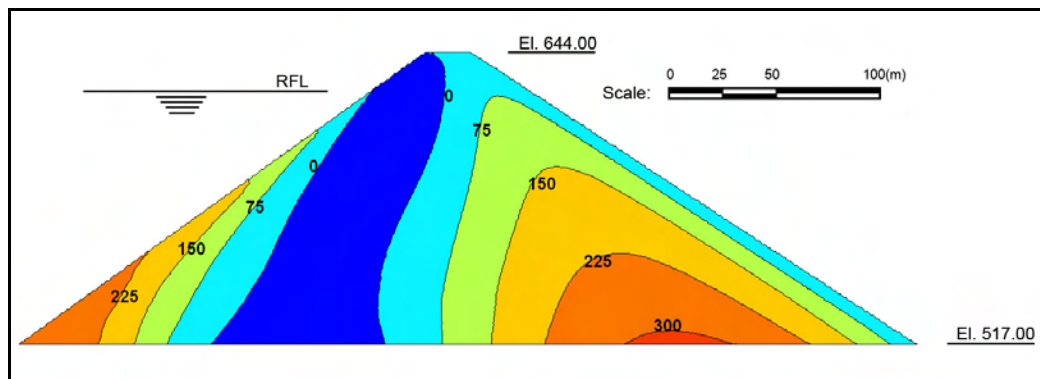



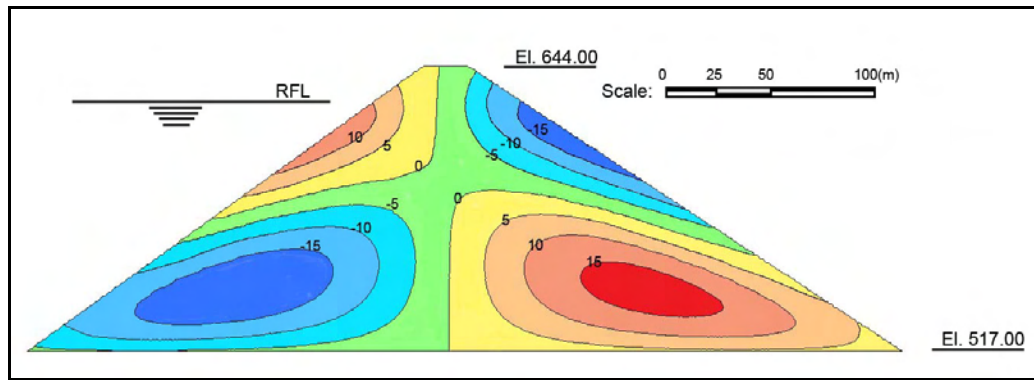
Figure 4.34 Shear stresses for RFC (stresses are in kPa)
 (positive values indicate )

When the horizontal displacement contours are examined, it is seen that for EoC, the upper part of the upstream face tended to move downstream while the lower part shows an opposite tendency. This behaviour is the same but mirrored at the downstream part. Since there were no instruments installed in Kürtün dam in order to observe the horizontal displacements, the results could not be compared with the observations (Figure 4.35).

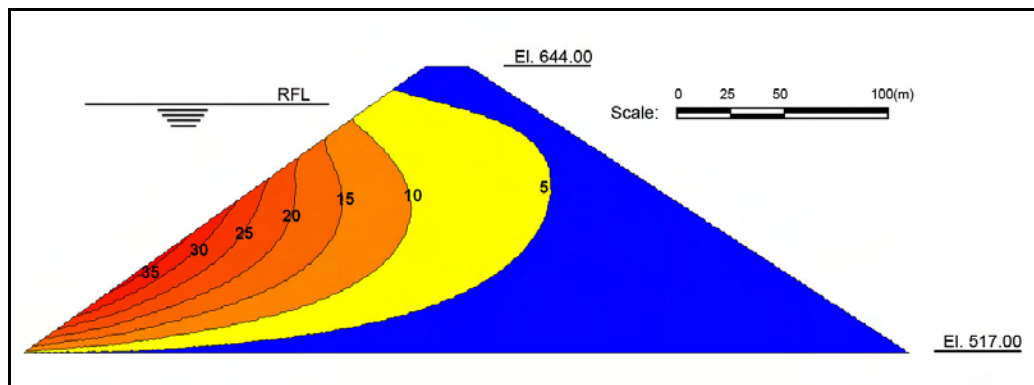
In the upstream half of the embankment, max horizontal displacement is calculated as 19.57 cm at 85.77 m away from dam centerline at El 547.50 (0.23 H, where H is dam height). In the downstream half, calculated max horizontal displacement is 17.22 cm at 91.37 m away from dam axis at El 547.50 (0.23 H). Calculated horizontal displacements are relatively small when compared with settlements. (Note that, RFC displacements are calculated separately from EoC displacements)

At RFC it is seen that, water load pushes the dam towards the downstream and horizontal displacements occur in the whole embankment towards downstream direction. Max calculated horizontal displacement is 37.72 cm which is found just under the concrete membrane at El 560.00 (0.32 H) (Figure 4.36).

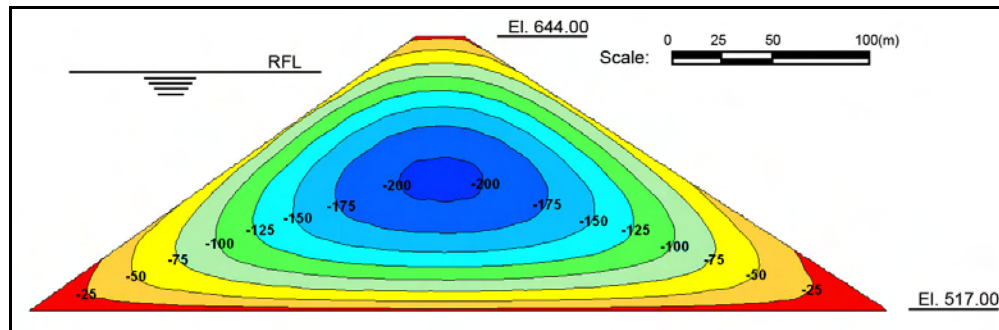
For EoC max calculated settlement is found as 205.13 cm (1.53 % of H), 4.65 m downstream from centerline at El 580.00 (0.47 H). For RFC, max. calculated settlement is found just under the concrete membrane as 54.10 cm (0.41 % of H) at El 563.13 (0.35 H) (Figures 4.37, 4.38) (Note that, RFC displacements are calculated separately from EoC displacements).



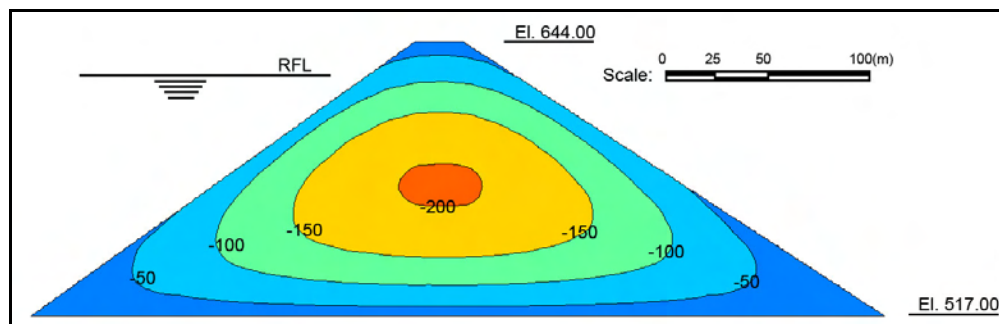
**Figure 4.35 Horizontal displacements for EoC (displacements are in cm)
(downstream is positive)**



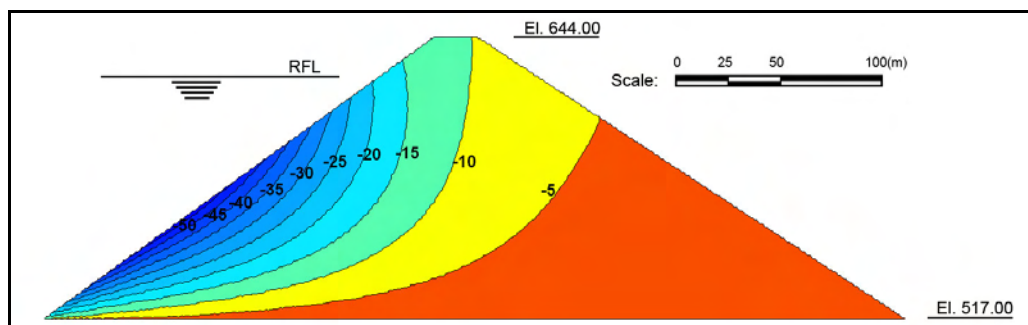
**Figure 4.36 Horizontal displacements for RFC (displacements are in cm)
(downstream is positive)**



**Figure 4.37a Vertical displacements for EoC with 25 cm contours
(negative values indicate settlement)**



**Figure 4.37b Vertical displacements for EoC with 50 cm contours
(negative values indicate settlement)**



**Figure 4.38 Vertical displacements for RFC (displacements are in cm)
(negative values indicate settlement)**

CHAPTER 5

SUMMARY and CONCLUSIONS

In this study two dimensional finite element analyses of Kürtün dam are carried out which is the first concrete face rockfill dam (CFRD) in Turkey. The following assumptions are made in the analysis:

- Grondiorite foundation of the dam is assumed to be rigid. This assumption can be considered reasonable when compared with relevant studies in the literature.
- Upstream membrane was assumed impervious without any cracks and modeled in five sections having different thicknesses due to increasing thickness of the membrane from the crest towards the upstream toe.
- The bond between concrete membrane and rockfill embankment was assumed to be totally prefect.
- The rockfill material is modeled using hardening soil model available in computer software. This model is based on Duncan and Chang's well known hyperbolic model.
- The model parameters are determined from the literature using hyperbolic parameters of CFRDs having similar deformation characteristics with Kürtün dam since no triaxial test results are available.

The following conclusions are achieved at the end of the study:

- When calculated stresses are compared with the observations, it is seen that cross-valley arching effect is significant for the end of construction (EoC) condition. This is clearly pronounced from the readings of the

instruments installed at El 555. The significance disappear towards upper elevations. This is attributed to the relatively narrow geometry of the valley.

- For EoC analyses, the calculated stress distributions are mirrored images of upstream and downstream parts of the embankment.
- For reservoir full condition (RFC, water level at El 630), both horizontal, vertical and shear stresses increase in the upstream part of the dam body considerably. However in the downstream part the increase is negligible.
- For RFC, as the water load modeled as a triangular distributed load, acting perpendicular to the membrane, calculated normal stresses are found to be higher than the readings in Axis G-G. However it can be concluded that overall agreement is satisfactory.
- When the settlements are examined, it is seen that arching effect is significant for EoC condition in lower elevations (i.e. El 555) increasing the differences between calculations and observations.
- Max vertical settlement is 205.13 cm (1.53 % of H), calculated at El 580.00 (0.47 H), 4.65 m downstream from dam centerline.
- It is found that, for EoC, vertical settlements recorded at El 625 was significantly lower than calculations. It is believed that, this difference is the result of relative changes in compaction effort. It is probable that, compaction effort kept higher at the upper elevations than the lower elevations and as a result lower settlement values are recorded.
- For RFC, calculated settlements are higher than the observations. This is probably due to the fact that, in the impounding rockfill behaves in a much stiffer response (like unloading) as compared with the construction condition. As a result unloading modulus controls the behaviour in impounding. However calculations indicate that unloading response of the rockfill material is not represented realistically by the computer software. When an unloaded region is assumed having 1.5 times greater deformation modulus than the primary loaded region, the results found more agreeable.

- It was seen that, Zone 3C material has a significant effect on the behaviour when modeled both as a weaker and as a stiffer material than Zone 3B material. However this effect is not clearly seen in the measurements. This is attributed to high compaction effort used in construction.
- When horizontal displacements are considered, it was found that, for EoC, upper half of upstream part of embankment moves downstream where lower half moves upstream. The same behaviour is observed but mirrored in the downstream part. The results could not be compared with the readings because horizontal displacement behaviour of Kürtün dam is not observed. However when the results are compared with relevant studies in the literature, it can be concluded that analyses do not represent the horizontal displacements realistically for EoC.
- For RFC, horizontal and vertical behaviour agree with the literature. Max horizontal and vertical displacements found to be occurred at about El 560-565 just under the concrete membrane which is in concordance with the previous work.
- When the rise in reservoir water level is considered, tensile strains are observed at some instruments located in the concrete membrane however at all water levels, computer analyses gives compressive strains. This difference is attributed to the assumption of totally perfect bonding between membrane and rockfill embankment.

As a conclusion, it can be said that two dimensional plane strain analysis results are encouraging. The location of instruments seem to be appropriate when the observations are compared with the calculations. But it is suggested to watch the horizontal displacement behaviour which is important in these type of structures.

When limitations of two dimensional plane strain analysis are considered, a three dimensional analysis is suggested to be carried out in order to see the effect of third dimension.

REFERENCES

1. Barton, N., and Kjaernsli, B., 1981. "Shear Strength of Rockfill", J. Geotech. Engrg., ASCE, 107, GT7, 873-891.
2. Byrne, P. M., Cheung, H., and Yan, L., 1987. "Soil Parameters for Deformation Analysis of Sand Masses", Can. Geotech. J., 24, 366-376.
3. Clements, R. P., 1984. "Post-Construction Deformation of Rockfill Dams", J. Geotech. Engrg., ASCE, 110, 7, 821-840.
4. Clough, R. W., and Woodward, R. J., 1967. "Analysis of Embankment Stresses and Deformations", J. of Soil Mech. and Found. Div., ASCE, 93, SM4, 529-549.
5. Cooke, J. B., 1984. "Progress in Rockfill Dams", (18th Terzaghi Lecture), J. Geotech. Engrg., ASCE, 110, 10, 1381-1414.
6. Cooke, J. B., and Sherard, J. L., 1987. "Concrete-Face Rockfill Dam: II. Design", J. Geotech. Engrg., ACSE, 113, 10, 1113-1132.
7. Duncan, J. M., and Chang, C. Y., 1970. "Nonlinear Analysis of Stress and Strain in Soil", J. of Soil Mech. and Found. Div., ASCE, 96, SM5, 1629-1653.
8. Duncan, J. M., Byrne, P., Wong, K. S., and Babry, P., 1980. "Strength, Stress-Strain and Bulk Modulus Parameters for Finite Element Analyses of Stresses and Movements in Soil Masses", Report No: UCB/GT/80-01, University of California, Berkeley.

9. Fitzpatrick, M. D., Cole, B. A., Kinstler, F. L., and Knoop, B. P., 1985. "Design of Concrete-Faced Rockfill Dams", Proc. of the Symp. "Concrete Face Rockfill Dams-Design, Construction, and Performance", ASCE, 410-434.
10. Frost, R. J., 1973. "Some Testing Experiences and Characteristics of Boulder-Gravel Fills in Earth Dams", ASTM, STP, 523, 207.
11. Fumagalli, E., 1969. "Tests on Cohesionless Materials for Rockfill Dams", J. of Soil Mech. and Found. Div., ASCE, 95, SM1, 313-332.
12. Hacas, J. E., Ramirez, C. A., and Regalado, G., 1985. "Construction and Performance of Salvajina Dam", Proc. of the Symp. "Concrete Face Rockfill Dams-Design, Construction, and Performance", ASCE, 286-315.
13. Hunter, G., and Fell, R., 2003. "Rockfill Modulus and Settlement of Concrete Face Rockfill Dams", J. Geotech. Geoenviron. Engng., ASCE, 129, 10, 909-917.
14. Janbu, N., 1963. "Soil Compressibility as Determined by Oedometer and Triaxial Tests", Proc. of the European Conf. on Soil Mech. and Found. Engng., Germany, vol.4, 19-25.
15. Khalid, S., Singh, B., Nayak, G. C., and Jain, O. P., 1990. "Nonlinear Analysis of Concrete Face Rockfill Dam", J. Geotech. Engng., ASCE, 116, 5, 822-837.
16. Kondner, R. L., 1963. "Hyperbolic Stress-Strain Response. Cohesive Soils", J. of Soil Mech. and Found. Div., ASCE, 89, SM1, 115-143.
17. Kulhawy, F. H., and Duncan, J. M., 1972. "Stresses and Movements in Oroville Dam", J. of Soil Mech. and Found. Div., ASCE, 98, SM7, 653-665.
18. Lefebvre, G., Duncan, J. M., and Wilson, E. L., 1973. "Three-Dimensional Finite Element Analysis of Dams", J. of Soil Mech. and Found. Div., ASCE, 99, SM7, 495-507.

19. Leps, T. M., 1970. "Review of Shearing Strength of Rockfill", J. of Soil Mech. and Found. Div., ASCE, 96, SM4, 1159-1170.
20. Liu, X., Wu, X., Xin, J., and Tian, H., 2002. "Three Dimensional Stress and Displacement Analysis of Yutiao Concrete Faced Rockfill Dam", Proc. of 2nd Int. Symp. On Flood Defense, Beijing.
21. Lowe, J., 1964. "Shear Strength of Course Embankment Dam Materials", Proc. 8th Int. Congress on Large Dams, 3, 745-761.
22. Marachi, N. D., Chan, C. K., and Seed, H. B., 1972. "Evaluation of Properties of Rockfill Materials", J. of Soil Mech. and Found. Div., ASCE, 98, SM1, 95-114.
23. Marsal, R. J., 1967. "Large Scale Testing of Rockfill Materials", J. of Soil Mech. and Found. Div., ASCE, 93, SM2, 27-43.
24. Nobari, E. S., and Duncan, J. M., 1972. "Movements in Dams due to Reservoir Filling", ASCE: Specialty Conf. On Performance of Earth and Earth Supported Structures, 797-815.
25. Pinto N. L. de S., Filho, M. P. L., and Maurer, E., 1985. "Foz do Areia Dam – Design, Construction, and Behaviour", Proc. of the Symp. "Concrete Face Rockfill Dams-Design, Construction, and Performance", ASCE, 173-191.
26. Plaxis ver. 7 - Material Models Manual.
27. Saboya, F. Jr., and Byrne, P. M., 1993. "Parameters for Stress and Deformation Analysis of Rockfill Dams", Can. Geotech. J., 30, 690-701.
28. Schanz, T., Vermeer, P. A., and Bonnier, P. G., 1999. "The Hardening Soil Model: Formulation and Verification", Beyond 2000 in Computational Geotechnics-10 Years of Plaxis, Balkema, Rotterdam.
29. Sharma, H.D. , 1976. "Nonlinear Analysis of a High Rockfill Dam with Earth Core", PhD Thesis, University of Roorkee, Roorkee, India.

30. Singh, B., and Varshney, R. S., 1995. "Engineering For Embankment Dams", A.A. Balkema Publishers, Brookfield.
31. TS 500, 2000. "Requirements for Design and Construction of Reinforced Concrete Structures", Turkish Standards Institution (TSE).
32. Varadarajan, A., Sharma, K. G., Venkatachalam, K., and Gupta, A. K., 2003. "Testing and Modeling Two Rockfill Materials", J. Geotech. Geoenv. Engrg., ASCE, 129, 3, 206-218.
33. Zeller, J., and Wullimann, R., 1957. "The Shear Strength of the Shell Materials for the Geo-Schenenalp Dam, Switzerland", Proc. 4th Inst. J. on Soil Mech. and Found. Engrg, London, 2, 399-404.